Circumventing Antibiotic Resistance:
A Two-Pronged Approach

Tolou Golkar Seisany

Department of Biochemistry
McGill University, Montréal
March 2022

A thesis submitted to McGill University in partial fulfillment
of the requirements of the degree of Doctor of Philosophy

Acknowledgments

I express my sincere gratitude to Albert Berghuis, my supervisor, my source of inspiration and support. Thank you for accepting me to become part of your research group, my second family from early on. Thanks for your always invaluable advice, outstanding patience, and tremendous encouragement and understanding.

My gratitude extends to my RAC members, David Thomas and Anthony Mittermaier, for their constructive guidance and insightful feedbacks during these years. Thank you for making my RAC meetings inspiring and motivational. I also offer my special thanks to Martin Scheming and Mehdi Talebzadeh for their help on the early stages of the ribosome project and to Tara Sprules for her assistance in NMR studies. I am also grateful to our collaborators at Clemson University and their group leader Dev Arya for our ongoing projects.

My heart is filled with thankfulness to all my current and previous lab members, my dear second family; Michal Zielinski, Jonathan Blanchet, Angelia Bassenden, Jaeok Park, Barry Sleno, Pedro Romero, Amy Yan, Dmitry Rodionov, Mark Hemmings, Ella Dekemp, Emma Kelly, and Juliana Munoz. I am deeply grateful to all of you for your unwavering support and intuitive suggestions at every stage of this journey. Our hearts are bound together forever. I particularly thank Kurt Dejgaard for proofreading this thesis, Jonathan Blanchet for the French translation of the abstract, and Kun Shi, the previous graduate student who gathered the fragment library. Additionally, I am grateful to the Department of Biochemistry, CIHR agency, and CRBS center for their funding aids which made this work possible.

Throughout my Ph.D. studies, I had the pleasure to work with four undergraduate students, Salma Youssef, Gautier Courbon, Émilie Desnoyers, and Danielle Courtemanche. This experience was a privilege, and I am honored to have this opportunity.

I'm deeply indebted to Kurt Dejgaard. Thank you for all your never-ending love and support. Your enthusiasm for science never ceases to amaze me. This life is more joyful with you.

And, of course, none of this could have happened without the support of my family and friends from all around the world. Mainly, I am forever thankful to my mom and dad. You are my symbols of love, strength, and steadfastness. I love you always, and I dedicate this thesis to both of you.

Abstract

The introduction of antibiotics into clinical use, revolutionized the treatment of many infectious diseases of bacterial origin. The discovery of Penicillin initiated a few frenzied decades of antibiotics discovery and development, which lamentably has fizzled out as we were unable to keep up the pace of discovery in the face of emerging resistant pathogens. Dissemination of antibiotic resistance genes and the evolution of antibiotic resistance mutations has resulted in the spread of multidrug-resistant bacteria, unresponsive to all antibiotics available for clinical use. The dangers of a post-antibiotic age prompted many policymakers to acknowledge this threat and, to some extent, revived the interest in the field of antibiotic discovery and drug development.

Alarmed by the prospects of antibiotic resistance, we participate in the global action plan to address this urgent public health problem. Focusing on two important classes of antibiotics, aminoglycosides and macrolides, we've looked at the three major molecular players in antibiotic resistance: the antibiotics themselves, the factor(s) that are responsible for resistance to these antibiotics and the antibiotics' target. For the aminoglycosides, one approach is to develop next-generation aminoglycosides that can evade resistance factor(s) but still recognize the target and enforce their antibacterial effect. With respect to the macrolides, another plausible strategy is to inhibit the resistance factor(s), thereby restoring macrolides' sensitivity.

In this thesis, we've pursued these two approaches with the aim to advance the field of drug design for next-generation aminoglycosides and macrolide adjuvant therapy by employing structural studies.

Firstly, we've examined the structural basis for the plazomicin mechanism of action and resistance to uncover new structural designs that enable this drug to escape resistance factors and yet recognize its target.

Secondly, targeting macrolide phosphotransferases, the most critical modifying enzymes for this class of antibiotics, we have worked on developing an inhibitor for these resistance-conferring enzymes that can be used as macrolide adjuvants.

Résumé

L'introduction des antibiotiques en utilisation clinique a révolutionné le traitement de nombreuses maladies infectieuses d'origine bactérienne. La découverte de la pénicilline a lancé quelques décennies frénétiques de découvertes et de développements d'antibiotiques, qui se sont lamentablement essoufflées car ces découvertes n'ont pas été en mesure de suivre le rythme face aux agents pathogènes résistants émergents. La diffusion de gènes de résistance aux antibiotiques et l'évolution des mutations de résistance ont entraîné la propagation de bactéries multi-résistantes, insensibles à tous les antibiotiques disponibles pour une utilisation clinique. Les dangers d'une ère post-antibiotique ont incité de nombreux décideurs à reconnaître cette menace et, dans une certaine mesure, ont ravivé l'intérêt pour le domaine de la découverte d'antibiotiques et du développement de médicaments adjuvants.

Alarmés par les perspectives de résistance aux antibiotiques, nous participons au plan d'action mondial pour faire face à cet urgent problème de santé publique. En nous concentrant sur deux classes importantes d'antibiotiques, les aminosides et les macrolides, nous nous sommes penchés sur les trois principaux acteurs moléculaires de la résistance aux antibiotiques : les antibiotiques eux-mêmes, le ou les facteurs responsables de la résistance à ces antibiotiques, et la cible des antibiotiques. Pour les aminosides, une tactique consiste à développer des aminosides de nouvelle génération qui peuvent échapper au(x) facteur(s) de résistance tout en reconnaissant la cible et en renforçant leur effet antibactérien. En ce qui concerne les macrolides, une autre stratégie plausible consiste à inhiber le(s) facteur(s) de résistance, rétablissant ainsi la sensibilité aux macrolides.

Dans cette thèse, nous avons poursuivi ces deux stratégies dans le but de faire progresser le développement d’aminosides de nouvelle génération et de médicaments pour la thérapie adjuvante des macrolides en faisant des études de biologie structurale.

En premier lieu, nous avons examiné la base structurale du mécanisme d'action et de résistance de la plazomicin afin de découvrir de nouvelles conceptions structurales qui permettraient à ce médicament d'échapper aux facteurs de résistance tout en reconnaissant sa cible.

Deuxièmement, en ciblant les macrolides phosphotransférases, les enzymes modificatrices les plus importantes pour la résistance à cette classe d'antibiotiques, nous avons travaillé au développement d'un inhibiteur de ces enzymes qui peut être utilisé comme adjuvant avec les macrolides.

List of Abbreviations

AD	**A**nno **D**omini
A-site	**A**minoacyl-site
AME	**A**minoglycoside **M**odifying **E**nzyme
AAC	**A**minoglycoside **Ac**etyltransferase
ANT	**A**minoglycoside **N**ucleotidyl**t**ransferase
APH	**A**minoglycoside **Ph**osphotransferase
ATP	**A**denosine-5′-**T**ri**p**hosphate
ARF	**A**DP **R**ibosylation **F**actor
AMR	**A**nti**m**icrobial **R**esistance
BC	**B**efore **C**hrist
CKI-7	**C**asein **K**inase-1 **I**nhibitor -7
CK2	**C**asein **K**inase-2
DOS	**D**e**o**xy**s**treptamine
Da	**Da**lton
ePKs	**E**ukaryotic **P**rotein **K**inase**s**
eEF1A	**E**ukaryotic **E**longation **F**actor 1A
eIF2	**E**ukaryotic **I**nitiation **F**actor2
FDA	**F**ood and **D**rug **A**dministration
GTP	**G**uanosine-5′-**T**ri**p**hosphate
HABA	**H**ydroxy-**A**mino**b**utyric **A**cid
HE	**H**ydroxy**e**thyl
ITC	**I**sothermal **T**itration **C**alorimetry
K_i	**I**nhibition constant
mRNA	**M**essenger **R**ibo**n**ucleic **A**cid
MPH	**M**acrolide **Ph**osphotransferase
MIC	**M**inimal **I**nhibitory **C**oncentration
NPET	**N**ascent **P**eptide **E**xit **T**unnel
NMR	**N**uclear **M**agnetic **R**esonance
Ni-NTA	**Ni**ckel-**Nit**rilo**a**cetic Acid
PTC	**P**eptidyl **T**ransferase **C**enter
rRNA	**R**ibosomal **RNA**
RAS	**Ra**t **S**arcoma Virus (protein)
RAN	**Ra**s-related **N**uclear (protein)
‘S’ in 70S, 50S. 30S, 16S, 23S, 5S	**S**vedberg unit **(**Sedimentation coefficient)
STD	**S**aturation **T**ransfer **D**ifference
tRNA	**T**ransfer **RNA**
WaterLOGSY	**Water**-**L**igand **O**bserved via **G**radient **S**pectroscop**y**

List of Tables

Chapter 1

1-1 The class and producing organism for the antibiotics shown in Figure 1-1.

Chapter 2

2-1 Data collection and refinement statistics of plazomicin bound to 70S ribosome and AAC(2′)-Ia.

Chapter 3

3-1 Data collection and refinement statistics of MPH(2′)-I in complex with the hit fragment and ABG-1.

List of Figures

Chapter 1

1-1 Timeline of antibiotics' clinical deployment and the first reported clinical resistance.

1-2 Chemical structure of aminoglycosides.

1-3 Outline of aminoglycoside binding sites on the ribosomal A-site.

1-4 Chemical structures of few clinically used macrolides.

1-5 Macrolides binding site on ribosomal 23S rRNA.

1-6 Plazomicin structure protects it from enzymatic inactivation by various AMEs.

1-7 Structural homology between MPH, APH, and ePK.

1-8 Sequence conservation of MPHs shown on MPH(2′)-I structure.

Chapter 2

2-1 Discovery maps of ribosome and AAC(2′)-Ia ligands.

2-2 Plazomicin bound to the 70S bacterial ribosome in complex with mRNA and tRNAs.

2-3 Structural comparison of apo and plazomicin-bound *T. thermophilus* ribosomal A-site.

2-4 The ribosomal A-site and AAC(2′)-Ia hydrogen bond interactions with plazomicin.

2-5 Alignment of aminoglycosides bound to the ribosomal A-site.

2-6 Comparison of plazomicin and acetylated-plazomicin binding to the ribosomal A-site and AAC(2′)-Ia.

2-7 Model of plazomicin bound to helix 69 of the ribosome.

2-8 Ribosome methylation and acetylated plazomicin clashes.

2-9 Proposed sites for next-generation aminoglycoside synthesis.

Chapter 3

3-1 Overview of the scheme followed for fragment screening and elaboration.

3-2 Binder identification on positive cocktails.

3-3 WaterLOGSY competition strategy using guanosine as a GTP-pocket competitor.

3-4 MPH(2′)-I structure in complex with 6-phenoxy pyridine 3-amine.

3-5 MPH(2′)-I hydrogen bond interaction with 6-phenoxy pyridine 3-amine and guanosine.

3-6 Hit-to-lead optimization strategies for 6-phenoxy 3-pyridine amine.

3-7 MPH(2′)-I hydrogen bond interactions with 6-(3-fluorophenoxy)-7H-purin-2-amine 1 (ABG-1) in *structures one* and *two*.

3-8 Inhibitory constant and kinetic parameters for the hit fragment, guanosine, and ABG-1.

3-9 Structural modeling of ABG-1 in the GTP pocket of human GTP-binding proteins.

3-10 Conservation prediction of ten residues surrounding ABG-1 is shown on MPH(2′)-I structure in complex with this molecule.

Chapter 4

4-1 Acetylation of plazomicin at 2′ position, using AAC(2′)-Ia in a biphasic reaction.

4-2 Mass spectrometry analysis of eluted samples after column chromatography.

4-3 Chemical structures of the four elaborated versions of ABG-1.

4-4 Chemical structures of the two proposed inhibitors based on *structure two* for ABG-1.

Table of Contents

Acknowledgments i
Abstract iii
Résumé v
List of Abbreviations vii
List of Tables viii
List of Figures ix
Table of Contents xi
Chapter 1 — Introduction 1
1.1 Preface 1
1.2 Antibiotics: Focus on Aminoglycosides and Macrolides 2
1.2.1 Brief History on Antimicrobials 2
1.2.2 Aminoglycosides: Spotlight on Plazomicin 4
1.2.2.1 Streptomycin to Plazomicin 4
1.2.2.2 Chemical Structure 5
1.2.2.3 Clinical Benefits 5
1.2.2.4 Mechanism of Action 7
1.2.3 Macrolides 9
1.2.3.1 Chemical Structure 9
1.2.3.2 Clinical Benefits 10
1.2.3.3 Mechanism of Action 11
1.3 Antibiotic Resistance: Focus on Aminoglycosides and Macrolides 15
1.3.1 Antibiotic Resistance is Ancient 15
1.3.2 Mechanisms of Resistance 16
1.3.3 Aminoglycosides Mechanisms of Resistance: Focus on Plazomicin 17
1.3.3.1 Change of Uptake and Efflux-mediated Resistance 17
1.3.3.2 Ribosomal Mutations 18
1.3.3.3 Ribosomal Methylations 18
1.3.3.4 Enzymatic Alteration of Aminoglycosides 19
1.3.4 Macrolides Mechanisms of Resistance 21
1.3.4.1 Efflux-mediated Resistance 21
1.3.4.2 Ribosome Protection 22

1.3.4.3 Ribosomal Mutations 22
1.3.4.4 Ribosomal Methylation 23
1.3.4.5 Enzymatic Alteration of Macrolides 24
1.3.5 Macrolide Phosphotransferases 25
1.3.5.1 Members of the Family 25
1.3.5.2 Brief on Structure 26
1.3.5.3 Conservation Studies 27
1.3.5.4 Substrate Specificity 29
1.4 Counteracting Antibiotic Resistance 30
1.4.1 Global Action Plan 30
1.4.2 New Antibiotics 31
1.4.3 Antibiotic Adjuvants 33
1.4.4 Innovative Therapies 33
1.5 Thesis Objectives 34
Chapter 2 — Structural Basis for Plazomicin Antibiotic Action and Resistance ... 36
2-1 Preface 36
2-2 Introduction 38
2-3 Results 41
2-3-1 Structure of Plazomicin Bound to the Ribosome•mRNA•tRNAs Complex 41
2-3-2 Structure of inactivated plazomicin bound to AAC(2′)-Ia 46
2-3-3 Comparison of plazomicin binding to target vs. resistance factor 47
2-4 Discussion 49
2-4-1 Mechanism of plazomicin antibiotic action 49
2-4-2 Mechanism of plazomicin resistance 51
2-4-3 Implications for further drug development 54
2-5 Conclusion 56
2-6 Experimental Procedures 57
2-6-1 Plazomicin Synthesis 57
2-6-2 Ribosome Purification 57
2-6-3 $tRNA^{fMet}$ and $tRNA^{Phe}$ Expression 57
2-6-4 $tRNA^{fMet}$ Purification 58
2-6-5 $tRNA^{Phe}$ Purification 58
2-6-6 mRNA Synthesis 59

2-6-7 Ribosome Complex-Formation 59
2-6-8 Ribosome Crystallization 59
2-6-9 Ribosome Data Collection, Structure Solution and Refinement 59
2-6-10 AAC(2')-Ia Cloning 60
2-6-11 AAC(2')-Ia Expression and Purification 61
2-6-12 AAC(2')-Ia Crystallization 62
2-6-13 AAC(2')-Ia Data collection, Structure Solution and Refinement 62
Chapter 3 — Inhibitor Development Against Kinases Involved in Macrolide Resistance 64
3-1 Preface 64
3-2 Introduction 66
3-3 Results and Discussions 70
3-3-1 Fragment screening with ligand-based NMR spectroscopy and binder identification 70
3-3-2 Potential GTP-pocket binders' characterization 70
3-3-3 Structure of MPH(2')-I complexed with 6-phenoxy pyridine 3-amine and structure-guided elaboration of this fragment 74
3-3-4 Structure of MPH(2')-I complexed with ABG-1 77
3-3-5 Inhibition studies 79
3-3-6 Possibility of cross-reactivity of MPH inhibitors with human GTP-binding proteins 81
3-3-7 All-inclusive MPH inhibitor design 83
3-4 Conclusion 84
3-5 Experimental Procedures 86
3-5-1 MPH(2')-I and MPH(2'')-II Expression, and Purification 86
3-5-2 Fragment-Based Library 86
3-5-3 6-(3-fluorophenoxy)-7H-purin-2-amine (ABG-1) Synthesis 87
3-5-4 NMR Studies 87
3-5-5 MPH-I Co-crystallization With 6-phenoxy pyridine 3-amine and 6-(3-fluorophenoxy)-7H-purin-2-amine 88
3-5-6 Data Collection, Structure Solution, and Refinement 90
3-5-7 Inhibition Assay 92
Chapter 4 — Thesis Conclusion 94
References 101
Appendix 119

Chapter 1 — Introduction

1.1 Preface

Sections 1.2.3.3, 1.3.4.3, 1.3.4.4, and 1.3.5 were partially adapted from Golkar, T., M. Zieliński and A. M. Berghuis (2018). "Look and outlook on enzyme-mediated macrolide resistance." Frontiers in microbiology **9**: 1942.

Individual Author Contributions in chapter one are as follows, with percent of overall contribution in parentheses:

Golkar, T. (75%): Preparation of the text and figures.

Berghuis, A. M. (25%): Editing of the text and figures.

1.2 Antibiotics: Focus on Aminoglycosides and Macrolides

1.2.1 Brief History on Antimicrobials

In our battle with microbial pathogens, we exploit the chemical weaponry of bioactive molecules that microbes themselves use to confront competitors. These molecules are used as antimicrobial drugs and have been a pillar of modern medicine since the middle of the 20th century. However, the use of these natural products dates back millennia. As documented in the Eber's papyrus, an Egyptian medical papyrus of herbal knowledge dating to circa 1550 BC, poultices of moldy bread and medicinal soil are among listed remedies (Haas 1999). Likewise, traces of tetracycline in human skeletal remains from ancient Sudanese Nubia dating back to 350-550 AD may indicate exposure to tetracycline-containing materials in the diet of these people (Bassett, Keith et al. 1980).

Prior to the discovery of penicillin by Alexander Fleming in 1928 (Fleming 1929), development of antimicrobial drugs, a proverbial "magic bullet" that selectively targets only disease-causing microbes, is widely accredited to Paul Ehrlich. Ehrlich and his team developed the synthetic arsenic-based drug, Salvarsan, to treat *Treponema pallidum*, the causative agent of syphilis, over a hundred years ago (Ehrlich and Halta 1910). Important in this context, Ehrlich introduced the systematic screening approach that has since become the foundation of drug discovery strategies in the pharmaceutical industry. This approach led to the discovery of Prontosil, an effective, broad-spectrum drug of the sulfonamide class of antimicrobials that were in clinical use prior to the clinical use of penicillin (Domagk 1935).

In the wake of Alexander Fleming's seminal work, Selman Waksman defined an *antibiotic as "a compound made by a microbe to destroy other microbes" (Waksman 1947)*. His studies were instrumental in identifying soil-dwelling actinomycetes as prolific producers of antibiotics. Neomycin and streptomycin are two examples of many antibiotics he discovered himself (Waksman, Schatz et al. 2010). His work initiated the golden age of antibiotic discovery from the 1940s to the 1960s (Figure 1-1). During this period, about 10 classes of antibiotics were introduced into clinics, more than 80% of which were isolated from actinomycetes (Table 1-1) (Hutchings, Truman et al. 2019).

Here, we focus on two classes of antibiotics and look deeper into their chemical structure, clinical benefits, and mechanism of action.

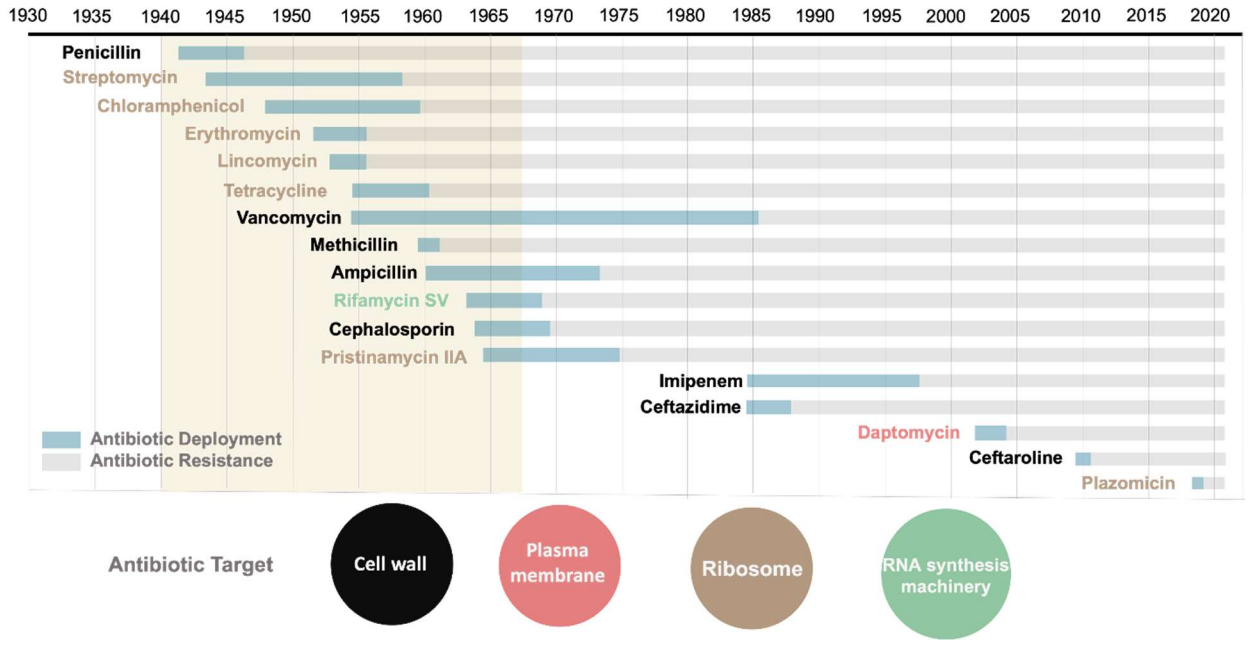

Figure 1-1. Timeline of antibiotics' clinical deployment and the first reported clinical resistance. Only natural antibiotics or semi-synthetic derivatives of natural antibiotics are shown here. At least one antibiotic is shown from each class. The golden age of discovery is highlighted in yellow. Antibiotics are colored based on their target.

Table 1-1. The class and producing organism for the antibiotics shown in Figure 1-1.

Antibiotic	Class	Producing organism
Penicillin	β-Lactam	*Penicillium spp.*
Streptomycin	Aminoglycoside	*Streptomyces griseus*
Chloramphenicol	Phenicols	*Streptomyces venezuelae*
Erythromycin	Macrolide	*Saccharopolyspora erythrea*
Lincomycin	Lincosamide	*Streptomyces lincolnensis*
Tetracycline	Tetracycline	*Streptomyces aureofaciens*
Vancomycin	Glycopeptide	*Streptomyces orientalis*
Methicillin	β-Lactam	2nd generation penicillin
Ampicillin	β-Lactam	3rd generation penicillin
***Rifamycin**	Ansamycin	*Amycolatopsis rifamycinica*
Cephalosporin	β-Lactam	fungus *Acremonium*
Pristinamycin IIA	Streptogramin A	*Streptomyces pristinaespiralis*
Imipenem	β-Lactam (subclass of carbapenem)	Semi-synthetic derivative of thienamycin (thienamycin from *Streptomyces cattleya*)
Ceftazidime	β-Lactam	3rd generation cephalosporin
Daptomycin	Lipopeptide	*Streptomyces roseosporus*
Ceftaroline	β-Lactam	5th generation cephalosporin
Plazomicin	Aminoglycoside	Semi-synthetic derivative of sisomicin (sisomicin from *Micromonospora inositola)*

*Rifamycin SV, which is a derivative of rifamycin, is clinically used.

1.2.2 Aminoglycosides: Spotlight on Plazomicin

1.2.2.1 Streptomycin to Plazomicin

Selman Waksman and Albert Schatz isolated the first aminoglycoside, streptomycin, in 1943 from *Streptomyces griseus* (Schatz, Bugle et al. 1944). Several other members of this class were introduced over the intervening years and are used in clinics, such as neomycin (1949, *S. fradiae*), gentamicin (1963, *Micromonospora purpurea*), tobramycin (1967, *S. tenebrarius*), amikacin (1972, derived from kanamycin) and the most novel aminoglycosides plazomicin (2010, derived from sisomicin) (Aggen, Armstrong et al. 2010, Krause, Serio et al. 2016). After almost four decades, Plazomicin became the first semi-synthetic next-generation aminoglycoside to be approved for clinical use by the FDA

and other sister agencies in other countries (Achaogen 2018, Chahine, Dougherty et al. 2021).

1.2.2.2 Chemical Structure

Aminoglycosides are aminocyclitol-containing molecules with either a streptamine or, in most cases, a 2-deoxystreptamine core. Most aminoglycosides have amino sugar rings substituted at positions 4, 5 or 4, 6 of the 2-deoxystreptamine (DOS) nucleus (Figure 1-2).

Plazomicin is distinguished from other 4, 6 disubstituted 2-DOS aminoglycosides by three key structural modifications (Figure 1-2. Number 7). Firstly, plazomicin lacks hydroxyl groups in the 3′ and 4′ positions. Secondly, it has a hydroxyethyl (HE) substituent in its N6′ position, and finally, the N1 position bears a hydroxy-aminobutyric acid (HABA) appendage. The importance of these modifications on plazomicin protection against aminoglycoside modifying enzymes will be discussed in section 1.3.3.4.

1.2.2.3 Clinical Benefits

Aminoglycosides are broad-spectrum antibiotics used to treat severe bacterial infections. They are particularly potent against members of the Gram-negative Enterobacteriaceae family (e.g., *Escherichia coli*, *Klebsiella pneumoniae*, *Enterobacter cloacae*), *Providencia* spp., *Proteus* spp., *Serratia* spp., *Pseudomonas* spp., and to a lesser extent *Acinetobacter* spp. They also have good activity against Gram-positive *Staphylococcus aureus*, including methicillin-resistant and vancomycin-intermediate and -resistant isolates. Furthermore, many *Mycobacterium* spp. (e.g., *Mycobacterium*

tuberculosis and *M. avium*) are also susceptible to aminoglycosides (Krause, Serio et al. 2016).

Plazomicin is specifically prescribed for the treatment of complicated urinary tract infections, including pyelonephritis caused by *E. coli*, *K. pneumoniae*, *Proteus mirabilis*, and *E. cloacae*. It also shows in vitro activity against *Pseudomonas aeruginosa and* methicillin-resistant *S. aureus* (Eljaaly, Alharbi et al. 2019).

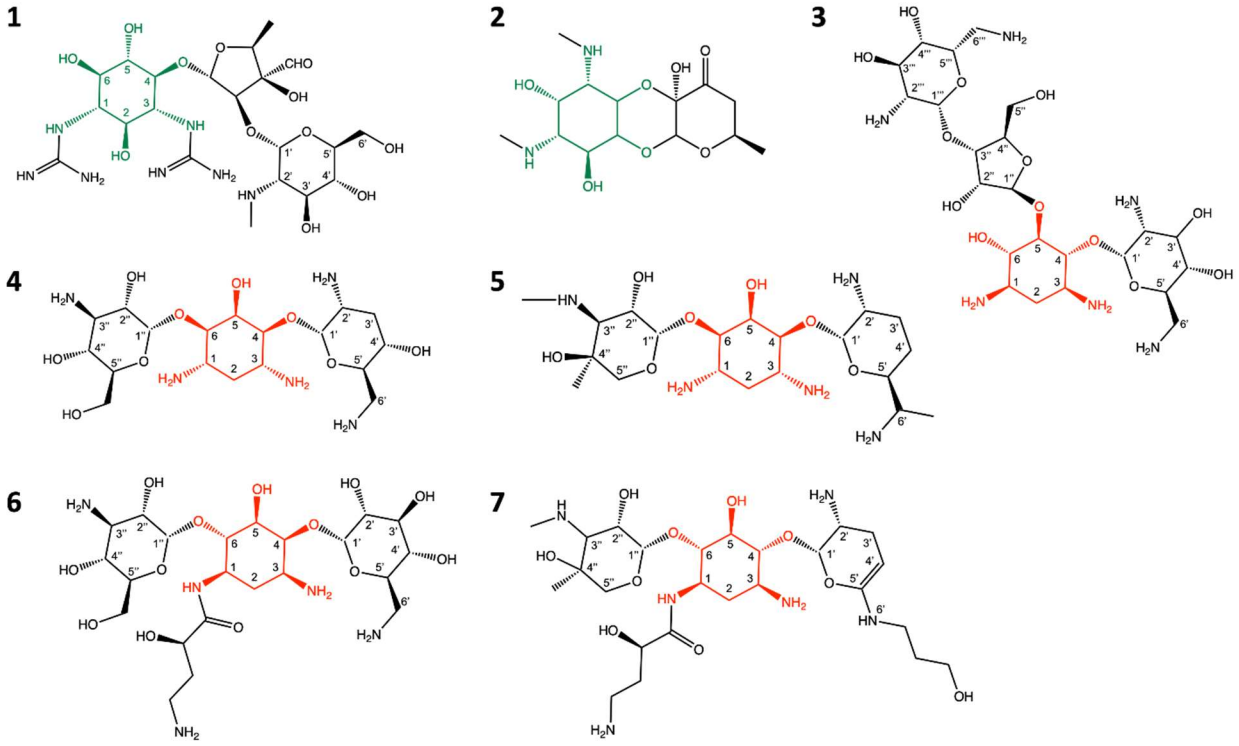

Figure 1-2. Chemical structure of aminoglycosides. The streptamine core is shown in green. The 2-deoxystreptamine (DOS) core is shown in red. **(1)** Streptomycin. **(2)** Spectinomycin. **(3)** 4,5-disubstituted 2-DOS aminoglycoside neomycin. **(4)** 4,6-disubstituted 2-DOS aminoglycoside tobramycin. **(5)** 4,6-disubstituted 2-DOS aminoglycoside gentamicin C1a. **(6)** 4,6-disubstituted 2-DOS aminoglycoside amikacin. **(7)** 4,6-disubstituted 2-DOS aminoglycoside plazomicin.

1.2.2.4 Mechanism of Action

Early studies on streptomycin-treated *E. coli* cells showed alteration in their cell membrane permeability, resulting in the relatively high excretion rate of certain ribonucleotides. A further examination revealed that this phenomenon is due to the interference in protein synthesis as RNA and DNA synthesis remained unchanged (Davis and Anand 1960). Subsequently, Spotts and Stanier hypothesized that the ribosomes were the sensitive elements (Spotts and Stanier 1961). Through in vitro studies of 70S ribosome reconstruction in which 30S subunits were taken from streptomycin-resistant strains of *E. coli*, the sensitivity to streptomycin was shown to reside on this subunit (Cox, White et al. 1964, Davies 1964). Ultimately, it was demonstrated that streptomycin could induce misreading during in vitro polypeptide synthesis (Davies, Gilbert et al. 1964, Davies and Davis 1968).

X-ray structural studies of the 30S ribosomal subunit of *Thermus thermophilus* brought considerable insights into the components and the function of the decoding site of the ribosome (Schluenzen, Tocilj et al. 2000, Wimberly, Brodersen et al. 2000). These observations, combined with the structural studies of different aminoglycosides bound to this region, brought the results of all previous years of investigations into perspective (Brodersen, Clemons Jr et al. 2000, Carter, Clemons et al. 2000).

Aminoglycosides bind to the A-site on 16S rRNA of the 30S ribosomal subunit. Their exact binding site and, therefore, their impact on the ribosome differ based on their chemical structure. However, the final consequence of these interactions is the same for all; inhibition of accurate protein synthesis, which precipitates aminoglycoside's bactericidal effects.

Spectinomycin binds in the minor groove at one end of helix 34 and interacts mainly with G1064, C1066, G1068, and C1192 (*E. coli* numbering). Its binding hinders tRNA translocation from the A- to P-site (Figure 1-3C). Streptomycin interacts with helices 1, 27,18, 44, and the ribosomal protein uS12 (Figure 1-3B). These interactions stabilize the ribosome in an error-prone state with a high affinity for tRNA, inducing the incorporation of non-cognate tRNAs. The preferential stabilization of this state also affects proof-reading mechanisms. The 4,5- and 4,6-disubstituted 2-DOS aminoglycosides sit at the base of helix 44 (Figure 1-3A). The pattern of hydrogen bond interactions differ, based on the structure of the aminoglycosides, but the prime ring and central ring play an essential role in these interactions. The binding of 4,5- and 4,6-disubstituted 2-DOS aminoglycosides initiates an erroneous decoding process in protein synthesis (Brodersen, Clemons Jr et al. 2000, Carter, Clemons et al. 2000, François, Russell et al. 2005).

Structural studies of neomycin, gentamicin, and paromomycin displayed another binding site for these three aminoglycosides. The site is located on helix 69 in the 23S rRNA of the 50S ribosomal subunit. It has been suggested that aminoglycoside binding to h69 restricts its helical dynamics, thereby stabilizing bridges between the ribosomal subunits, resulting in inhibition of ribosome recycling (Borovinskaya, Pai et al. 2007). Binding of other 4,5- and 4,6-disubstituted 2-DOS aminoglycosides to this location has not been reported and warrants further investigation.

As we will discuss later (section 1.3.3.3), ribosomal methylation on 16S rRNA at helix 44 makes a pathogen resistant to plazomicin. This observation suggests that as other 4,6-disubstituted 2-DOS aminoglycosides, plazomicin binds to the 16S rRNA at the

A-site of the 30S ribosomal subunit. Still, structural studies on its binding to the bacterial ribosome demand further elucidation (see Section 1.5).

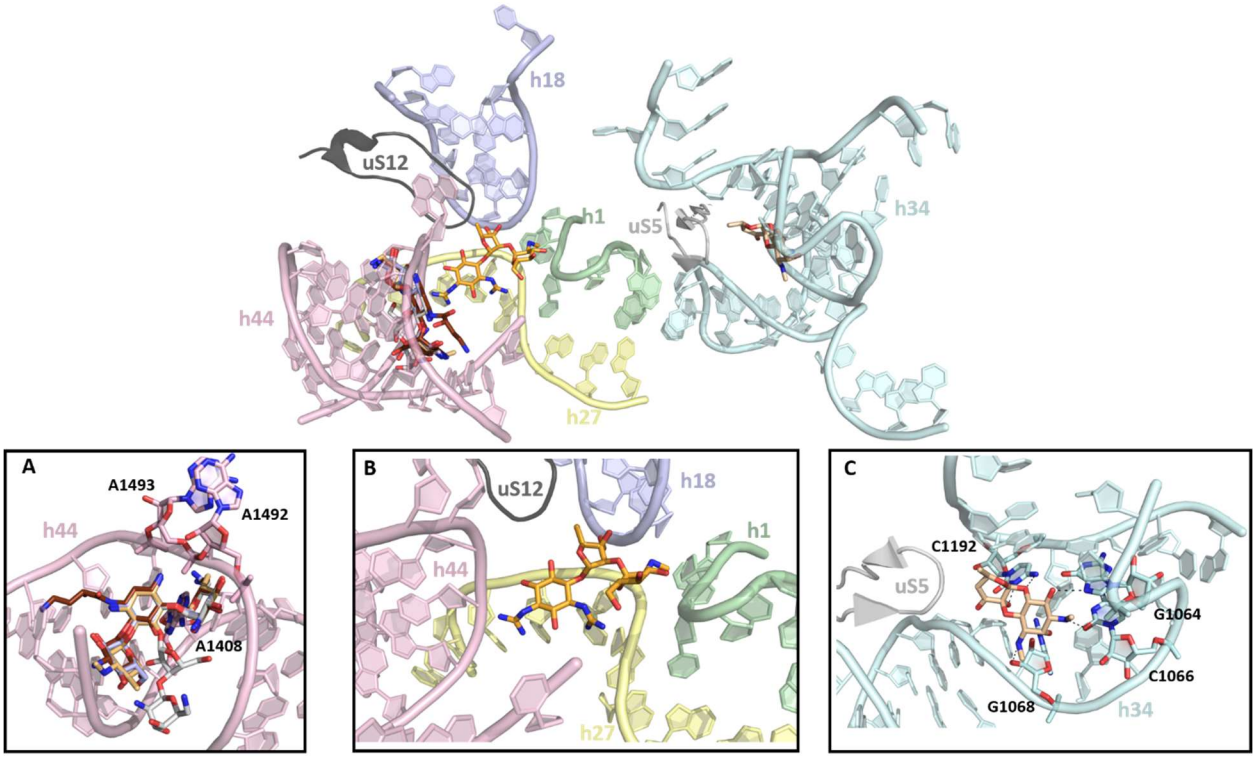

Figure 1-3. Outline of aminoglycoside binding sites on the ribosomal A-site. The top panel shows the different helices of 16S rRNA engaged in aminoglycosides interactions on ribosomal A-site. Helix1 is in light green, helix18 is in light purple, helix27 is in yellow, helix44 is in light pink, and helix34 is in light blue. Ribosomal proteins uS12 and uS5 are shown in dark gray and light gray, respectively. **(A)** Neomycin (light gray) (PDB code: 2ET4), gentamicin C1a (yellow) (PDB code: 2ET3) , amikacin (brown) (PDB code: 4P20), and tobramycin (light blue) (PDB code: 1LC4) sit at the base of h44. Residues 1492, 1493, and 1408 are depicted as sticks and colored in light pink. **(B)** Streptomycin makes interactions with h1, h18, h27, h44, and uS12 (PDB code: 1FJG). **(C)** Spectinomycin makes interactions mainly with four residues on h34. These residues are depicted as sticks and colored in light blue (PDB: 1FJG).

1.2.3 Macrolides

1.2.3.1 Chemical Structure

The first clinically used macrolide, erythromycin, was first isolated in 1949 from the soil-dwelling bacterium *Saccharopolyspora erythrea* and used in clinics in 1952. Clinically

relevant macrolides consist of a 14- to 16-membered macrolactone ring substituted by hydroxyl or alkyl groups and sugar moieties at C5 or C5/C3 positions. C5 position can hold a desosamine or mycaminose sugar. In the case of mycaminose, a second sugar, mycarose, is linked to this moiety, creating a disaccharide at the C5 position. C3 can hold a cladinose sugar which, in the case of next-generation macrolides, known as ketolides, is replaced with a 3-ketone (Figure 1-4).

1.2.3.2 Clinical Benefits

Erythromycin has primarily been used to treat respiratory, skin, and soft tissue infections, especially in patients allergic to penicillin. Erythromycin has poor oral bioavailability and shows a high incidence of gastrointestinal adverse effects. It is also inefficient against *Haemophilus influenzae* and *Moraxella catarrhalis.* These limitations urged the development and discovery of new macrolides such as azithromycin (15-membered, C-9a tertiary amino derivative of erythromycin), clarithromycin (14-membered, 6-O-methyl derivative of erythromycin), and spiramycin (16-membered, isolated from *S. ambofaciens*) (Jelić and Antolović 2016). The removal of the cladinose in ketolides increases both acid stability and antibacterial potency against bacteria resistant to macrolides by the efflux mechanism.

As a result of these modifications, macrolides are now effective in the treatment of Gram-positive (e.g., *Streptococcus pneumoniae*, *Streptococcus pyogenes*, *Staphylococcus aureus*), Gram-negative bacterial pathogens (e.g., *H. influenzae, M. catarrhalis*), and even some atypical pathogens (e.g., *Neisseria gonorrhoeae*) (Zhanel, Dueck et al. 2001, Zuckerman, Qamar et al. 2011).

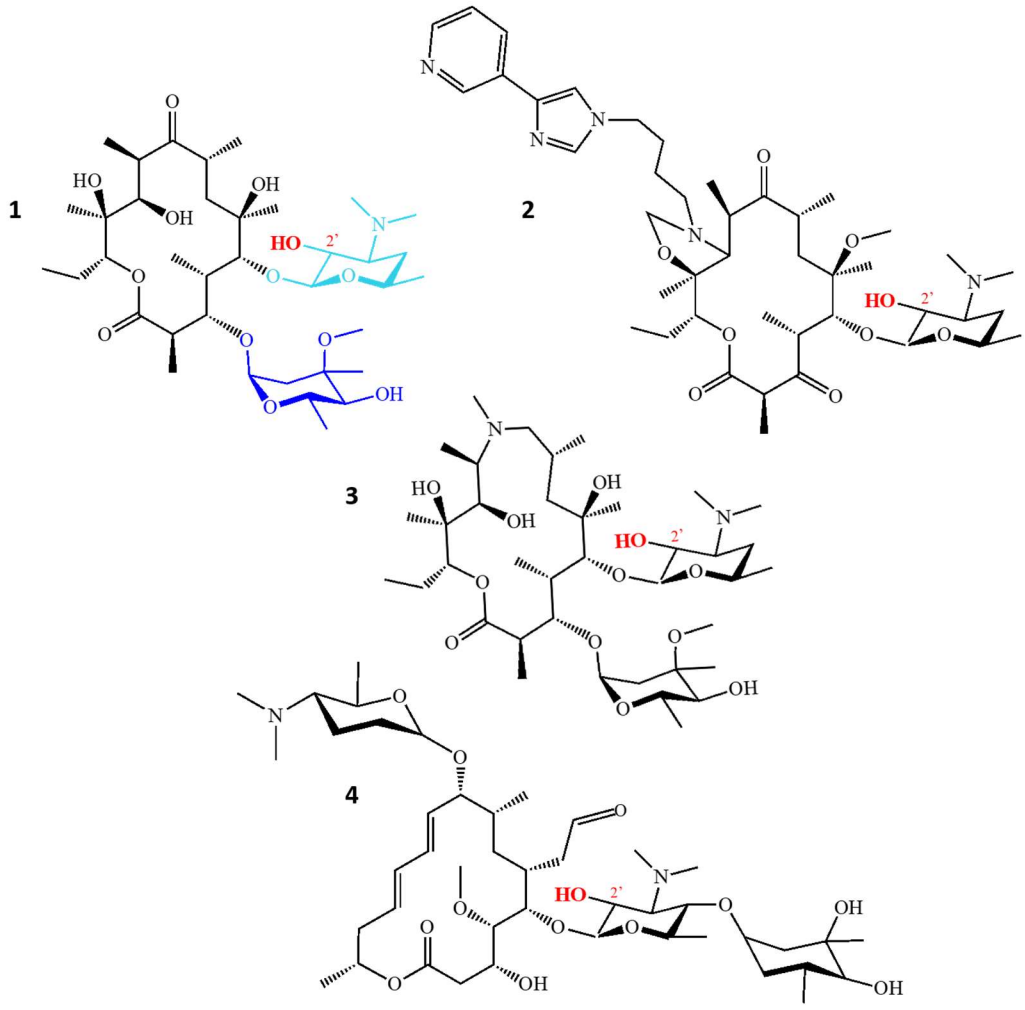

Figure 1-4. Chemical structures of few clinically used macrolides. Desosamine moiety is shown in light blue, and cladinose sugar is shown in dark blue on erythromycin structure. The 2′-OH position, which is the site of modification by macrolide phosphotransferases, is shown in red in all structures. **(1)** 14-membered erythromycin. **(2)** 14-membered ketolide, telithromycin. **(3)** 15-membered azithromycin. **(4)** 16-membered spiramycin I.

1.2.3.3 Mechanism of Action

Through the study of the effects of erythromycin on bacteria, it was found early on that macrolides had an impact on protein synthesis (Taubman, So et al. 1963). Subsequent studies revealed that this was due to the binding of the macrolide to the

ribosome (Taubman, Jones et al. 1966). Around this time, studies of chloramphenicol binding to the 50S ribosome, and interference of this binding by different classes of antibiotics, suggested that macrolides interact with the 50S subunit at a related site (Vazquez 1966). This binding was also confirmed through binding studies of erythromycin to ribosomes from antibiotic-sensitive and -resistant *Bacillus subtilis* 168 (Oleinick and Corcoran 1969), through the fragment reaction studies (Celma, Monro et al. 1970) and by dimethyl sulfate and kethoxal probing (Moazed and Noller 1987). Furthermore, this binding was shown genetically through two chloramphenicol-erythromycin resistance mutations on *E. coli* 23S rRNA (Ettayebi, Prasad et al. 1985). However, it took some time before the exact location and mechanism of ribosome binding and inhibition was confirmed through X-ray crystal structures of the 50S and 30S ribosomal subunits and the intact 70S ribosome (Ban, Nissen et al. 2000, Wimberly, Brodersen et al. 2000, Schlünzen, Zarivach et al. 2001, Schlünzen, Harms et al. 2003, Tu, Blaha et al. 2005).

Macrolides bind to the 23S rRNA in the nascent peptide exit tunnel (NPET) of the 50S ribosomal subunit, immediately adjacent to the peptidyl transferase center (PTC). Despite the chemical diversity of macrolides, there is an extensive similarity in how they bind to the ribosome (Figure 1-5). First of all, the lactone rings, which possess a hydrophobic and a hydrophilic face, invariably bind to the ribosome with their hydrophobic face. The desosamine moiety at the C5 position makes specific hydrogen bond interactions with the nucleotide residues A2058 and A2059 (*E. coli* numbering). Furthermore, for those macrolides that possess a sugar at the C3 position, this cladinose group makes specific interactions with the base of nucleotide 2505, though this only

contributes incrementally to the affinity of the macrolide for the 50S subunit (Hansen, Ippolito et al. 2002).

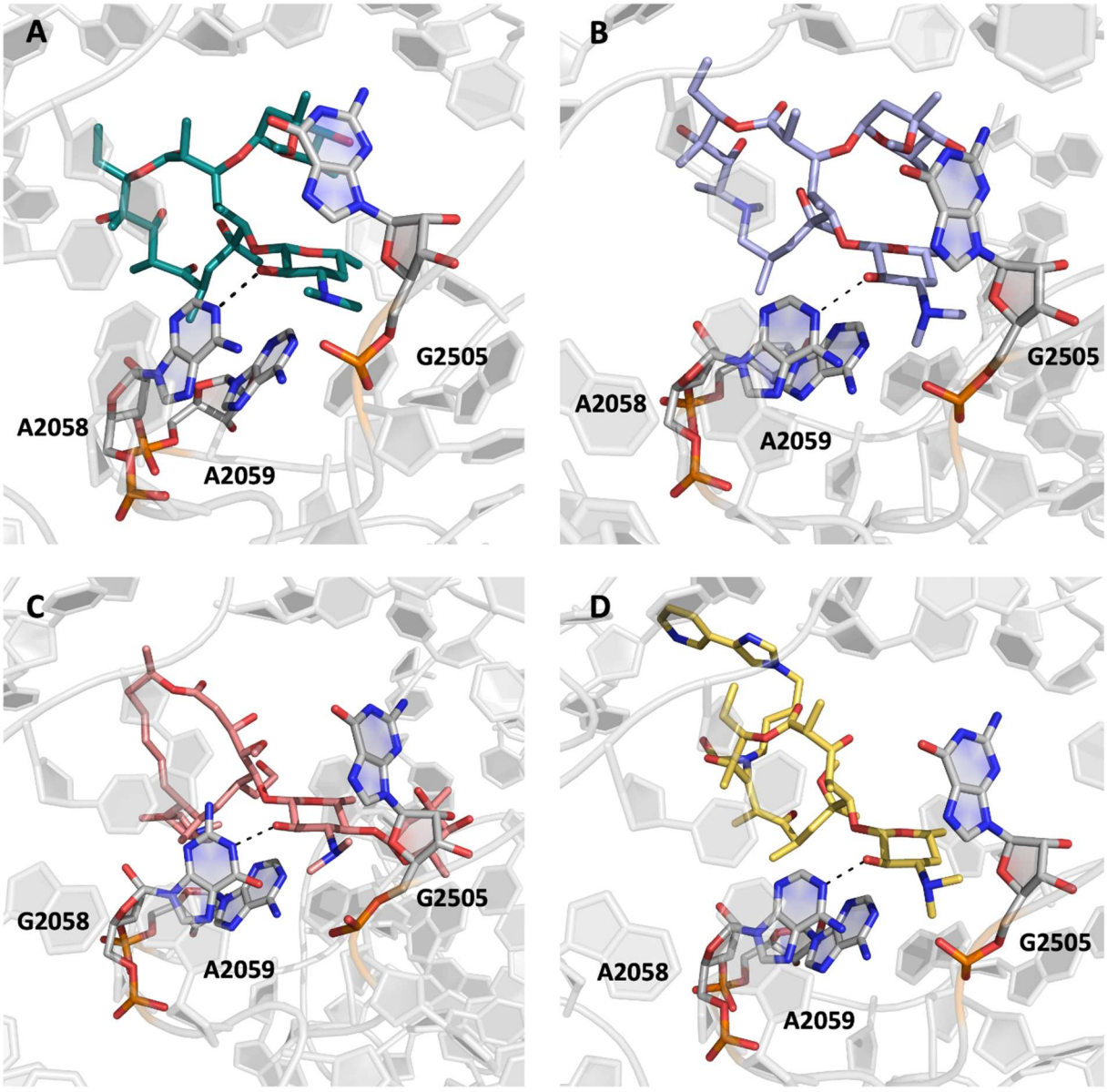

Figure 1-5. Macrolides binding site on ribosomal 23S rRNA. Four macrolide-bound ribosome structures are shown in four panels. The three important residues for macrolides' interactions at this site (*E. coli* numbering) are depicted as sticks and colored in gray. The hydrogen bond is depicted as a black dashed line. Note that in panel (C) the corresponding residue for *E. coli* A2058 is guanine in *Haloarcula marismortui,* which makes this organism much more resistant to macrolides than those that have an adenine at this position (Hansen, Ippolito et al. 2002). (A) Erythromycin bound to *E. coli* ribosome (PDB code: 4V7U). (B) Azithromycin bound to *Thermus thermophilus* ribosome (PDB code: 4V7Y). (C) Spiramycin I bound to *Haloarcula marismortui* (PDB code: 1KD1), and (D) Telithromycin bound to *E. coli* ribosome (PDB code: 4V7S).

Traditionally, it has been thought that macrolides stop translation simply by clogging the NPET, thereby blocking the passage of all the newly synthesized polypeptides. However, new data gathered by ribosome profiling over the past several years have shown that macrolides can inhibit the synthesis of a subset of proteins (Ingolia, Ghaemmaghami et al. 2009). These proteins contain a macrolide arrest motif (MAM) in their amino acid sequence. For example, for telithromycin ketolide, a Lys/Arg-X-Lys/Arg motif accounts for the arrest sites in nearly 80% of the cases. Still, cladinose-containing erythromycin or azithromycin inhibit translation not only at this motif but at a wider array of MAMs (Davis, Gohara et al. 2014).

Depending on their structure, macrolides can significantly vary in their bacteriostatic or bactericidal ability (Svetlov, Vázquez-Laslop et al. 2017). Recent studies have shown that the kinetics of binding and dissociation from the ribosome rather than mere affinity is the crucial parameter distinguishing between bacteriostatic and bactericidal macrolides. For instance, drugs with extended alky-aryl side chain, such as that seen in the structure of telithromycin (Figure 1-4, number 2), exhibit much slower dissociation kinetics which correlates to their bactericidal activity. In comparison, antibiotics that do not carry such an appendage rapidly vacate the ribosome and exhibit primarily bacteriostatic action (Credito, Ednie et al. 1999).

1.3 Antibiotic Resistance: Focus on Aminoglycosides and Macrolides

1.3.1 Antibiotic Resistance is Ancient

In 1940, a few years before the widespread clinical use of penicillin, Abraham and Chain reported an *E. coli* strain that could enzymatically inactivate penicillin (Abraham and Chain 1940). The spread of resistance and the appearance of different resistant-*Staphylococcus aureus* strains was already documented by 1942 (Rammelkamp and Maxon 1942), when the first trials of penicillin in the war setting were conducted in the military hospitals in north Africa (Fraser 1984). The proportion of infections caused by these penicillin-resistant pathogens rose rapidly, and by the late 1960s, more than 80 percent of both community and hospital-acquired strains of *S. aureus* were penicillin-resistant (Lowy 2003).

The concomitant appearance of resistant pathogens with the clinical deployment of antibiotics (Figure 1-1) can be interpreted to mean that antibiotic resistance is a modern phenomenon, and it is exclusively associated with the use and/or misuse of antibiotics in humans and animals. However, as much as it might be valid for the clonal dissemination of pathogenic bacteria with resistance mechanisms related to the mutations of target molecules, the majority of antibiotic resistance are most likely cases of acquired resistance, in which acquisition of antibiotic resistance genes is mostly through lateral transfer of genes from taxonomically and ecologically distant bacteria existed thousands of years ago (Aminov and Mackie 2007, D'Costa, King et al. 2011).

1.3.2 Mechanisms of Resistance

Antibiotic resistance can appear as a result of possible modifications enforced on bacteria at three levels: (1) Alterations to the bacterial cell wall or membrane, which restrain antibiotic uptake or force its efflux, (2) Adjustments at the level of the antibiotic target, which can ultimately interfere with antibiotic binding or restore target functionality despite antibiotic binding and (3) Enzymatic-alterations to the antibiotic itself, which impedes drug-target interaction. The underlying factors for each of these modifications differ for diverse antibiotics, yet all end up with the same outcome; the appearance of resistant bacteria.

Examples on the first level of modifications can be changes that physically block the passage of the antibiotic into the cell or reduce its permeability across the outer or plasma membrane (Nikaido 1994, Delcour 2009). There are also efflux pumps as resistance factors that actively export antibiotics against their concentration gradient (Du, Wang-Kan et al. 2018),

At the second level, there are various examples of target adjustments including, changes of the pentapeptide stem of Lipid II at the outer leaflet of the cell membrane (Ahmed and Baptiste 2018), alteration of the Lipid A Component of Lipopolysaccharide (Boll, Radziejewska-Lebrecht et al. 1994), ribosomal mutations (Long and Vester 2012), ribosomal methylation (Kehrenberg, Schwarz et al. 2005), and ribosomal protection (Nguyen, Starosta et al. 2014). All of these changes can either reduce the affinity of the target to the antibiotic or sterically remove the antibiotic. In addition, there are also ribosomal protection mechanisms in which the protection factor induces conformational

changes within the ribosome that restore its functionality despite the presence of the bound antibiotic (Tomlinson, Thompson et al. 2016).

And last but not least is the enzymatic modification of antibiotics. This can be done through different mechanisms, including antibiotic acetylation (Sugantino and Roderick 2002), nucleotidylation (Morar, Bhullar et al. 2009), phosphorylation (Stogios, Cox et al. 2016), hydrolysis (Oefner, d'Arcy et al. 1990), thiolation (e.g., thiol-dependent antioxidant system (Ouyang, Li et al. 2020)), and glycosylation (Sobhanifar, Worrall et al. 2016).

The following section discusses the various resistance mechanisms for aminoglycoside and macrolide class of antibiotics which follow the three modes of alterations mentioned above.

1.3.3 Aminoglycosides Mechanisms of Resistance: Focus on Plazomicin

1.3.3.1 Change of Uptake and Efflux-mediated Resistance

Transport of aminoglycosides across the bacterial cell membrane requires energy and involves an oxygen-dependent proton motive force. Therefore, anaerobic bacteria are intrinsically resistant to aminoglycosides (Bryan and Kwan 1981). Moreover, any mutations that lead to defective electron transport chain components will confer resistance (Muir, Hanwell et al. 1981). Bacterial efflux systems that can confer resistance to aminoglycosides are few. Still, one of the main pumps in Gram-negative bacteria is a multi-drug transporter and a member of the resistance-nodulation-division (RND) family of efflux pumps. These efflux pumps have been identified in many Gram-negative bacterial species, including *E. coli*, *S. enterica*, *A. baumannii* , *P. aeruginosa*, and *Burkholderia pseudomallei* (Li, Plésiat et al. 2015).

1.3.3.2 Ribosomal Mutations

Aminoglycoside resistance can emerge from point mutations in the *rrs* gene, the coding gene for 16S rRNA. However, these mutations are not very common due to often lethal consequences. Besides, most bacterial species maintain numerous copies of rRNA genes, meaning; they need to acquire the same mutation in each rRNA of the genome to confer resistance. However, many Mycobacterium species keep just one copy of each rRNA; therefore, rRNA mutations can be an effective way to circumvent antibiotic activity (Espejo and Plaza 2018). One viable mutation that has been found in clinically isolated strains of resistant *Mycobacterium tuberculosis, M. avium, and M. abscessus* is A1408G in h44, which disrupts an essential hydrogen bond interaction between the aminoglycoside prime ring and this residue (Alangaden, Kreiswirth et al. 1998, Kim, Kim et al. 2021) (Refer to Figure 1-3). As a side remark, the substitution of guanine in this residue is one of the critical differences between prokaryotic and eukaryotic ribosomes (Recht, Douthwaite et al. 1999).

In addition to h44 mutations, mutations in ribosomal protein uS12 and uS5 can lead to streptomycin resistance in *M. tuberculosis* and spectinomycin resistance in *N. gonorrhoeae*, respectively (see Figure 1-3) (Springer, Kidan et al. 2001, Unemo, Golparian et al. 2013).

1.3.3.3 Ribosomal Methylations

Besides mutations, methylation of the 16S rRNA at the aminoglycoside binding site can also confer resistance for this class of antibiotics (except for streptomycin and spectinomycin). 16S rRNA methyltransferases (16S-RMTases) implicated in

aminoglycoside resistance are divided into two groups, N7-G1405 16S-RMTases (e.g., ArmA, RmtA) and N1-A1408 16S-RMTases (NpmA), depending on the nucleotide position to be modified at the A-site of 16S rRNA. The first group can confer resistance to 4,6-disubstituted 2-DOS, but not to 4,5-disubstituted 2-DOS aminoglycosides. However, the second group confers pan-aminoglycoside resistance to both 4,5- and 4,6-disubstituted DOS aminoglycosides. The clinical prevalence of these resistance-conferring methyltransferases is still low and exclusively limited to Gram-negative pathogens to date, but this may change (Wachino and Arakawa 2012, Doi, Wachino et al. 2016).

Studies have reported plazomicin resistance in clinical pathogens harbouring N7-G1405 16S-RMTases (Aggen, Armstrong et al. 2010, Livermore, Mushtaq et al. 2011, Castanheira, Davis et al. 2019, Galani, Nafplioti et al. 2019). These reports may seem disappointing news for the most novel aminoglycoside, but we need to consider that plazomicin was explicitly designed to overcome the action of aminoglycoside modifying enzymes discussed in the next section.

1.3.3.4 Enzymatic Alteration of Aminoglycosides

Enzymatic modification of aminoglycosides is the most prevalent mechanism of resistance in clinical settings. Aminoglycoside modifying enzymes (AMEs) catalyze the modification at different hydroxyl and amino groups of the 2-DOS nucleus or the sugar moieties. There are well more than 100 aminoglycoside modifying enzymes identified to date, which include O-nucleotidyltransferases (ANTs), O-phosphotransferases (APHs), or N-acetyltransferases (AACs) (Ramirez and Tolmasky 2010). In addition, some

examples of bifunctional enzymes have also been reported (Tenorio, Zarazaga et al. 2001, Kim, Hesek et al. 2006, Kim, Villegas-Estrada et al. 2007). Successful distribution of these enzymes among bacteria makes this resistance mechanism universal in almost all bacteria.

The Nomenclature currently in use to identify aminoglycoside modifying enzymes consists of a three-letter identifier of the activity, followed by the site of modification between parenthesis (class), a roman number particular to the resistant profile they confer to the host cells (subclass), and a low case letter that is an individual identifier (Shaw, Rather et al. 1993).

Structural modifications specific to plazomicin protect this aminoglycoside from enzymatic inactivation by several AMEs. On the 3′ and 4′ positions, removal of hydroxyl groups protects it from ANT(4′) and APH(3′). ANT(4′) impacts both amikacin and tobramycin, and APH(3′) impacts only amikacin. The addition of HE tail at its 6′ position provides protection against AAC(6′), which causes resistance to tobramycin, gentamicin, and amikacin. Lastly, the HABA tail at the N1 position blocks AAC(3) and ANT(2″), which both cause gentamicin and tobramycin resistance, and APH(2″), which causes resistance to gentamicin, tobramycin, and amikacin (Figure 1-6).

Despite its resilience towards most AMEs, plazomicin has shown to be still susceptible to the action of enzymes capable of modifying amino moieties at the 2′ position. Plazomicin was found to be inactive against a *Providencia stuartii* isolate with the AAC(2′)-Ia enzyme, concluded by elevated minimum inhibitory concentrations (MIC) (Aggen, Armstrong et al. 2010, Livermore, Mushtaq et al. 2011). AAC(2′)-Ia mediates inactivation of aminoglycosides such as tobramycin, gentamicin, and plazomicin by

catalyzing the acetylation of the 2′ amino groups of these antibiotics using acetyl-CoA (Figure 1-6). AAC(2′)-Ia is chromosomally restricted in *P. stuartii* and has not been a predominant factor in antimicrobial resistance in the past. Still, the increased use of plazomicin may expand its clinical prevalence (Bassenden, Dumalo et al. 2021).

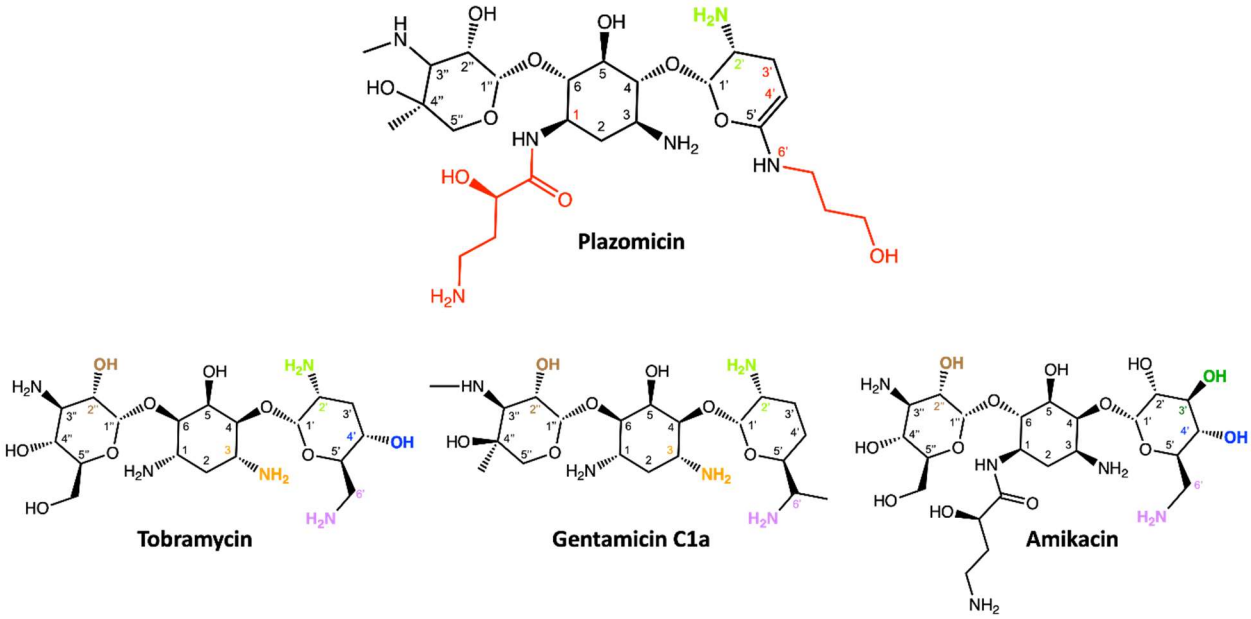

Figure 1-6. Plazomicin structure protects it from enzymatic inactivation by various AMEs. Plazomicin structure is shown in comparison with tobramycin, gentamicin C1a, and amikacin structure. Plazomicin HABA tail and HE group are shown in red. The site of modification by different AMEs is shown in different colors. ANT(4′) modification site is in blue, APH(3′) modification site is in dark green, AAC(6′) modification site is in purple, AAC(3) modification site is in orange, ANT(2″) modification site is in brown, and AAC(2′)-Ia modification site is shown in light green.

1.3.4 Macrolides Mechanisms of Resistance

1.3.4.1 Efflux-mediated Resistance

Several different families of pumps have been discovered that contribute to macrolide resistance, including the major facilitator superfamily (MFS), the ATP-binding

cassette (ABC) superfamily, the multi-drug and toxic compound extrusion (MATE) family, the resistance-nodulation-division (RND) superfamily, and the small multi-drug resistance (SMR) family (Gomes, Martínez-Puchol et al. 2017). Efflux systems in MFS and ABC and RND superfamilies can use 14- and 15-membered macrolides as substrates, including the ketolide telithromycin. Some members of MFS superfamily (e.g., EmrAB-TolC) are also active against 16-membered macrolides like josamycin (Elkins and Mullis 2007, Gomes, Martínez-Puchol et al. 2017).

1.3.4.2 Ribosome Protection

The Cryo-EM structure of one protection factor (MsrE from ABC superfamily of proteins) in complex with the 70S ribosome has revealed that this protein binds the ribosomal E-site, with its antibiotic resistance domains (ARDs) reaching into the peptidyl-transferase center (PTC) deep into the ribosomal exit tunnel. At this site, it sterically mediates the release of macrolides from the ribosome (Su, Kumar et al. 2018).

1.3.4.3 Ribosomal Mutations

Besides the ribosomal protection mechanism, there are two main types of modifications to the ribosome which mediate resistance to macrolides; mutations and methylations. Mutations of the residue A2058 (*E. coli* numbering) in the 23S rRNA to guanine, cytosine, or uracil have been reported in macrolide resistance (Refer to Figure 1-5). Furthermore, numerous other mutations have been described in both domains II and V of 23S rRNA that confer resistance to various macrolides (Pfister, Jenni et al. 2004, Tu, Blaha et al. 2005, Descours, Ginevra et al. 2017).

Mutations in some of the ribosomal proteins are also capable of conferring resistance. Specifically, alterations have been identified in the uL4 and uL22 ribosomal proteins. These alterations are single amino acid changes or could also consist of insertion/deletion of one or more amino acids to these proteins. Mutations in uL4 and uL22 have been proposed to confer resistance through changing the shape of the peptide exit tunnel and distortion of the macrolide-binding site, which results in altered binding kinetics for macrolides (Gabashvili, Gregory et al. 2001, Moore and Sauer 2008, Lovmar, Nilsson et al. 2009, Wekselman, Zimmerman et al. 2017).

1.3.4.4 Ribosomal Methylation

The most prominent type of ribosomal modification is the methylation of the 23S rRNA by the members of the Erm family of methyltransferases. These enzymes catalyze the methylation of the N6 position of residue A2058 in the 23S rRNA. Recent structural studies of the A2058-dimethylated 70S ribosome and its comparison with unmethylated structure revealed that this alteration makes the coordination of a conserved water molecule between the N6 position of A2058, phosphate of G2505, and dimethylamino group of a macrolide impossible (Svetlov, Syroegin et al. 2021). Thus, dimethylation of this residue confers high resistance to macrolides and ketolides. It is important to note that the macrolide binding site on the bacterial ribosome is also exploited by streptogramins B and lincosamides for binding and exerting an antibacterial effect. Consequently, dimethylation by Erm methyltransferases also confers high resistance to these antibiotics, though the resistance mechanism for each of these antibiotics differs at the molecular level (Roberts 2008).

1.3.4.5 Enzymatic Alteration of Macrolides

Thus far, two classes of enzymes have been identified in bacteria that confer resistance to macrolide antibiotics: macrolide phosphotransferases (MPHs) and erythromycin esterases (Eres). In addition, there is also a third class of enzymes that glycosylate various macrolides. Glycosylation of macrolides is one protection mechanism for the Streptomyces that produce these antimicrobial agents. These enzymes inactivate macrolides and hence protect the producing bacteria from their own antibacterial agents (Bolam, Roberts et al. 2007).

Erythromycin esterases cleave the macrolactone ring of macrolides by hydrolyzing its ester bond. Thus far, four members have been identified in this family named EreA, EreB, EreC, and EreD. EreA appears to be the enzyme most often identified in clinical strains such as *Pseudomonas spp*., *Vibrio cholera*, MRSA, and *Klebsiella oxytoca* and confers resistance to the majority of clinically used macrolides. In addition, the structure of one member of this family (EreC) has been published recently and provides insights into the catalytic mechanism of these enzymes (Zieliński, Park et al. 2021).

The next section focuses on macrolide phosphotransferases, which are the most prevalent resistant-conferring modifying enzymes for this class of antibiotics.

1.3.5 Macrolide Phosphotransferases

1.3.5.1 Members of the Family

The first MPH enzyme was identified in a clinical *E. coli* strain in 1988. Subsequently, it was shown that this enzyme could phosphorylate the hydroxyl group located at the 2′ position of the desosamine or mycaminose moiety of all clinically relevant macrolides (Figure 1-4) (O'Hara, Kanda et al. 1988, O'Hara, Kanda et al. 1989). The modified macrolides are no longer capable of binding effectively to the 23S rRNA of the 50S ribosomal subunit, which alters their antibiotic effects.

Following this discovery, several more enzymes have been found that show similar activity, and so far, at least 15 gene subtypes of MPHs have been reported (Kono, O'Hara et al. 1992, Kim, Baek et al. 1996, Matsuoka, Endou et al. 1998, Roberts, Sutcliffe et al. 1999, Matsuoka, Inoue et al. 2003, Schlüter, Szczepanowski et al. 2007, Roberts 2008, Pawlowski, Wang et al. 2016, Pawlowski, Westman et al. 2018).

Among the fifteen gene subtypes of MPHs, *mph*(A), (B), and (C) are encoded on mobile genetic elements and found in clinical isolates of *E. coli*, Salmonella sp., Klebsiella sp., and *S. aureus*. Six more MPHs are encoded on mobile genetic elements but have thus far only been found in non-pathogenic bacteria, such as *Exiguobacterium* and *Brachybacterium*. However, this could readily change. The remaining six mph genes are chromosomally encoded and only found in non-pathogenic bacteria, such as *Brachybacterium faecium* and *Bacillus subtilis* 168.

1.3.5.2 Brief on Structure

The first solved structures of MPH(2′)-I and MPH(2′)-II (products of *mph*(A) and *mph*(B) genes) in their apo state, in complex with GTP analogs, and in complex with several macrolides, confirmed that MPHs are members of a large superfamily that also includes eukaryotic protein kinases (ePKs) and aminoglycoside phosphotransferases (APHs) (Fong, Burk et al. 2017). The archetypal structure of the members of this superfamily is composed of an N-terminal lobe that contains a five-stranded β-sheet and C-terminal lobe that contains several α-helices. In between these two lobes is the binding site for a tri-phosphate nucleotide that is used as the phosphoryl donor. The C-terminal lobe contains the substrate-binding site, but the specific local architecture for this section can vary significantly between various members of the superfamily. For the two MPH enzymes, the architecture of their N-terminal lobe is similar to that seen for the N-terminal lobes of Ser/Thr and Tyr protein kinases, and APHs (Hon, McKay et al. 1997) (Figure 1-7). The C-terminal lobe is largely identical to those observed in a sub-family of APHs, the APH(2″) group with whom they share approximately 17% sequence identity (Shi and Berghuis 2012). On the other hand, MPHs deviate from archetypical ePKs and APHs in the region between the N- and C-terminal lobes. In ePKs and APHs, the lobes are connected by a loop, 5–12 residues in length, while in MPH (2′)-I and MPH(2′)-II the linker region is significantly longer, spanning approximately 25 residues (Fong, Burk et al. 2017).

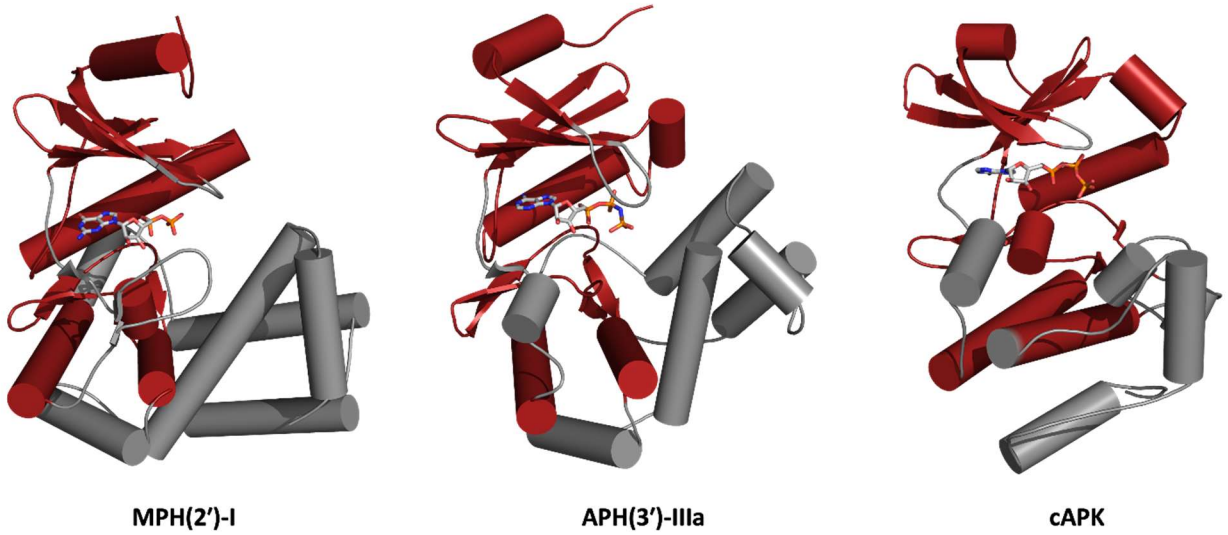

Figure 1-7. Structural homology between MPH, APH, and ePK. The structures of MPH(2′)-I (PDB: 5IGP), APH(3′)-IIIa (PDB: 3TM0), and residues 35–280 of the catalytic subunit of cAMP-dependent protein kinase (cAPK) (PDB: 1ATP) are shown. The homologous segments which are mainly seen in the N-terminal lobes of the proteins, are depicted in red.

1.3.5.3 Conservation Studies

The sequence conservation in MPHs is not extensive except for the residues required for catalysis and residues in the nucleotide-binding pocket (Figure 1-8). However, as the structures of MPH(2′)-I and MPH(2′)-II reveal, this does not impact the fold of these enzymes, as their structures are highly similar (Fong, Burk et al. 2017).

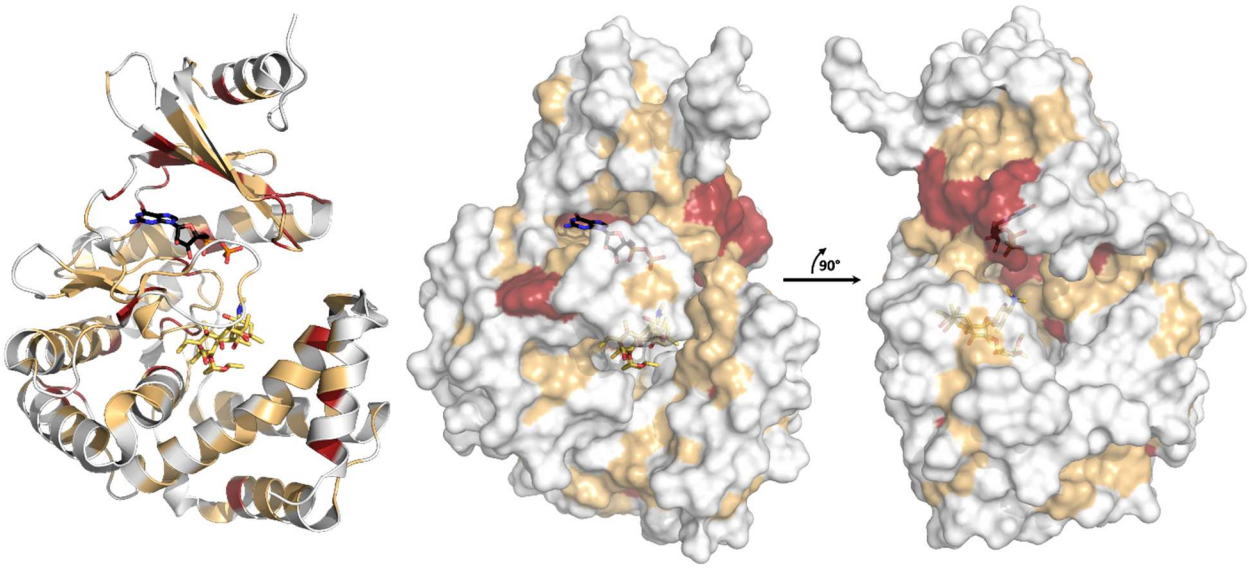

Figure 1-8. Sequence conservation of MPHs shown on MPH(2′)-I structure. The structure of MPH(2′)-I in complex with GDP (in black) and erythromycin (in yellow) is shown here (PDB: 5IGP). The color coding used illustrates sequence conservation within the 14 MPHs enzymes [only a partial sequence is available for the *mph* d gene]. Dark orange indicates completely conserved residues, light orange residues are conserved among more than seven members, and white residues are not conserved. The surface representation of the enzyme is shown in two faces.

Residue comparisons in the macrolide binding area of MPHs reveal that this site is not at all conserved (Figure 1-8). However, delving deeper into this, the chemical character of the macrolide binding pocket is similar in MPHs: generally hydrophobic with a region of negative charge around the conserved proton abstracting catalytic base (Fong, Burk et al. 2017). Structural studies of MPH(2′)-I and MPH(2′)-II showed the relatively non-specific hydrophobic nature of the macrolide binding site, and the fact that many of the interactions between the macrolides and the enzymes involve the macrolactone ring would facilitate the accommodation of a range of macrolide substrates.

1.3.5.4 Substrate Specificity

Macrolide phosphotransferases can confer resistance to a wide range of macrolide substrates, but this topic has not yet been thoroughly investigated, and much remains unknown about their substrate specificity profile. Comparing substrate specificity of the clinically relevant MPH(2′)-I and -II reveal that MPH(2′)-I can only efficiently inactivate 14- and 15-membered lactone macrolides, whereas MPH(2′)-II can additionally inactivate 16-membered lactone macrolides and the ketolide, telithromycin (Kono, O'Hara et al. 1992, Fong, Burk et al. 2017). A similar observation has been made for MPH(2′)-XII and XIII (products of *mph*(L) and *mph*(M) genes), with MPH(2′)-XII mirroring the substrate profile of MPH(2′)-I and MPH(2′)-XIII, reflecting the substrate profile of MPH(2′)-II (Wang, Sui et al. 2015). Also, MPH(2′)-III (product of *mph*(C) gene) has been shown to have the same broad substrate specificity as MPH(2′)-II (Chesneau, Tsvetkova et al. 2007).

MPH(2′)-IX (product of *mph*(I)) from the environmental bacterium *Paenibacillus sp. LC231* and MPH(2′)-XI (product of *mph*(K)) from *B. subtilis 168* are unable to confer resistance to macrolides with a C3 cladinose in cell-based assays. Although, biochemical analysis of drug modification for both enzymes showed that they can use C3 cladinose containing macrolides as substrates, but cannot inactivate 14-membered and 15-membered lactone macrolide as efficiently as macrolides without this moiety (Pawlowski, Wang et al. 2016, Pawlowski, Stogios et al. 2018). Intriguingly, MPH(2′)-X (product of *mph*(J) gene), which is a closer homolog to MPH(2′)-IX than MPH(2′)-XI, is able to effectively provide resistance to several cladinose-containing macrolides (Pawlowski, Westman et al. 2018). This observation underscores that sequence similarity among MPHs offers no indication of what the substrate profile for these enzymes might be.

1.4 Counteracting Antibiotic Resistance

1.4.1 Global Action Plan

Antimicrobial resistance (AMR) is a crisis that must be addressed with the utmost urgency as it is one of the greatest health threats we face as a global community. By looking only at part of its impacts, the data reveal that a continued rise in resistance will result in 300 million deaths over the next 30 years, and by 2050 the world's gross domestic product will be 2 to 3.5% lower than it otherwise would be. This would cost the world up to 100 trillion USD (O'Neill 2014).

To counter this crisis, the World Health Organization (WHO) set out a global multi-faceted action plan in which public education on antimicrobial resistance, research and surveillance on this topic, optimization in the consumption of antimicrobials, reduction in the incidence of infections, and sustainable investments in new medicines and diagnostic tools are targeted. As this plan emphasizes, a practical approach to overcome this plight involves coordination among numerous international sectors and actors (Mendelson and Matsoso 2015).

Following this plan, the WHO published a list of global priority pathogens with the objective of encouraging the prioritization of funding and aligning the research in the battle against resistance (Shrivastava, Shrivastava et al. 2018). These pathogens include 12 species of bacteria grouped under three priority tiers (critical, high, and medium) according to their antibiotic resistance. The Gram-negative *Acinetobacter baumannii, Pseudomonas aeruginosa, Enterobacteriaceae, Neisseria gonorrhoea, and Gram-*

positive Streptococcus pneumoniae and Staphylococcus aureus are some examples of these global priority pathogens.

Following are some available avenues in therapeutic developments that can play an essential role in controlling bacterial infections and antibiotic resistance.

1.4.2 New Antibiotics

Since the discovery of the first antibiotic, the quest to increase the number of these essential armamentaria has never stopped (Traxler and Kolter 2015). Unfortunately, the rise in the number of these drugs continued for just a few decades, and since 1987, after lipopeptides, no new class of natural products has been introduced into clinics (Hutchings, Truman et al. 2019) (Figure 1-1 and Table 1-1).

Besides the discovery approach towards new natural products, semi-synthetic innovative chemical alterations in the framework of existing antibiotics are also being pursued. Just as it was discussed for the plazomicin structure, these modifications in aminoglycosides are rationally designed to overcome the activity of different AMEs. For example, dibekacin, which is the first aminoglycoside of this kind, is a modified version of kanamycin in which the removal of the 3′-OH group block the action of APH(3′). Amikacin was also developed based on the kanamycin structure by the addition of a HABA tail on the N1 position. The substitution of this appendage prevents the binding of amikacin in the aminoglycoside-binding pocket of some AMEs (Kondo and Hotta 1999, Bassenden, Rodionov et al. 2016, Ramirez and Tolmasky 2017). The same approach has been deployed to develop next-generation macrolides, such as telithromycin ketolide with alkyl-

aryl side chain, that remain active against macrolide-resistant strains (Fernandes, Martens et al. 2017).

On this track, the idea of using fully synthetic routes to antibacterial molecules, a tried-and-tested strategy, as we discussed at the beginning of this chapter, is also being examined. There are for now only a few fully synthetic antibacterial compound classes that have found their way into clinics, such as quinolone (and later fluoroquinolone) and oxazolidinone (Lesher, Froelich et al. 1962, Slee, Wuonola et al. 1987). However, mechanisms of resistance, to an extent much greater than expected, has been seen for even these groups of drugs (Eliopoulos, Meka et al. 2004, Hernández, Sanchez et al. 2011). Recently, another team pursued a full structural exploration of the lincosamides and introduced a new class of fully synthetic compounds called oxepanoprolinamides (Mitcheltree, Pisipati et al. 2021), effective against *Enterococcus faecium*, *S. aureus*, *K. pneumoniae*, *A. baumannii*, *P. aeruginosa*, and *Enterobacter* species, the leading cause of nosocomial infections throughout the world (Santajit and Indrawattana 2016).

Antibiotic hybrids, which are defined as synthetic constructs of two antibiotic molecules that are covalently linked, represent yet another strategy towards treating drug-resistant bacteria (Gupta and Datta 2019). The most widely studied hybrid compounds contain the fluoroquinolone class of antibiotics linked to another antibacterial agent (Endres, Bassères et al. 2017). As we will discuss shortly, this approach can also be utilized to generate antibiotic-adjuvant hybrids.

1.4.3 Antibiotic Adjuvants

The concept of antibiotic adjuvants deals with the ability of a molecule to potentiate and improve the effectiveness of an antibiotic. Here, the antimicrobial drugs are combined with chemical entities which most often do not possess antimicrobial actions on their own. The adjuvant can enhance the uptake of an antibiotic (e.g., outer membrane permeabilizers (Gordon, Png et al. 2010)), suppress its efflux (e.g., efflux pump inhibitors (Van Bambeke and Lee 2006)), block the action of an enzyme that modifies the antibiotic target (e.g., methyltransferases inhibitor (Hajduk, Dinges et al. 1999)), or inhibit the activity of the antibiotic modifying enzyme (e.g., β-lactamase inhibitors). The most successful of these, so far, are β-lactamase inhibitors (Drawz, Papp-Wallace et al. 2014).

1.4.4 Innovative Therapies

Our increased understanding of the mechanisms of antibiotic resistance, bacterial pathogenesis and inter-communication have revealed more potential strategies to develop novel drugs for the treatment of bacterial infections. These promising avenues include, but are not limited to, antivirulence therapy (Rasko and Sperandio 2010), antibacterial vaccines (Priebe and Goldberg 2014, Redi, Raffaelli et al. 2018), use of antibodies or antibody-drug conjugates (Theuretzbacher and Piddock 2019), and bacteriophage therapy (Rohde, Wittmann et al. 2018).

1.5 Thesis Objectives

The body of work behind this thesis aligns with the global action plan advised by the WHO to counter antibiotic resistance. By focusing on two clinically essential classes of antibiotics, aminoglycosides and macrolides, we pursue a two-pronged approach to overcome antibiotic resistance. Firstly, we employ structural strategies to gain insight into details of antibacterial action for the most novel aminoglycoside, plazomicin. Then, we combine this knowledge with structural studies of the plazomicin clinical resistome and suggest specific structural modifications to this last-resort antibiotic to enhance its efficacy. Next, in our second approach, we direct our attention to the macrolide phosphotransferases, the most clinically critical group of macrolide modifying enzymes. Here, we explore the possibility of developing a macrolide adjuvant that can block the activity of these enzymes.

In chapter two, we focus on plazomicin and address the following questions:

- How does plazomicin, with two synthetically added tails to its structure, accommodate the bacterial ribosome and its modifying enzyme?
- How can plazomicin exert a bactericidal effect through its binding to the bacterial ribosome?
- What are the consequences of ribosome methylation and plazomicin acetylation on plazomicin binding to its target?
- What are the implications of these structural studies for any next-generation drug designs?

In chapter three, we focus on fragment-based drug design tactics to develop an adjuvant for macrolide phosphotransferases. Here we undertake the following topics:

- How can we use fragment libraries to screen for hit compounds against our targets?
- How can structural studies assist in the hit fragment(s) elaborations?
- How can enzyme kinetics guide us in the further evolution of an inhibitor?
- What are the challenges to making an inclusive inhibitor for all MPHs?
- How can the off-target effects of an inhibitor be examined?

Chapter 2 — Structural Basis for Plazomicin Antibiotic Action and Resistance

2-1 Preface

The FDA approval of plazomicin in 2018 broadened the clinical library of aminoglycosides available for use against emerging bacterial pathogens. Plazomicin was purposefully designed to counter the resistance conferred by aminoglycoside modifying enzymes and fulfilled its mission almost entirely. Nevertheless, instances of resistance have been reported in clinical settings for AAC(2′)-Ia resistance enzyme. Structural studies of plazomicin in complex with both its target and resistance factor will provide a roadmap for next-generation drug development that aims to ease the impact of antibiotic resistance.

This chapter presents the first solved crystal structure of plazomicin bound to its target, the bacterial ribosome. Moreover, the crystal structure of AAC(2′)-Ia, the only clinically reported modifying enzyme for plazomicin, bound to plazomicin is also described. This chapter provides us with structural insights into the mechanism of plazomicin action and the mechanisms of clinical resistance. The structural data reveal that plazomicin exclusively binds to the 16S ribosomal A site, where it likely interferes with the fidelity of mRNA translation. The unique extensions to the core aminoglycoside scaffold incorporated into the structure of plazomicin do not interfere with ribosome binding, which is analogously seen in the binding of this antibiotic to the AAC(2′)-Ia resistance enzyme. Furthermore, the data provide a structural rationale for resistance conferred by drug acetylation and ribosome methylation, i.e., the two mechanisms of

resistance observed clinically. Finally, the crystal structures of plazomicin in complex with both its target and the clinically relevant resistance factor provide us with suggestions for next-generation drug development.

Individual Author Contributions are as follows, with percent of overall contribution in parentheses:

Golkar,T. (50%): Experimental design; 70S ribosome purification, tRNA expression and purification, crystallization; data collection and analysis; preparation of the manuscript.

Bassenden, A. V. (25%). Experimental design; AAC(2')-Ia expression, purification and crystallization; data collection and analysis; preparation of the manuscript.

Maiti, K. and Arya, D. P. (5%): Plazomicin synthesis

Schmeing, T. M. (5%): Aid in 70S ribosome purification.

Berghuis, A.M. (15%): Supervisory guidance of experimental design; editing of the manuscript.

2-2 Introduction

It is widely recognized that antibiotic resistance poses a serious threat to global public health. The high consumption of antibiotics in our food chain and health care systems has drastically waned the effectiveness of antibacterial treatments, severely compromising our ability to manage infections (Roca, Akova et al. 2015). Despite numerous programs to reduce usage and control prescription, resistance to clinically used antibiotics remains widespread, and the number of bacterial pathogens presenting multidrug resistance continues to rise (Roca, Akova et al. 2015).

To alleviate the pressure on our current armament of antibiotics, much effort has been directed at creating new treatment options (Tacconelli, Carrara et al. 2018). The results from these efforts have thus far been limited, highlighting the difficulties in developing new antibiotics in the context of resistance (Sommer, Munck et al. 2017). However, a newly developed aminoglycoside antibiotic, plazomicin (marketed as Zemdri), was approved for clinical use by the U.S. Food and Drug Administration (FDA) in 2018; and since then, sister agencies in other countries have also approved its use. Like other aminoglycosides, plazomicin binds to the 16S rRNA at the aminoacyl-tRNA site (A-site) of the 30S ribosomal subunit, interfering with protein translation (Carter, Clemons et al. 2000, Magnet and Blanchard 2005). Plazomicin's in vitro activity displays similar MIC ranges against Gram-negative and Gram-positive bacteria as other commonly used aminoglycosides, such as gentamicin, tobramycin, and amikacin (Livermore, Mushtaq et al. 2011, Castanheira, Deshpande et al. 2018, Cox, Ejim et al. 2018, Castanheira, Davis et al. 2019, Eljaaly, Alharbi et al. 2019, Galani, Nafplioti et al. 2019, Shaeer, Zmarlicka et al. 2019, Walkty, Karlowsky et al. 2019). Clinical studies have proven plazomicin effective

in the treatment of complicated urinary tract infections and pyelonephritis (Achaogen 2018) and have shown activity against emerging clinical drug-resistant bacteria, including *Enterobacteriaceae*, *Pseudomonas aeruginosa* and *Staphylococcus* spp, such as methicillin-resistance *S. aureus* (Shaeer, Zmarlicka et al. 2019, Walkty, Karlowsky et al. 2019)

Chemically, plazomicin is derived from sisomicin, an aminoglycoside that closely resembles gentamicin, with synthetic modifications incorporated at the N1 and N6′ positions of the antibiotic (Aggen, Armstrong et al. 2010). The N1 position is extended by appending a hydroxy-aminobutyric acid (HABA) substituent, and the N6′ is modified through the addition of a hydroxyethyl (HE) substituent. The presence of these chemical alterations allows plazomicin to evade the action of nearly all clinically relevant resistance mechanisms, which are largely mediated by aminoglycoside modifying enzymes (AMEs) (Cox, Ejim et al. 2018). Notably, plazomicin is impervious to the action of AAC(3) and AAC(6′), the most common aminoglycoside acetyltransferases in *P. aeruginosa* (Poole 2005), as well as ANT(2″) and APH(2″), the most common AMEs in the *Enterobacteriaceae* family (Ramirez and Tolmasky 2010). Plazomicin also lacks hydroxyl groups at the 3′ and 4′ positions, protecting it against the activity of AMEs ANT(4′) and APH(3′) (Eljaaly, Alharbi et al. 2019). Although the chemical modifications incorporated in the structure of plazomicin substantially increase its resilience against the activities of most AMEs, this antibiotic has shown to be still susceptible to the action of enzymes capable of modifying amino moieties at the 2′ position. Specifically, AAC(2′)-Ia is reported to cause plazomicin resistance at elevated minimum inhibitory concentrations (MIC) (Livermore, Mushtaq et al. 2011). Additionally, plazomicin is incapable of circumventing

some of the target alteration mechanisms of resistance, mediated by 16S ribosomal methyltransferases (Livermore, Mushtaq et al. 2011, Castanheira, Deshpande et al. 2018, Castanheira, Davis et al. 2019, Galani, Nafplioti et al. 2019).

Here, we present the crystal structure of plazomicin bound to its target the 70S ribosome in complex with mRNA and tRNAs. This structure sheds light on the structural basis for plazomicin's antibiotic properties and provides insights into the effectiveness of target alteration-based resistance mechanisms. Additionally, the crystal structure of inactivated plazomicin in complex with AAC(2′)-Ia is presented. This structural information combined with that from the plazomicin bound ribosome provides foundational data for addressing resistance to one of the newest antibiotics presently available for clinical use.

2-3 Results

2-3-1 Structure of Plazomicin Bound to the Ribosome•mRNA•tRNAs Complex

The crystal structure of the *T. thermophilus* ribosome in complex with plazomicin was determined to 3.27 Å. The crystal form used for this was previously exploited for the elucidation of the interactions between the ribosome and several other antibiotics (Selmer, Dunham et al. 2006, Svetlov, Plessa et al. 2019) and contains two copies of the 70S ribosomes in complex with mRNA and three tRNAs in the asymmetric unit. As has been observed for the other isomorphous crystal structures (Selmer, Dunham et al. 2006, Svetlov, Plessa et al. 2019), the presented 70S ribosome complex structure does not contain two of the ribosomal proteins bL12 and bS1. Also, disorder in some of the components is noted; most relevant, the tRNA positioned in the E-site contains segments that could not be modeled due to disorder. Data collection details and final refinement statistics are given in Table 2-1.

Examination of discovery maps for the ribosome complex unambiguously identified that plazomicin binds to the highly conserved decoding region of the aminoacyl-tRNA site (A-site) on 16S rRNA in both ribosome complexes in the asymmetric unit (Figure 2-1a). Specifically, plazomicin binds in the major groove of the 16S rRNA of the small ribosomal subunit at the base of helix 44, where two conserved adenine residues at positions 1492 and 1493 (*E. coli* numbering) flip out of the helix (Figure 2-2 and Figure 2-3). This site corresponds to what had been predicted based on resistance conferred by ribosomal methyltransferases and also corresponds to where structurally related aminoglycosides interact with the bacterial ribosome (François, Russell et al. 2005). It is

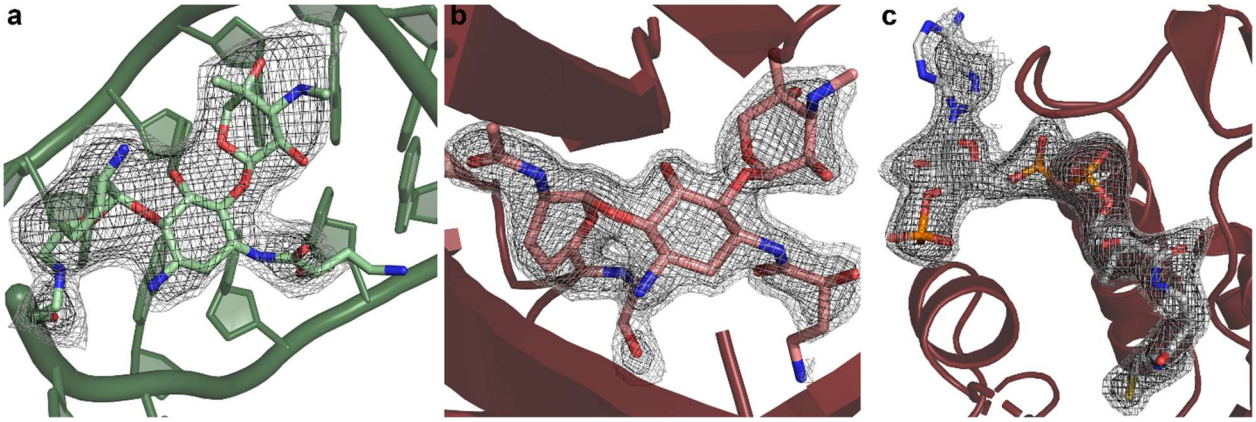

Figure 2-1. Discovery maps of ribosome and AAC(2′)-Ia ligands. (a) View of the ribosomal A-site (dark green) bound to plazomicin (light green). **(b)** View of AAC(2′)-Ia (dark red) bound to acetylated plazomicin (salmon). **(c)** View of AAC(2′)-Ia bound to CoA (light grey). The Fo-Fc discovery maps are contoured at 3σ (dark grey) and 2σ (light grey), respectively, in all panels. Note, discovery maps are calculated in the early stages of refinement, prior to the inclusion of the modelled ligands. As these maps do not contain model bias with respect to ligands, they can be used to confirm the presence of these ligands in the structure.

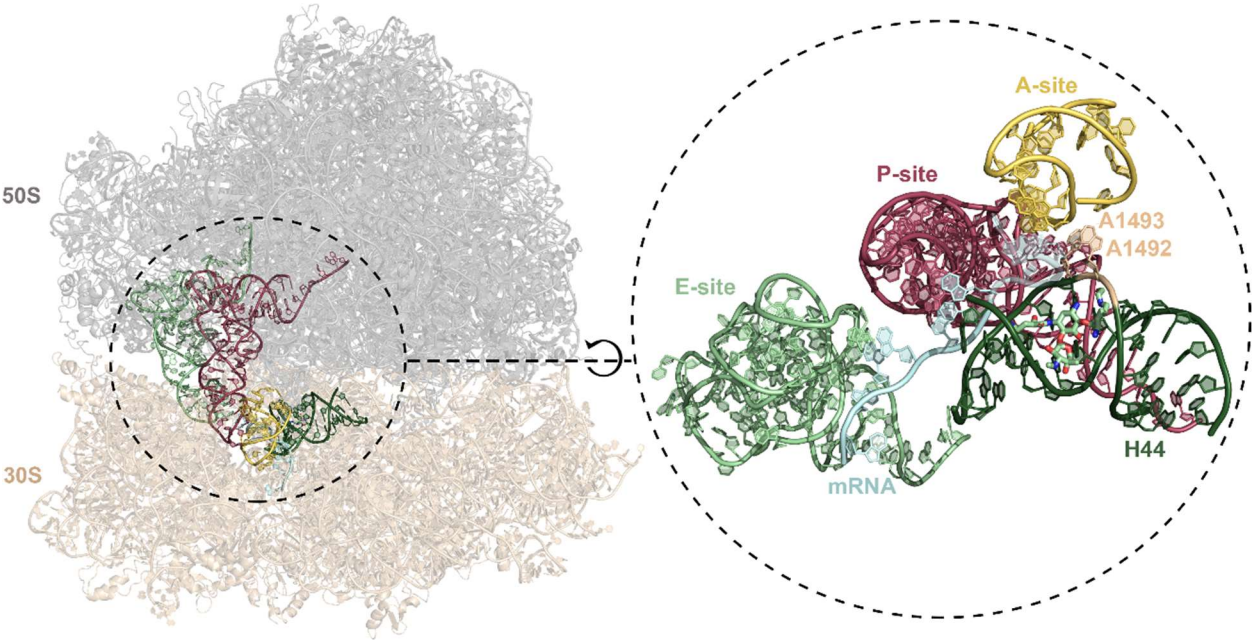

Figure 2-2. Plazomicin bound to the 70S bacterial ribosome in complex with mRNA and tRNAs. Panel insert shows details of the A-site (yellow), P-site (maroon), E-site (light green), Helix44 (dark green), H44 residues 1492 and 1493 (wheat) and mRNA (light blue), as well as the plazomicin binding site.

noteworthy that in some crystal structures of aminoglycoside ribosome complexes, a second aminoglycoside binding site has been identified, i.e., helix 69 of the 23S rRNA of the large ribosomal subunit (Borovinskaya, Pai et al. 2007). However, the structure presented here does not reveal any additional binding sites for plazomicin beyond the ribosomal A-site.

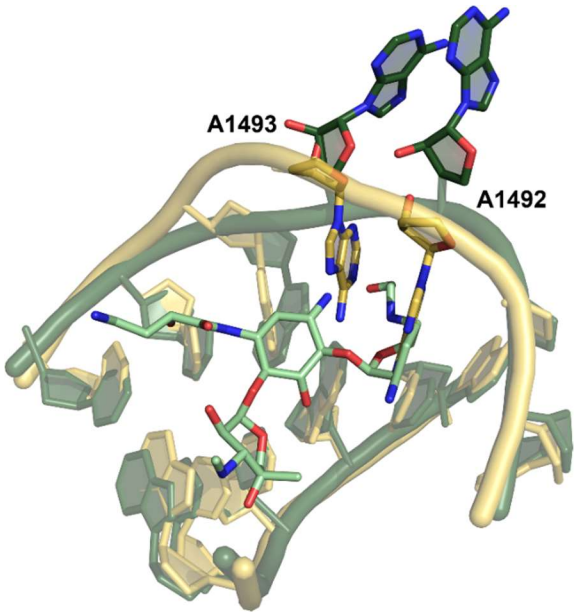

Figure 2-3. Structural comparison of apo and plazomicin-bound *T. thermophilus* ribosomal A-site. The ribosomal A-site apo structure (yellow, PDB ID: 1FKA) and the plazomicin-bound structure (dark green) are depicted, where residues A1492 and A1493 are shown in stick representation, highlighting their displacement upon plazomicin (light green) binding.

The crystal structure allowed for the identification of specific interactions between plazomicin and the rRNA (Figure 2-4a, b). The N1 and N3 amino groups on the central ring of the aminoglycoside interact with nucleotides G1494 and U1495, respectively, while the O5 hydroxyl on the central ring interacts with nucleotides C1407 and G1494. Furthermore, the synthetically added HABA tail of plazomicin forms a hydrogen bond with the uracil base of U1498. Moreover, the stacked arrangement of plazomicin's prime ring

and the purine ring of G1491 allows the hydroxyl and amino groups on the 6′-HE tail to form a pseudo-base-pair with A1408. Finally, the double-prime ring forms hydrogen bonds to the Hoogsteen sites (N7 and O6) of nucleotide G1405, as well as phosphate oxygens of U1405 and U1406.

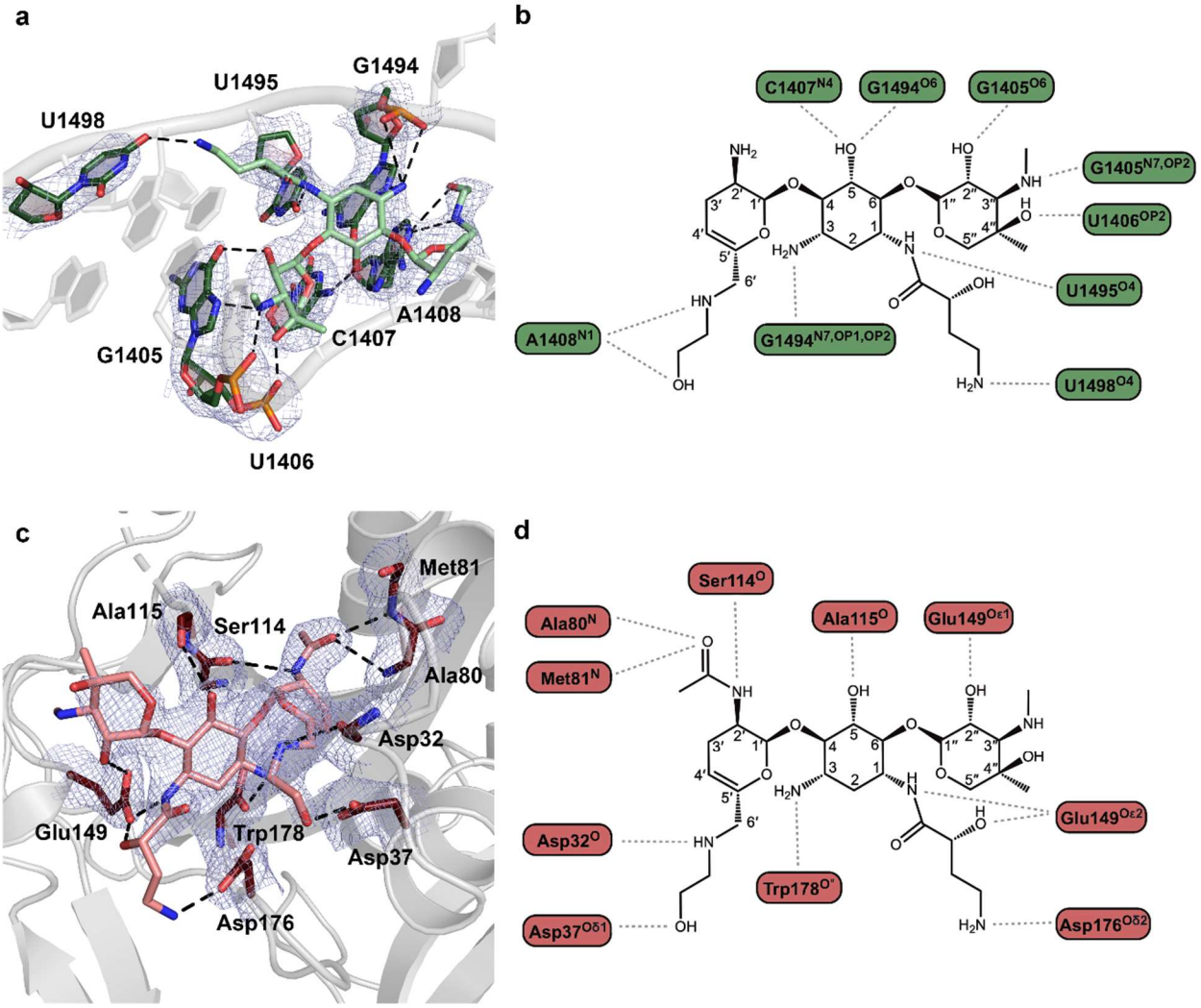

Figure 2-4. The ribosomal A-site and AAC(2′)-Ia hydrogen bond interactions with plazomicin. (a) Ribosomal A-site bases involved in interactions depicted as sticks and colored in dark green, plazomicin colored in light green. Hydrogen bonds are depicted as black dashed lines. The composite 2Fo-Fc map is contoured to 1σ and colored in blue. (b) A 2-dimensional representation of hydrogen bond interactions between plazomicin and the ribosomal A-site. (c) AAC(2′)-Ia residues involved in interactions depicted as sticks and colored in dark red, acetylated plazomicin colored in salmon. The composite 2Fo-Fc map is depicted as in (a). (d) A 2-dimensional representation of hydrogen bond interactions between acetylated-plazomicin and AAC(2′)-Ia.

A comparison of plazomicin binding to the ribosomal A-site with other related 4,6-disubstituted aminoglycosides, including gentamicin, tobramycin, and amikacin shows that the binding mode of these aminoglycosides shares many similarities. Most notably, the interactions made by the central deoxystreptamine ring are highly conserved. Moreover, plazomicin and amikacin show similar conformation in their shared HABA synthetic additions at their N1 positions. However, the conformation of the prime ring in plazomicin is slightly different from the other ribosome-bound aminoglycosides due to the contribution of the hydroxyl group on the HE tail of plazomicin in pseudo-base-pair formation between the prime ring and A1408 (Figure 2-5).

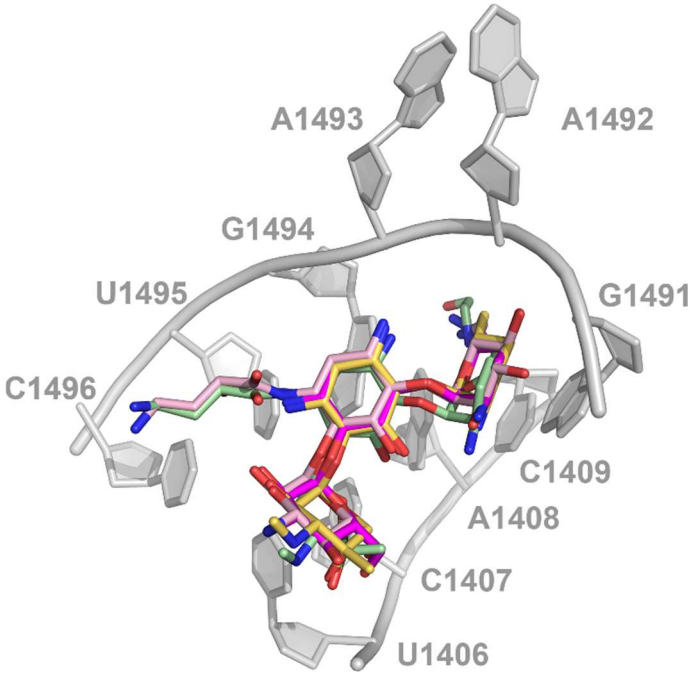

Figure 2-5. **Alignment of aminoglycosides bound to the ribosomal A-site.** Depicted are amikacin (light pink, PDB ID: 4P20), gentamicin (yellow, PDB ID: 2ET3), plazomicin (light green), and tobramycin (magenta, PDB ID: 1LC4). The ribosomal A-site is shown in grey.

2-3-2 Structure of inactivated plazomicin bound to AAC(2')-Ia

The high-resolution crystal structure of acetylated-plazomicin and CoA bound to AAC(2′)-Ia from *Providencia stuartii* was determined at 2.0 Å. The overall structure of the enzyme has been previously reported in a different crystal form with different ligands (Cox, Ejim et al. 2018). Also, we have reported structures of AAC(2′)-Ia in complex with different aminoglycosides that employ the same crystal form used here (Bassenden, Dumalo et al. 2021). As expected, there are no major differences observed in the fold of the enzyme in all of these various AAC(2′)-Ia structures. Also, the structures all confirm AAC(2′)-Ia exists as a homodimer under physiological conditions, as is anticipated for the AAC class of AMEs (Burk, Ghuman et al. 2003). The data collection details and final refinement statistics for this crystal structure are given in Table 2-1.

Crystals of AAC(2′)-Ia were grown in the presence of the substrates plazomicin and acetyl-CoA. However, discovery maps unequivocally identified the enzymatically modified plazomicin and CoA in the active site in each unit of the dimeric structure, indicating that the acetylation reaction had occurred during crystallization and that the product bound state of the enzyme was captured (Figure 2-1b, c).

The AAC(2′)-Ia plazomicin binding pocket primarily wraps around the central and prime rings of the aminoglycoside, while the double-prime ring is relatively solvent-exposed. The pattern of hydrogen bonds between AAC(2′)-Ia and acetylated-plazomicin reveals that the majority of interactions occur at the central ring and the prime ring, the latter being the site of 2′-aminoglycoside modification (Figure 2-4c, d). Although the enzyme forms few interactions with the double-prime ring of plazomicin, Glu149 forms an

interaction with the 2″-hydroxyl group of the aminoglycoside. At the central ring, the enzyme forms hydrogen-bond interactions with the 3-amine and 5-hydroxyl group of plazomicin using Trp178 and Ala115, respectively. At the prime ring, the majority of the interactions take place at the 2′-site of modification. The Ser114 interacts with the 2′-amine, while residues Ala80 and Met81 interact with the oxygen of the 2′-acetyl modification. Of particular interest is AAC(2′)-Ia's ability to accommodate the two synthetic additions of plazomicin, as it is this feature that allows the enzyme to confer resistance to the newest aminoglycoside antibiotic. The N1 HABA tail extends away from the central ring in a solvent-exposed region, though the N1 secondary amine moiety forms hydrogen bonds with Glu149 and Asp176. The N6′ HE extension sits in a crescent-shaped tunnel of the enzyme and forms hydrogen bond interactions with residues Asp32 and 37.

2-3-3 Comparison of plazomicin binding to target vs. resistance factor

There is much similarity observed in how plazomicin interacts with the ribosome in comparison with its clinically relevant resistance enzyme AAC(2′)-Ia. First, the conformation of plazomicin and the inactivated acetylated plazomicin is very similar, with the main differences being rotations of ~15-35˚ in the four glycosidic bonds that connect the prime ring and double-prime ring to the central deoxystreptamine ring, culminating in ~60˚ and ~40˚ hinge rotations for the prime and double-prime rings, respectively. Additionally, a 180˚ flip in how the HABA tail links to the N1 group is noted (Figure 2-6a). Secondly, nearly all of the hydrogen bonds formed by the latest aminoglycoside with its target are conserved in the structure of the AAC(2′)-Ia resistance factor (Figure 2-4).

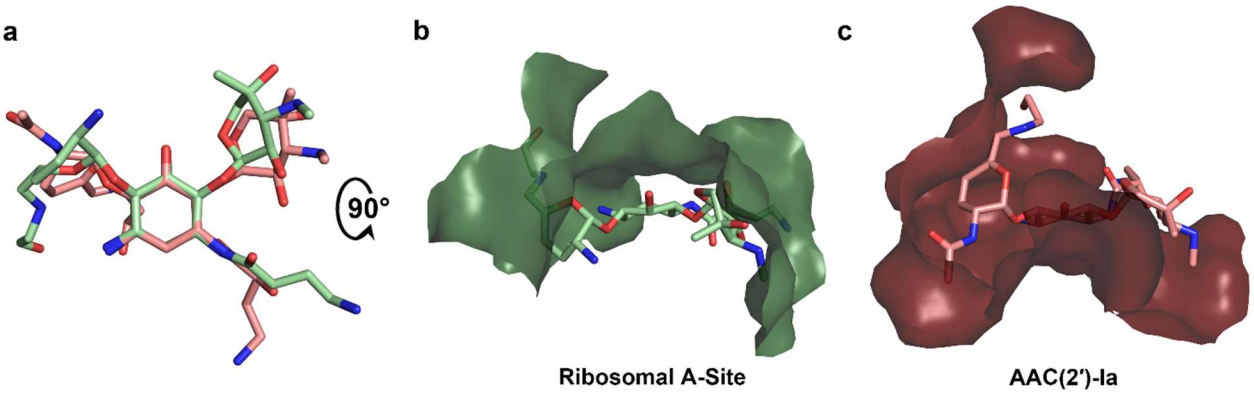

Figure 2-6. Comparison of plazomicin and acetylated-plazomicin binding to the ribosomal A-site and AAC(2′)-Ia. (a) Overlay of ribosome-bound plazomicin (light green) and the AAC(2′)-Ia-bound acetylated-plazomicin (salmon) using the aminoglycoside's central ring as the common structural motif. (b) Plazomicin binding site in the ribosomal A-site. (c) Acetylated-plazomicin binding site in AAC(2′)-Ia. Perspective is flipped 90˚ from panel (a) in panels (b) and (c). The color scheme is as per Figure 2-4.

The similarities in both aminoglycoside conformation and hydrogen bond interactions in the ribosome and various AMEs have previously been noted for naturally occurring aminoglycosides, such as kanamycin and gentamicin (Fong and Berghuis 2002, Bassenden, Rodionov et al. 2016). While there are striking similarities in the binding pose and hydrogen bond interactions, the van der Waals interactions made by plazomicin with the 16SrRNA bears little resemblance to how this same antibiotic interacts with AAC(2′)-Ia. In fact, most of the van der Waals interactions made by these two macromolecules are at opposite faces of the antibiotic (Figure 2-6b, c). Substantial differences in van der Waals interactions have also been seen when examining aminoglycoside interactions with several other AMEs (Fong and Berghuis 2002, Bassenden, Rodionov et al. 2016). Importantly, it is the substantial differences in van der Waals interactions among AMEs, specifically with respect to the ribosome, that enables plazomicin to evade resistance by, for example, AAC(3), ANT(2″) and APH(2″) (Eljaaly, Alharbi et al. 2019).

2-4 Discussion

The determination of the three-dimensional structures of both the ribosome complex and AAC(2′)-Ia bound to the newest aminoglycoside antibiotic to near-atomic resolution allows for a mechanistic analysis of how plazomicin exerts a bactericidal effect and how clinically relevant resistance is achieved. In turn, this information can be exploited for the design of next-generation aminoglycosides that are less susceptible to existing methods of resistance.

2-4-1 Mechanism of plazomicin antibiotic action

The structure of plazomicin bound to the 70S bacterial ribosome in complex with mRNA and tRNAs reveals that it specifically binds to the 16S rRNA ribosomal A-site (Figure 2-2). This site also coincides with the physiologically relevant binding site for plazomicin, confirmed by resistance-conferring ribosomal methylation sites, which all concentrate at this location (see below). The structural consequence of plazomicin binding is that bases A1492 and A1493 are extruded from helix 44 of the 16S rRNA. This conformation of the ribosomal A-site resembles the state in which the codon-anticodon helix is recognized through a minor groove interaction and enables cognate tRNA accommodation (Lescoute and Westhof 2006, Steitz 2008). Locking the ribosomal A-site in this conformational state following plazomicin binding can, therefore, induce the incorporation of near- and non-cognate tRNAs into the ribosome during the decoding process (Carter, Clemons et al. 2000). The overall impact is that the fidelity of mRNA translation is compromised through the binding of plazomicin. It has been speculated that the resultant production of aberrant proteins induces stress on bacteria, including

compromised membrane integrity, which ultimately precipitates a bactericidal effect (Krause, Serio et al. 2016). This mode of action is identical to what has been proposed for other aminoglycosides that bind to the ribosomal A-site (Carter, Clemons et al. 2000).

An additional mechanism by which aminoglycosides exert antibiotic activity has been proposed, i.e., inhibition of ribosome recycling via binding to helix 69 of the 23S rRNA (Borovinskaya, Pai et al. 2007). As mentioned above, the structure of the plazomicin-ribosome complex does not reveal aminoglycoside binding in helix 69. Moreover, modeling of plazomicin into this location based on the gentamicin binding pose reveals this to be impossible due to predicted steric clashes of the N1 HABA extension with G1910, U1911, C1920 and G1921 (Figure 2-7). Therefore, based on structural data, it is unlikely that plazomicin interferes with ribosome recycling.

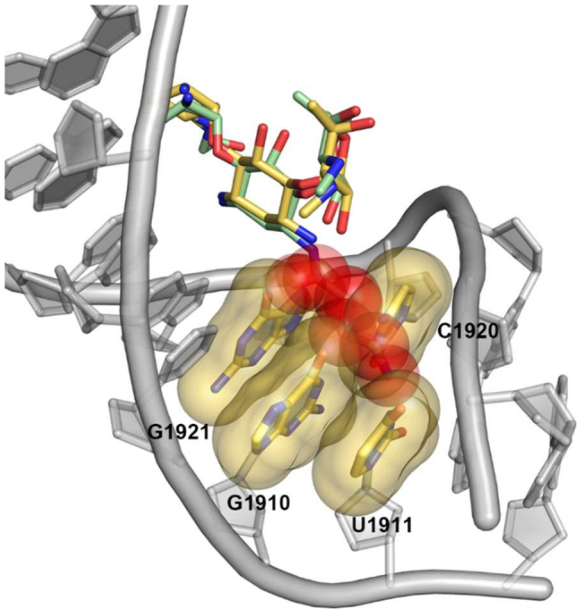

Figure 2-7. Model of plazomicin bound to helix 69 of the ribosome. Model based on gentamicin-bound structure (PDB ID: 4V53). The ribosome structure is colored in grey, and bases predicted to clash with plazomicin are colored in yellow and depicted as surfaces. Gentamicin is shown in yellow, while the modeled plazomicin is shown in light green. The HABA tail of plazomicin is shown as red spheres.

2-4-2 Mechanism of plazomicin resistance

Resistance to plazomicin has been noted through two main mechanisms: drug modification and target alteration. The clinically identified mechanism of drug modification is the acetylation of plazomicin at the 2′ position catalyzed by AAC(2′)-Ia (Aggen, Armstrong et al. 2010). Clinically observed plazomicin resistance through target alteration has been affected by ribosomal 16S rRNA methylation, specifically methylation of G1405 by enzymes such as ArmA (Castanheira, Deshpande et al. 2018).

Plazomicin acetylation – While there are well over 100 different AMEs that have been identified in pathogenic bacteria, making covalent modification of aminoglycosides the most prominent mechanism of resistance to this class of antibiotics, AAC(2′)-Ia is unique in that it is presently the only AME that can efficiently use plazomicin as a substrate (Bacot-Davis, Bassenden et al. 2016). The structure of the plazomicin enzyme complex shows the reason for this, i.e. the aminoglycoside binding pocket of AAC(2′)-Ia can accommodate both the HABA and HE extensions, while the enzyme remains perfectly poised to modify one of the functional groups on the antibiotic. Other AMEs may be able to accommodate one or both of the synthetic extensions of plazomicin, but this is invariably accompanied by a dramatic reduction in enzyme efficiency. For example, APH(2″)-Ia has been shown to accept aminoglycosides containing the HABA tail, but this coincides with a compromised ability to phosphorylate these antibiotics (Caldwell and Berghuis 2018).

The structure of the plazomicin bound ribosome complex sheds light on the consequences of 2′ acetylation for the antibiotic properties of this aminoglycoside.

Modeling of the inactivated plazomicin into the ribosomal A-site reveals that the carbonyl group of the additional acetyl moiety would inevitably cause steric clashes with O6 and/or N7 of G1491 (Figure 2-8). It is conceivable that the extent of the steric clash can be reduced by allowing for substantial conformational strain in the acetylated plazomicin structure, but the overall energetics would remain unfavourable.

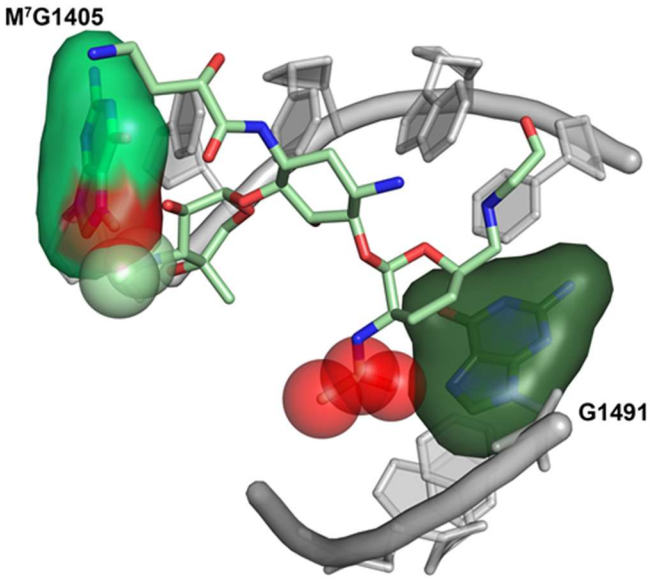

Figure 2-8. Ribosome methylation and acetylated plazomicin clashes. Methylation and acetylation sites are colored in red. M7G1405 is shown as a surface colored in neon green clashing with the 3″ group of plazomicin, shown as spheres. G1491 is shown as a surface colored in dark green clashing with the acetyl group of plazomicin, shown as spheres.

Moreover, this steric clash is aggravated by the actuality that all the groups involved in interactions are hydrogen acceptors, including G1491 N7, implying that the loss of water-mediated hydrogen bonds upon 2′-acetylated-plazomicin binding cannot be compensated by new hydrogen bonds between the acyl carbonyl group and G1491. Finally, the 2′ amino group in plazomicin is most likely protonated, creating a positive

charge at this site that forms favourable charge interactions with three negatively charged phosphate backbone groups that are positioned within 7Å. Upon acetylation, the charge on the 2′ group is removed, abolishing this favourable charge interaction. While separately the steric clash/strain, loss of hydrogen bonds, and loss of charge interactions may be insufficient to prevent binding of acetylated plazomicin; together, these three factors result in 2′-acetylation by AAC(2′)-Ia to confer resistance to plazomicin.

Ribosome Methylation – Various 16S rRNA methyltransferases mediate the methylation of the N7 position of G1405 resulting in m^7G1405, which precipitates resistance to plazomicin. Most notable is ArmA, which is found in *Enterobacteriaceae* family including *Klebsiella pneumoniae* (Castanheira, Davis et al. 2019, Galani, Nafplioti et al. 2019). The plazomicin bound ribosome complex structure, again, enables the rationalization of why the addition of a methyl group to a select RNA base confers resistance. Modeling of m^7G1405 reveals that, in addition to abolishing the potential hydrogen bond between N7 and the secondary amine on the plazomicin double-prime ring, the methylation would also create severe steric clashes with this ring (Figure 2-8). An additional aspect of methylation is that this modification introduces a positive charge within the ribosomal A-site, which is generally unfavourable for promoting interactions with aminoglycosides, given their predominantly positive charge. This charge contribution to effecting resistance echoes that of acetylation, where a positive charge on the antibiotic is removed. The modeling of the impact of the m^7G1405 alteration on resistance for other aminoglycosides that target the ribosomal A-site mirrors the explanation provided here (Juhas, Widlake et al. 2019).

2-4-3 Implications for further drug development

Much of next-generation aminoglycoside development has exploited two complementary strategies: the removal of functional groups so as to circumvent modification by AMEs, and the addition of synthetic extensions so as to interfere with AME binding. However, both strategies have caveats since many of the functional groups are required for ribosomal A-site binding, and extensions on the core chemical structure can also prevent binding to the 16S rRNA. The development of plazomicin successfully used both strategies by using sisomicin as its core, lacking functional groups on the 3′ and 4′ positions and incorporating extensions on the N1 and N6′ positions. Nonetheless, both 2′ acetylation of plazomicin and G1405 methylation cause high-level resistance.

While neither 2′ acetylation nor G1405 methylation are currently wide-spread mechanisms of aminoglycoside resistance, with continued usage of plazomicin, the incidence will inevitably rise. The three-dimensional structural data presented can provide helpful insights into the development of plazomicin derivatives with decreased susceptibility to resistance while maintaining antibiotic activity. Addressing modification of the 2′ amine group by AMEs is perhaps relatively straightforward through adding an extension at this location, analogous to how 6′ acetylation in plazomicin is prevented by the HE tail. The effectiveness of this strategy has been demonstrated in related 4,5-disubstituted aminoglycosides (Sati, Sarpe et al. 2019). Alternatively, the 2′ amine group could be substituted by a hydroxyl, as is the case in amikacin and isepamicin, for example (Figure 2-9). In theory, this substitution could be susceptible to 2′ phosphorylation or adenylation by AMEs, but enzymes with this activity have never yet been identified (Bacot-Davis, Bassenden et al. 2016). A concern with either of these approaches is that

the overall positive charge of the antibiotic is reduced, which might negatively impact the affinity for the ribosome, as has been noted in the development of other next-generation aminoglycosides (Sati, Sarpe et al. 2019). Our structural data reveals that despite the differences in van der Waals interactions between the ribosomal A-site and AAC(2′)-Ia (Figure 2-6), there are very few synthetically feasible extensions to be made to the plazomicin structure that would provide another solution for preventing 2′ acetylation. One of the possibilities might be alterations at the 4″ methyl location, which in the ribosome points away from helix 44, while in AAC(2′)-Ia an appropriate extension may create clashes with S116 (Figure 2-9).

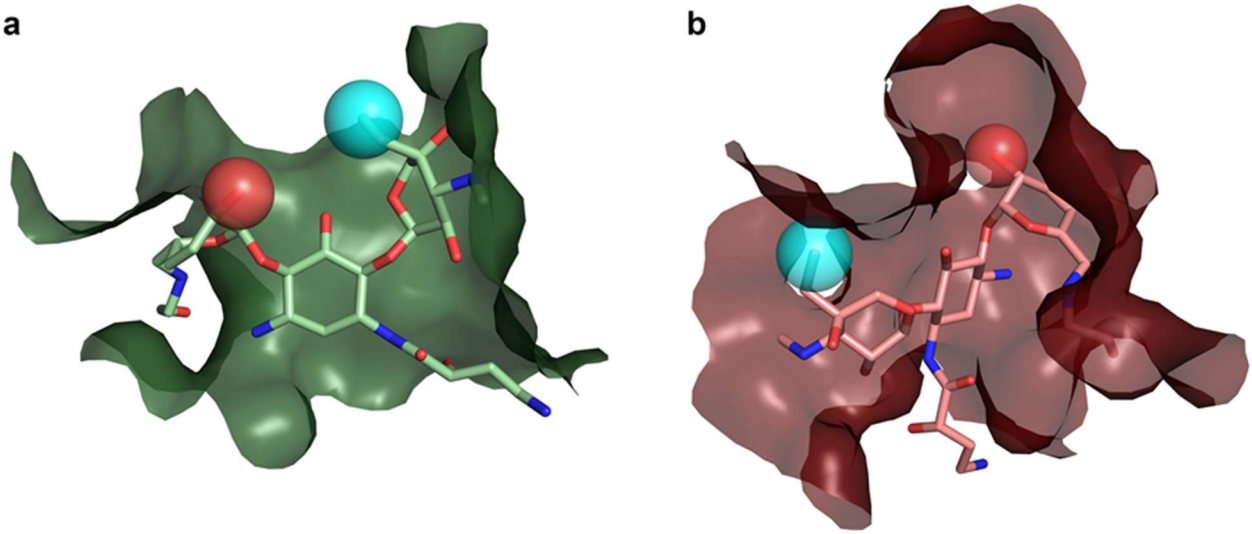

Figure 2-9. Proposed sites for next-generation aminoglycoside synthesis. Shown are (a) the ribosomal A-site plazomicin binding site, and (b) the AAC(2′)-Ia acetylated-plazomicin binding site, colored as per Figure 1. Depicted in both panels is a proposed extension to the 4″ methyl group (light blue sphere), and a proposed hydroxyl substitution at the 2′ amine (red sphere) to plazomicin for next-generation aminoglycoside design.

Addressing resistance conferred through G1405 methylation is perhaps even more challenging since this target alteration impacts binding of the plazomicin double-prime ring. There are aminoglycoside antibiotics that exploit the ribosomal A-site, which are

unaffected by the presence of an m^7G1405, i.e., 4,5-disubstituted aminoglycosides and unusual aminoglycosides such as the 4-monosubstituted apramycin. However, all of these lack the 6-linked double-prime ring. Therefore, circumventing resistance by ribosomal methyltransferases, such as ArmA and RmtA will require a core structure that considerably departs from plazomicin.

2-5 Conclusion

In summary, the structural data presented here reveals both the mechanism by which plazomicin exerts its antibiotic activity, as well as the structural basis for clinically observed resistance. The synthetic modifications made to the sisomicin scaffold afford plazomicin protection to nearly all of AMEs. However, this antibiotic is also not immune to resistance mechanisms. Our analysis reveals that further alteration to the scaffold may confer additional protection to drug modification. Unfortunately, avoiding resistance caused by target modification with the plazomicin scaffold appears unlikely. This highlights the importance of curtailing the spread of resistance while simultaneously expanding our armament of antibiotics.

2-6 Experimental Procedures

2-6-1 Plazomicin Synthesis

Synthesis of plazomicin was performed starting from commercially available sisomicin sulfate as recently reported (Sonousi, Sarpe et al. 2018) in the modified version of the original report by Moser (Aggen, Armstrong et al. 2010).

2-6-2 Ribosome Purification

70S ribosomes were purified from HB8 *Thermus thermophilus* cells using the Selmer *et al.* purification protocol, with minor modifications to the final step. Here, zonal ultracentrifugation was replaced by three steps of 10-40% sucrose gradient preparation, ultracentrifugation, and fraction collection (Selmer, Dunham et al. 2006).

2-6-3 $tRNA^{fMet}$ and $tRNA^{Phe}$ Expression

The $tRNA^{fMet2(MetY)}$ and $tRNA^{PheV}$ plasmids, encoded in pBS $tRNA^{fMet2}$ and pBSTNAV2/$tRNA^{PheV}$, respectively, were generously provided by Ramakrishnan Lab (MRC laboratory of molecular biology, UK) and Innis Lab (European Institute of Chemistry and Biology, France). The vectors were used to transform HMS174(DE3) competent cells. Cells were subsequently grown in 2YT medium at 37 ˚C for approximately 20 hours. Cells were then harvested by centrifugation at 6000g for 15 minutes at 4˚C and resuspended in 1 mM TRIS-HCl, pH 7.5, and 10 mM magnesium acetate. The $tRNA^{bulk}$ was extracted by organic RNA extraction method using a phenol solution saturated with o.1 M citrate buffer, pH 4.3 (Zubay 1962). Amino acids bound to tRNA were removed by incubation in 1.5 M TRIS-HCl, pH 8.8, at 37° C for 2 hours.

2-6-4 tRNA^{fMet} Purification

The extracted tRNA^{bulk} was applied to a series of four HiTrap™ Q HP 5 mL columns (Cytiva) equilibrated in 20 mM TRIS-HCl, pH 7.5, 8 mM $MgCl_2$, 200 mM NaCl, and 0.1 mM EDTA and eluted using a 20-35% gradient of equilibration buffer supplemented with 1 M NaCl (Guillon, Meinnel et al. 1992). tRNA^{fMet} fractions were identified using urea-PAGE and pooled. Pure tRNA^{fMet} was concentrated to approximately 100-150 µM and exchanged into a final storage buffer consisting of 10 mM ammonium acetate, pH 5.0, and 50 mM KCl using Amicon® concentrators. tRNA^{fMet} was subsequently flash-frozen and stored at -80 ˚C until further use for complex formation.

2-6-5 tRNA^{Phe} Purification

tRNA^{Phe} was purified using the Junemann and Cayama methods (Jünemann, Wadzack et al. 1996, Cayama, Yépez et al. 2000). Briefly, tRNA^{bulk} peak fractions from the anion-exchanged material were pooled and applied to the HiPrep™ Phenyl HP 16/10 column (Cytiva) equilibrated in 50 mM ammonium acetate, pH 5.3, 10 mM magnesium acetate, and 1.5 M ammonium sulfate and eluted using the same buffer in the absence of ammonium sulfate. Peak fractions containing tRNA^{Phe} were identified using urea-PAGE and pooled. The resulting material was then applied on a Symmetry300™ C4 (Waters) column equilibrated in 10 mM ammonium acetate, pH 5.5, 10 mM magnesium acetate, and 400 mM NaCl and eluted using equilibration buffer supplemented with 60% Methanol. tRNA^{Phe} was then precipitated using 3 M sodium acetate and 100% ice-cold ethanol in a 1:25 ratio. Pure tRNA^{Phe} was buffer exchanged, concentrated, and stored as described for tRNA^{fMet}.

2-6-6 mRNA Synthesis

The mRNA oligos with the sequence 5′-GGCAAGGAGGUAAAAAUGUUCUAA-3′ were chemically synthesized by Integrated DNA Technologies (Coralville, IA). The codons for $tRNA^{fMet}$ and $tRNA^{Phe}$ are underlined.

2-6-7 Ribosome Complex-Formation

Ribosome-mRNA-tRNA complexes were formed following Polikanov *et al.* method (Polikanov, Osterman et al. 2014, Polikanov, Szal et al. 2014). Plazomicin was added to this complex with the final concentration of 125 μM during a 10-minute equilibration step executed at 37° C.

2-6-8 Ribosome Crystallization

Crystals of the 70S ribosome complex were grown at 19-21°C using the sitting-drop vapour diffusion method. Drops contained a 1:1 ratio of the 70S ribosome complex and reservoir solution consisting of 100 mM TRIS-HCl, pH 7.6, 3-3.2% (w/v) PEG 20K, 7-12% (v/v) MPD, 100-200 mM arginine, and 0.5 mM β-mercaptoethanol. Crystals were sequentially transferred into a cryo-protecting solution consisting of 100 mM TRIS-HCl, pH 7.6, 3.2% PEG 20K, 10 mM magnesium acetate, 10 mM NH_4Cl, 50 mM KCl, 6 mM BME, and 40% (v/v) MPD and flash-frozen in liquid nitrogen.

2-6-9 Ribosome Data Collection, Structure Solution and Refinement

Diffraction data for optimized crystals of the 70S ribosome complex were collected at CMCF beamline 08ID-1 at the Canadian Light Source (100 K, 0.97857 Å). The dataset

was then processed using the *xia2* pipeline (Winter 2010), [*DIALS* (Winter, Waterman et al. 2018)]. The structure was determined using Fourier synthesis performed by *phenix.refine* (Adams, Afonine et al. 2010) using a previously solved 70S ribosome complex bound to paromomycin (PDB ID: 4V51) stripped of all non-protein and -RNA atoms. The structure was then refined by iterative cycles of reciprocal-space refinement with *phenix.refine* and real-space refinement and model building in *Coot* (Emsley, Lohkamp et al. 2010). The ligand restraints for plazomicin were generated using *eLBOW* (Moriarty, Grosse-Kunstleve et al. 2009). The missing bL36, uL10, and uL11 proteins from 4V51 were modelled using a second 70S ribosome complex (PDB ID: 4V5P). Final Ramachandran statistics are as follows: 67.3% favored, 13.0% outliers. The data collection and final refinement statistics of the model are listed in Table 2-1.

The final structure consists of the entire 70S ribosome in complex with its tRNA and mRNA ligands (except for the bL12 and bS1). The E-site is occupied with a noncognate tRNA, and the decoding region of the A-site is occupied by plazomicin. uL1, bL25, bL31 and uS2 were either poorly ordered or completely disordered.

2-6-10 AAC(2')-Ia Cloning

The *aac(2')-Ia* gene from *Providencia stuartii* was synthesized and subcloned into pET-15b expression vector between the *NdeI* and *BamHI* restriction sites with an N-terminal HIS-tag followed by a thrombin cleavage site and verified by DNA sequencing using the BioBasic Inc. gene synthesis service. The resulting vector was used to transform *E. coli* BL21(DE3) cells.

2-6-11 AAC(2')-Ia Expression and Purification

Protein expression was carried out using the Studier method for auto-induction, as previously described (Studier 2005, Bassenden, Rodionov et al. 2016). Cells were then harvested by centrifugation at 6000g for 15 minutes at 4˚C and resuspended in 40 mL of lysis buffer containing 50 mM TRIS-HCl, pH 8.0, 200 mM NaCl, 10 mM β-mercaptoethanol, 10% (v/v) glycerol and one EDTA-free protease inhibitor tablet (Roche). Cells were then lysed by sonication, and cell debris was subsequently removed by centrifugation at 50000g for 30 minutes at 4˚C. The supernatant was further clarified by filtration through a 0.22 µm syringe-driven filter. The resulting material was applied on a 26mm i.d.x50mm Ni-IDA-Sepharose® column equilibrated in 50 mM TRIS-HCl, pH 8.0, 200 mM NaCl, 10 mM β-mercaptoethanol, 10% (v/v) glycerol and eluted stepwise with starting buffer supplemented with 150 mM imidazole. AAC(2′)-Ia containing fractions were identified by SDS-PAGE and pooled. 50 µL of 1 unit μL^{-1} Thrombin was added to the pool and incubated overnight at 22˚C to remove the N-terminal HIS-tag. The pool was then applied on a HiTrap™ Benzamidine FF column (Cytiva) attached in series with the Ni-IDA-Sepharose® column equilibrated in the aforementioned buffer to remove thrombin and the HIS-tag from the AAC(2′)-Ia sample. AAC(2′)-Ia fractions were desalted on HiPrep 26/10 Desalting column (Cytiva) equilibrated in 25 mM BIS-TRIS propane pH 7.5, 10 mM β-mercaptoethanol and 10% (v/v) glycerol. The desalted material was applied on DEAE Sepharose® FF 26mm i.d. x 140mm column equilibrated in the identical buffer and eluted with 0–400 mM NaCl gradient over 16 column volumes. Peak fractions from the DEAE column were pooled, and buffer exchange was then performed on the same desalting column equilibrated in the final storage buffer consisting of 10 mM HEPES, pH

6.6, and 1 mM TRIS (2-carboxyethyl) phosphine hydrochloride (TCEP). AAC(2′)-Ia was then concentrated to 10 mg mL^{-1} and stored at 4˚C. Lastly, the enzymatic activity of the purified AAC(2′)-Ia was confirmed using a previously established assay (Serpersu, Özen et al. 2008).

2-6-12 AAC(2')-Ia Crystallization

Crystals of the AAC(2′)-Ia-acetylated plazomicin-CoA complex were grown at 4˚C using the sitting-drop vapour diffusion method. Drops contained a 1:1 ratio of 10 mg mL^{-1} of AAC(2′)-Ia in storage buffer supplemented with 10 mM acetyl-CoA and 10 mM plazomicin. Crystals of the AAC(2′)-Ia complex grew when reservoir solution consisted of 0.2 M LiCl and 40% (v/v) MPD.

2-6-13 AAC(2')-Ia Data collection, Structure Solution and Refinement

Diffraction data for optimized crystals of the AAC(2′)-Ia-acetylated plazomicin-CoA complex were collected at CMCF beamline 08ID-1 at the Canadian Light Source (100 K, 0.97857 Å). The dataset was then processed using the *xia2* pipeline (Winter 2010), [*CCP4* (Collaborative 1994)*, POINTLESS* (Evans 2006)*, XDS* (Kabsch 2010)]. The structure was determined using Fourier synthesis performed by *phenix.refine (Adams, Afonine et al. 2010)* using a concurrently solved acetylated netilmicin-CoA complex stripped of all non-protein atoms. The structure was then refined by iterative cycles of reciprocal-space refinement with *phenix.refine* and real-space refinement and model building in *Coot* (Emsley, Lohkamp et al. 2010). The ligand restraints for CoA and acetylated plazomicin were generated using *eLBOW* (Moriarty, Grosse-Kunstleve et al.

2009). Final Ramachandran statistics are as follows: 98.2% favored, no outliers. The data collection and final refinement statistics of the model are listed in Table 2-1.

Table 2-1 Data collection and refinement statistics of plazomicin bound to 70S ribosome and AAC(2′)-Ia.

	T. thermophilus Ribosome • tRNAs • mRNA • Plazomicin	AAC(2′)-Ia • CoA • Acetylated Plazomicin
Data collection		
Space group	P 21 21 21	P 32 2 1
Cell dimensions		
***a*, *b*, *c* (Å)**	209.5, 449.4, 619.6	73.5, 73.5 147.1
α , β , γ (°)	90, 90, 90	90, 90, 120
Resolution (Å)	127.5-3.27 (3.38-3.27)*	58.43-1.95 (2.02-1.95)
R_{merge}	0.214 (1.27)	0.052 (0.96)
I / σ	5.94 (1.2)	18.9 (2.1)
Completeness (%)	99.7 (97.5)	98.8 (97.5)
Redundancy	6.5 (5.4)	8.1 (7.0)
Refinement		
Total no. reflections	5816392 (463077)	273465 (23176)
R_{work} / R_{free}	0.214 / 0.277	0.192 /0.225
No. atoms	296449	3096
Macromolecules	294983	2756
Ligand/ion	1464	224
Water	2	116
***B*-factors (Å²)**	86.8	48.9
Macromolecules	87.0	46.9
Ligand/ion	61.7	58.0
Water	56.9	47.4
R.m.s. deviations		
Bond lengths (Å)	0.012	0.006
Bond angles (°)	1.82	0.80

One crystal used for data collection of each structure. *Values in parentheses are for the highest-resolution shell.

Chapter 3 — Inhibitor Development Against Kinases Involved in Macrolide Resistance

3-1 Preface

In the previous chapter, we aimed at contributing to the development of next-generation aminoglycosides through structural studies of the antibiotic in complex with the target, the bacterial ribosome, and the resistance factor. This structure-guided design of next-generation antibiotics represents one approach in our quest to negate antibiotic resistance. In our second approach, we focus on the resistance factor itself with the aim to abrogate its activity. Adopting this strategy, we expect to restore antibiotic sensitivity to the resistant bacteria.

In this chapter, we describe our endeavors to develop an inhibitor against phosphotransferases that confer resistance to the macrolide class of antibiotics. Using fragment-based drug design tactics, ligand-based NMR screening and X-ray crystallography, we present a crystal structure of a hit fragment and its structurally-designed variant (ABG-1) bound to MPH(2′)-I. Inhibition studies of ABG-1 define it as a GTP-competitive inhibitor for both MPH(2′)-I and MPH(2′)-II enzymes. Also, comparison of the inhibition constant for the hit fragment and ABG-1, points to the success of our elaboration strategies for it. Furthermore, we present conservation studies on the residues that encompass the binding pocket of ABG-1. These studies propose ABG-1's potential to act as an inclusive inhibitor towards all reported macrolide

phosphotransferases. Finally, the off-target activity for this molecule was explored by applying structural modeling on a few eukaryotic GTP-binding proteins.

Adapted from Golkar, T., Courtemanche, D., Sprules, T., Blanchet, J., and Berghuis A. M. (2022)." Inhibitor Development Against Kinases Involved in Macrolide Resistance." *Manuscript in preparation.*

Individual Author Contributions are as follows, with percent of overall contribution in parentheses:

Golkar,T. (65%): Experimental design; NMR studies; protein purification and crystallization; data collection and analysis; preparation of the manuscript.

Courtemanche, D. (10%): Performing steady-state kinetics.

Sprules, T. (5%): NMR experimental design.

Blanchet, J. (5%): Aid in protein purification.

Berghuis, A.M. (15%): Supervisory guidance of experimental design; editing of the manuscript.

3-2 Introduction

Antibiotic resistance is one of the most pressing challenges to global health. In 2019, the World Health Organization (WHO) declared it as one of the top 10 public health threats facing humanity (WHO 2021). Bacterial isolates resistant to all antibiotics available for clinical use have been reported. Pan drug-resistant bacteria include, but are not limited to, *Klebsiella pneumoniae*, *Pseudomonas aeruginosa,* and *Acinetobacter baumannii* (Chen 2017, Lim, Chua et al. 2018, Nichols 2019) and may represent a prelude to a post-antibiotic era, in which minor injuries and common infections pose a lethal threat.

At the same time, the evolution of antibiotic-resistant bacteria seems inevitable. Phylogenetic insights and metagenomic analyses into the evolution and diversity of several antibiotic resistance genes indicate that at least some of these genes have a long evolutionary history of diversification. These studies imply that antibiotic resistance is a natural phenomenon that predates the modern selective pressure of clinical antibiotic use and began well before the antibiotic era (D'Costa, King et al. 2011). However, it is undeniable that the ever-increasing production and consumption of existing antibiotics for different purposes, including the controversial practice of feeding them to food-production animals at subtherapeutic levels for growth promotion, contribute an evolutionary factor to the dissemination of antibiotic resistance genes (Aminov and Mackie 2007).

Considering these facts, overcoming antibiotic resistance may be difficult, if not impossible, to achieve. Nevertheless, approaches to minimize the impacts of resistance are currently being pursued, and development of antibiotic adjuvants is one of them. These drugs can inhibit resistance mechanisms and thus potentiate already existing antibiotics (Bernal, Molina-Santiago et al. 2013, Melander and Melander 2017, Douafer,

Andrieu et al. 2019). Successful advancements in β-lactamase inhibitors as adjuvants to the β-lactam class of antibiotics is one promising example of this group of drugs, where enzymatic activity of a resistance-inducing antibiotic modifying enzyme is targeted (Yahav, Giske et al. 2020).

In this study, we follow along the same path for the macrolide class of antibiotics. Macrolides are among the most prescribed antibiotics and have a wide range of activity towards Gram-positive (e.g., *Streptococcus pneumoniae, Streptococcus pyogenes*, *Staphylococcus aureus*), some Gram-negative (e.g., *Haemophilus influenzae, Moraxella catarrhalis*), as well as atypical pathogens (e.g., *Chlamydia trachomatis, Treponema pallidum*, *Mycoplasma pneumoniae).* Given their extensive use, dissemination of antibiotic-resistant genes and spread of pathogenic bacteria that have become resistant to them, were expected (Zhanel, Dueck et al. 2001, Zuckerman, Qamar et al. 2011).

As our target enzymes, we have chosen the two main clinically relevant macrolide phosphotransferases (MPHs), MPH(2′)-I and -II. These enzymes mediate the transfer of the γ-phosphate group from GTP onto the 2′-OH group of macrolide substrates. The modified macrolides are no longer capable of binding effectively to the 50S ribosomal subunit and are thus unable to exert their antibiotic effect. (Fyfe, Grossman et al. 2016, Fong, Burk et al. 2017, Golkar, Zieliński et al. 2018, Gomes, Ruiz-Roldán et al. 2019).

The feasibility of developing an inhibitor for MPHs can be justified by the accomplishments achieved in the field of inhibitor development for eukaryotic protein kinases (ePKs) (Melnikova and Golden 2004, Attwood, Fabbro et al. 2021), considering that ePKs have striking structural similarities to macrolide (and aminoglycoside)

phosphotransferases (Martin, Jullien et al. 1988, Hon, McKay et al. 1997, Fong, Burk et al. 2017). Additionally, these structural similarities provoked the idea of repurposing ATP competitive kinase inhibitors against these antibiotic kinases, and several known ATP competitive inhibitors of ePKs were assayed for their activity toward aminoglycoside phosphotransferases (APHs). Isoquinoline sulfonamide derivatives, notably CKI-7, were among the first compounds discovered to inhibit some APHs, such as APH(3′)-IIIa (Daigle, McKay et al. 1997, Fong, Xiong et al. 2011, Shi, Caldwell et al. 2013). Likewise, a library of 80 chemically diverse protein kinase inhibitors was also tested in a high throughput manner against MPHs and APHs. This screening study clearly showed that although some of the inhibitors can be used against ATP-binding APHs, none were capable against MPHs, which are GTP-kinases (Shakya, Stogios et al. 2011).

Here, we utilize a fragment-based drug discovery approach (Murray and Rees 2009, Li 2020) to develop a GTP-competitive inhibitor for MPH(2′)-I and -II. The nucleotide-binding pocket of these enzymes is targeted as this area is the most conserved region among MPH enzymes (Golkar, Zieliński et al. 2018). We report, here, high-resolution crystal structures of a hit fragment and elaborated variant of this hit fragment (called ABG-1) in the GTP-binding pocket of MPH(2′)-I. As expected based on our structures, Inhibition studies of the hit fragment and ABG-1 revealed a significant increase in the inhibition constant for ABG-1 compared to the original hit fragment. These studies also confirmed ABG-1 as a GTP-competitive inhibitor for MPH(2′)-I and MPH(2′)-II enzymes. In addition, based on conservation analyses on 14 subtypes of MPHs for the residues surrounding the binding pocket, the elaborated variant of the hit fragment may be used as an all-inclusive framework for MPH enzymes' inhibition. Furthermore,

modeling studies on nine eukaryotic GTP-binding proteins present encouraging results in eliminating concerns over off-target effects for this molecule.

3-3 Results and Discussions

3-3-1 Fragment screening with ligand-based NMR spectroscopy and binder identification

MPH(2′)-I and MPH(2′)-II were screened against an in-house fragment library composed of 257 compounds grouped into 34 cocktails (see Appendix) using Water-Ligand Observed via Gradient SpectroscopY (WaterLOGSY) (Dalvit, Fogliatto et al. 2001) and Saturation Transfer Difference (STD) experiments (Mayer and Meyer 2001). Although STD experiments were done on all cocktails, among cocktails that contain fragments with binding affinity signals to MPH(2′)-I and MPH(2′)-II, there were only two cocktails with both STD and WaterLOGSY positive results. The rest were only positive for WaterLOGSY experiments. Inconsistencies between data obtained by STD vs. WaterLOGSY have been reported, and this has largely been attributed to WaterLOGSY being a more sensitive technique (Antanasijevic, Ramirez et al. 2014, Antanasijevic, Kingsley et al. 2016, Chu, Zhou et al. 2017); therefore, we decided to pursue the results of the WaterLOGSY experiments.

The cocktails with the positive WaterLOGSY binding spectra for both MPH(2′)-I and MPH(2′)-II enzymes were selected. Further, 1D proton spectra of the compounds in each of these cocktails were compared to the WaterLOGSY positive peaks to distinguish the candidate binder and 16 candidate binders were characterized (Figure 3-1 and 3-2).

3-3-2 Potential GTP-pocket binders' characterization

The previous experiments did not provide information on the possible binding sites for the characterized 16 candidate binders. As mentioned before, as we aim to develop

an effective inhibitor against all macrolide phosphotransferases, we need to target the GTP-binding pocket of these enzymes. Hence, 'GTP-binding pocket' binders were identified using competition WaterLOGSY experiments at the next step. These experiments were carried out using guanosine and each candidate binder on MPH(2′)-I. Our interpretation strategy for competition experiments is shown in Figure 3-3. If both the candidate binder and guanosine showed binding spectra in the WaterLOGSY experiment, this binder is not in competition with guanosine for the GTP-binding pocket and potentially binds somewhere else. On the other hand, if guanosine spectra turn out to be the only binding spectra, then the binder competes with guanosine. Out of sixteen, four of these binders showed a competing nature with guanosine (Figure 3-2).

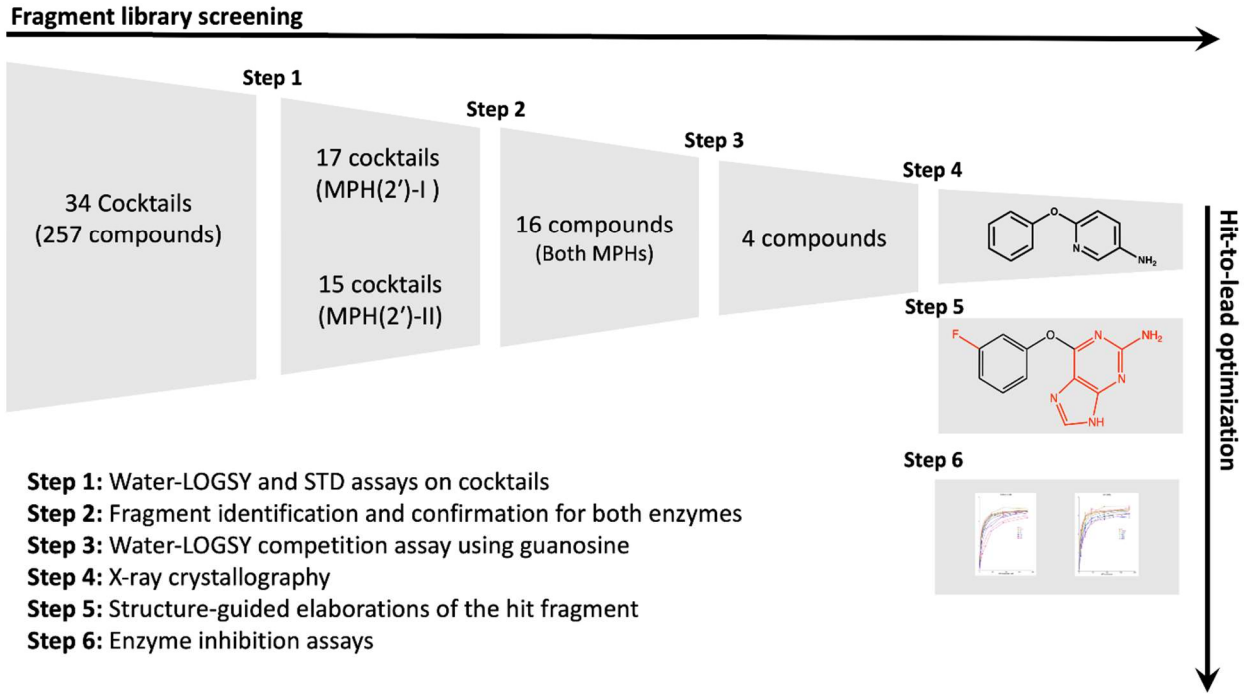

Figure 3-1. Overview of the scheme followed for fragment screening and elaboration.

The four selected fragments displayed binding spectra for both MPH(2′)-I and MPH(2′)-II enzymes in the previous experiments. As a result, we are confident that they are ‘GTP-pocket’ binders for both proteins.

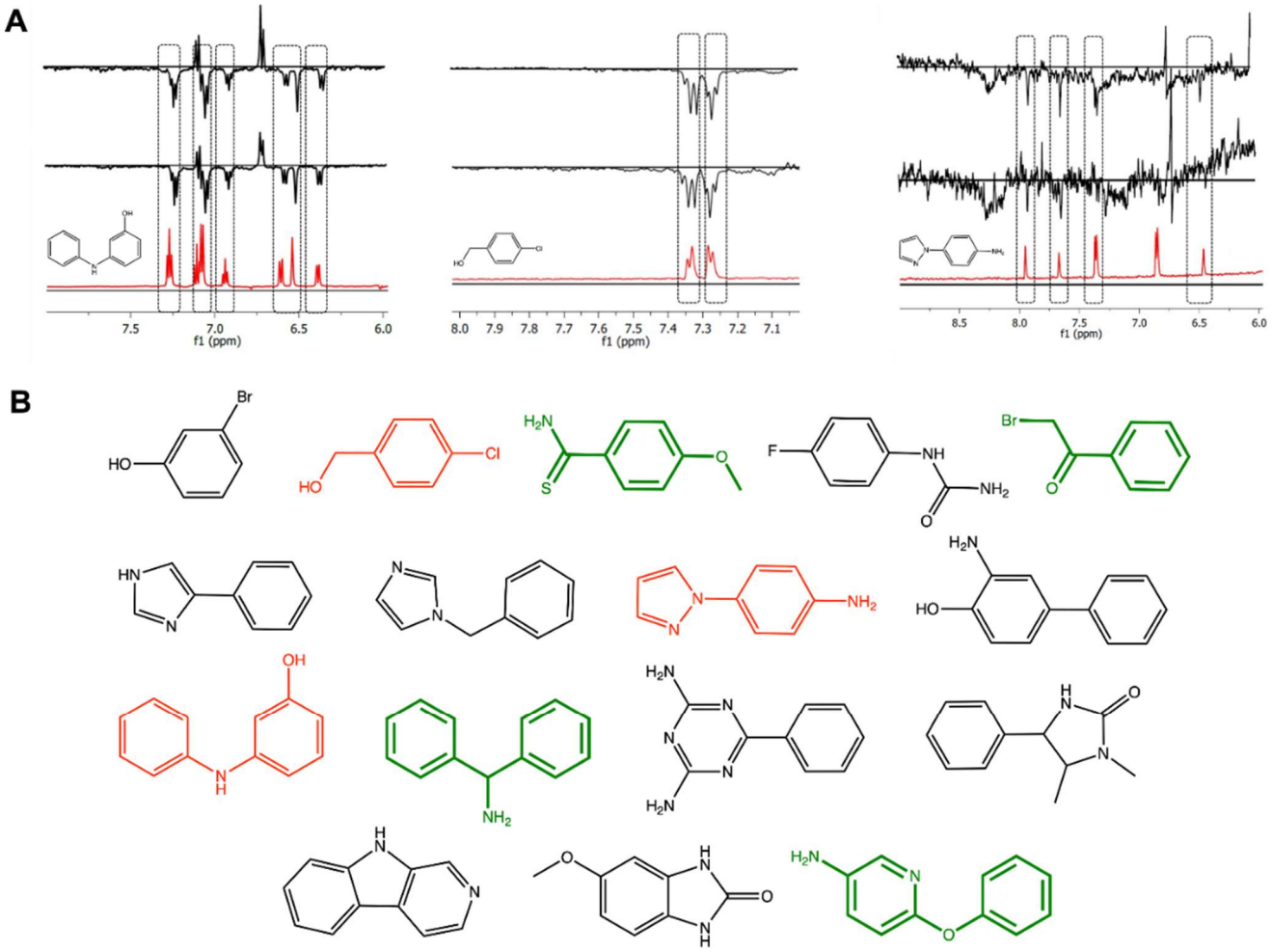

Figure 3-2. **Binder identification on positive cocktails.** Binding spectra are defined as negative peaks for WaterLOGSY experiments. **(A)** For all three examples, MPH(2′)-I WaterLOGSY proton spectrum of the cocktail is shown on top. MPH(2′)-II WaterLOGSY proton spectrum of the cocktail is shown in the middle and the compound 1D proton spectrum is shown at the bottom. Binding spectra of cocktail 18 are shown on the left, cocktail 31 in the middle, and cocktail 29 on the right. **(B)** The 16 candidate binders that characterized following the previous procedure. The three red fragments are the ones shown as an example in (A). the four bolded green binders are the ‘GTP-pocket’ binders identified following WaterLOGSY competition assays.

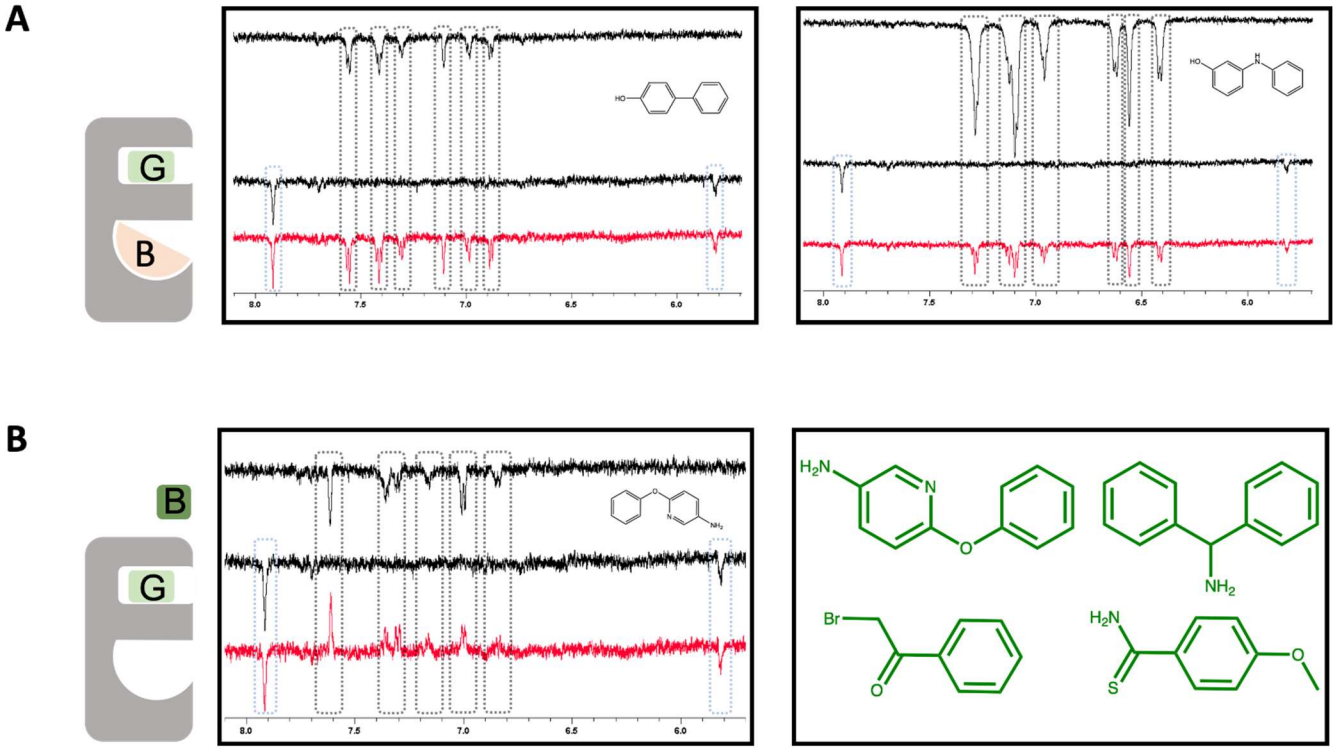

Figure 3-3. WaterLOGSY competition strategy using guanosine as a GTP-pocket competitor. Binding spectra are defined as negative peaks for WaterLOGSY experiments against MPH(2′)-I . In the schematic figure of the enzyme, the guanosine is depicted as a light green rectangle sitting in the GTP pocket of the protein. The binder is depicted as a light pink semi-circle in (A) and a dark green rectangle in (B). **(A)** Two examples of binders that are not competing with the guanosine. On the left panel, the WaterLOGSY binding spectra for: 2-amine 4-phenylphenol (top), guanosine (middle), and both guanosine and this binder (bottom). On the right panel the WaterLOGSY binding spectra for: 3-hydroxy diphenylamine (top), guanosine (middle), and both guanosine and this binder (bottom). **(B)** On the left, one example of the binder that competes with guanosine. The WaterLOGSY binding spectra for: 6-phenoxy 3-pyridine amine (top), guanosine (middle), and both guanosine and this binder (bottom). On the right, chemical structures of the four ′GTP-Pocket′ binders' fragments.

3-3-3 Structure of MPH(2')-I complexed with 6-phenoxy pyridine 3-amine and structure-guided elaboration of this fragment

Despite pursuing crystallization attempts for MPH(2′)-I in complex with all four ′GTP-pocket′ binders, we have thus far only been successful in obtaining a crystal structure for one of them.

Crystal structure of MPH(2′)-I in complex with 6-phenoxy pyridine 3-amine was determined at 2.29 Å. Comparison of 6-phenoxy pyridine 3-amine binding to MPH(2′)-I, with guanosine binding to this protein, revealed this hit fragment's competing nature with guanosine (Figure 3-4). The data collection details and final refinement statistics for this crystal structure are given in Table 3-1.

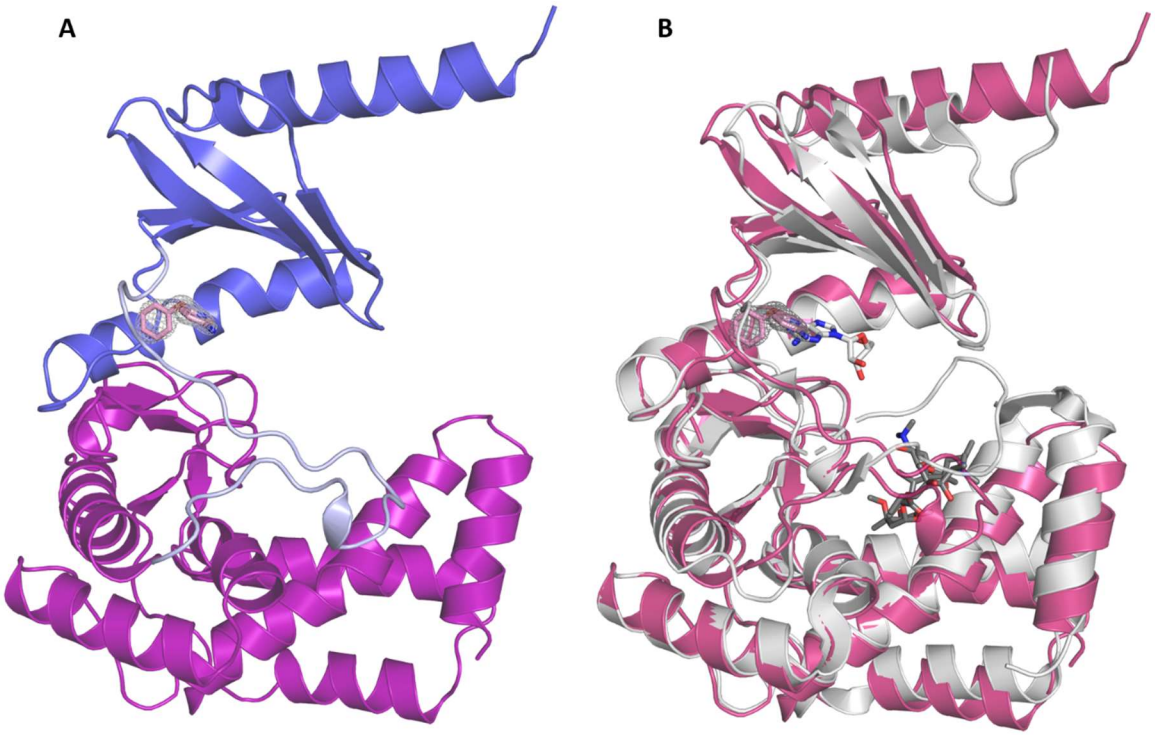

Figure 3-4. MPH(2′)-I structure in complex with 6-phenoxy pyridine 3-amine. (A) Cartoon representation of MPH(2′)-I structure is depicted in dark blue at the N-terminal lobe, light blue at the linker segment region and violet at the C-terminal lobe. The hit fragment, 6-phenoxy pyridine 3-amine is shown in light pink. The 2Fo–Fc map is countered to 1σ and colored in light gray. **(B)** Superposition of our structure in pink with MPH(2′)-I structure in complex with guanosine and azithromycin (PDB code: 5IGI) in gray. Guanosine is shown in gray and azithromycin is shown in dark gray.

As shown in Figures 3-5 and 3-6, the phenyl ring of this hit fragment is sandwiched between the hydrophobic side chain of Ala80, Pro82, Leu97, Leu207, and Gly 216. These residues form a pocket at the edge of the nucleotide-binding site of the MPH(2′)-I protein. It consists of residues from the N-terminal lobe, the beginning of the linker region, and the core subdomain of the C-terminal lobe (see Figure 3-4A). This

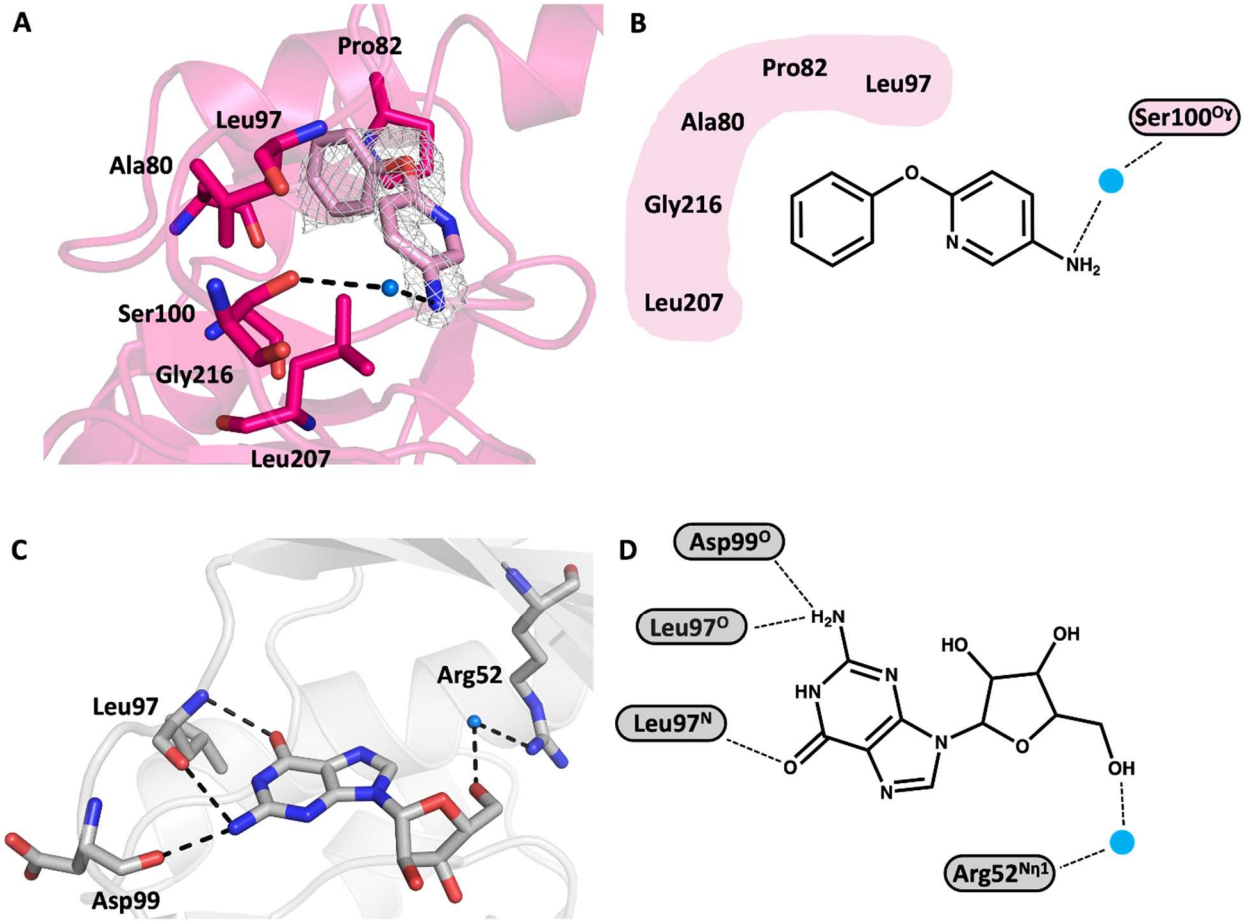

Figure 3-5. MPH(2′)-I hydrogen bond interactions with 6-phenoxy pyridine 3-amine and guanosine. **(A)** MPH(2′)-I residues involved in water-mediated hydrogen bond interaction with 6-phenoxy pyridine 3-amine and formation of hydrophobic pocket depicted as sticks and colored in dark pink. 6-phenoxy pyridine 3-amine colored in light pink. Hydrogen bonds are depicted as black dashed lines. The water molecule is depicted as a blue sphere. The Fo–Fc discovery map is countered to 2σ and colored in gray. **(B)** A 2-dimensional representation of water-mediated hydrogen bond interaction between 6-phenoxy pyridine 3-amine and MPH(2′)-I. The side chain of the residues in the pink shell contributes to the hydrophobic pocket formation. **(C)** MPH(2′)-I residues involved in hydrogen bond interactions with guanosine are depicted as sticks and colored in gray. Guanosine is colored in gray. Hydrogen bonds are depicted as black dashed lines (PDB code: 5IGI). **(D)** A 2-dimensional representation of hydrogen bond interactions between guanosine and MPH(2′)-I.

small pocket does not overlap with the guanosine binding site. In contrast, the 3-aminopyridine ring extends into the nucleotide pocket and overlaps the binding position of the pyrimidine ring of the pyrimidine-imidazole ring system in guanosine. The amino group of this ring makes one water-mediated hydrogen bond interaction with Ser100.

The next step in the process of inhibitor development demands a further elaboration of the hit fragment. Analysis of this structure and its comparison with the structure of MPH(2′)-I in complex with guanosine shows two possible alteration sites: phenyl ring and 3-aminopyridine ring.

Expansion of the molecule at the side of the phenyl ring can be implemented by adding a fluorine group to its meta-position. As shown in Figure 3-6A, there is a solvent-exposed pocket at this side that can accommodate an additional group. Furthermore, adding a halogen group is a common elaboration strategy in any therapeutic or diagnostic small molecule synthesis. It can enhance a number of physicochemical and pharmacokinetic properties, such as improved metabolic stability and enhanced membrane permeation (Gillis, Eastman et al. 2015).

The enlargement strategy at the 3-aminopyridine ring was inspired by the positioning of the guanine ring in the structure of MPH(2′)-I in complex with guanosine (Figure 3-5 and Figure 3-6B). As the pyrimidine ring of guanosine overlaps the binding position of the 3-aminopyridine ring, we decided to merge this ring to our fragment. We speculated that the amino group of this ring would have the same hydrogen bond interaction seen for guanosine in the designed molecule (Figure 3-6C).

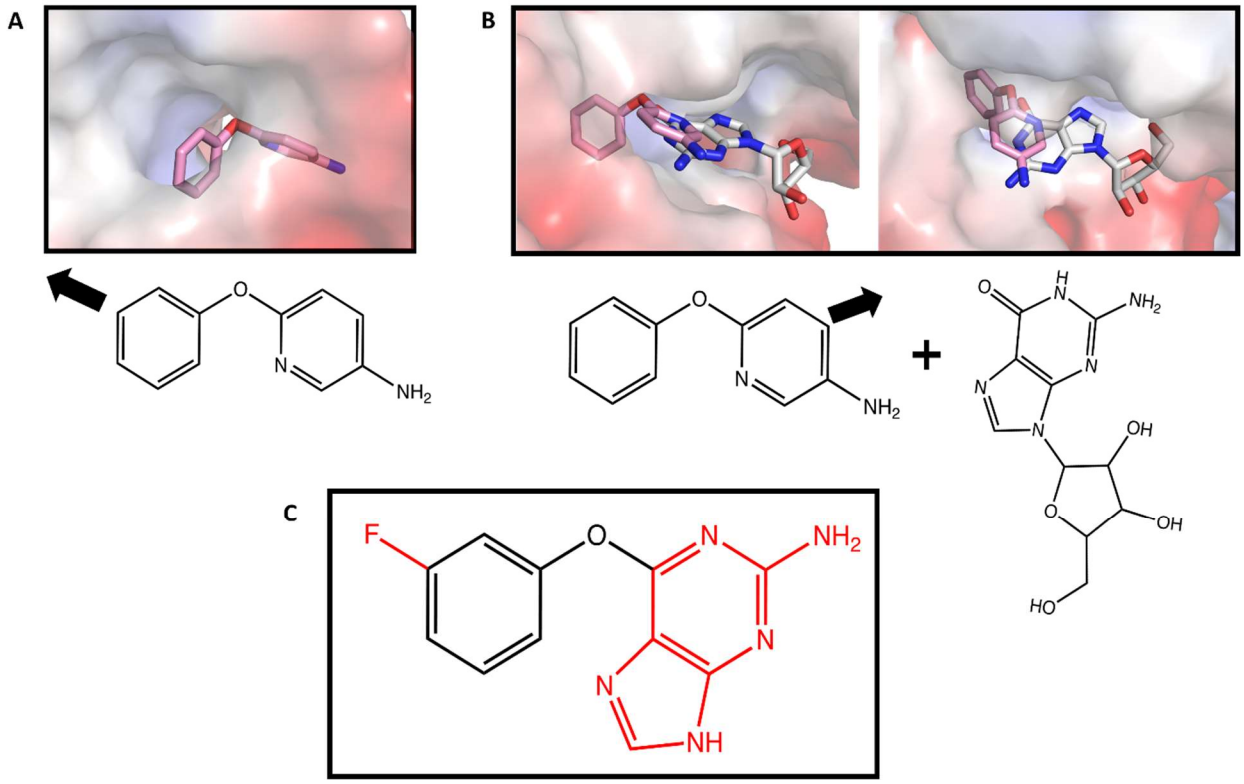

Figure 3-6. Hit-to-lead optimization strategies for 6-phenoxy 3-pyridine amine. (A) The elaboration potential on the meta position of the phenyl group is shown on the left. (B) The substitution potential of 3-aminopyridine with guanine is shown on the right. (C) The chemical structure of the proposed lead, 6-(3-fluorophenoxy)-7H-purin-2-amine, is shown with the elaborated groups in **red**. This molecule named ABG-1.

3-3-4 Structure of MPH(2')-I complexed with ABG-1

We have solved six MPH(2′)-I structures in which the elaborated molecule, 6-(3-fluorophenoxy)-7H-purin-2-amine (named ABG-1), occupies one binding position in the GTP-binding pocket of this protein. The determined binding site for ABG-1 is similar in all these structures and therefore being allocated as the primary binding site for this molecule. One of these structures (chosen based on the resolution and data completeness for all shells) was refined and is shown in Figure 3-7A,B. At the same time, another MPH(2′)-I structure with *two* bound ABG-1 was solved in a different crystallization

condition. This structure displays a secondary binding site for this molecule (Figure 3-7C,D). The data collection details and final refinement statistics for both crystal structures are given in Table 3-1.

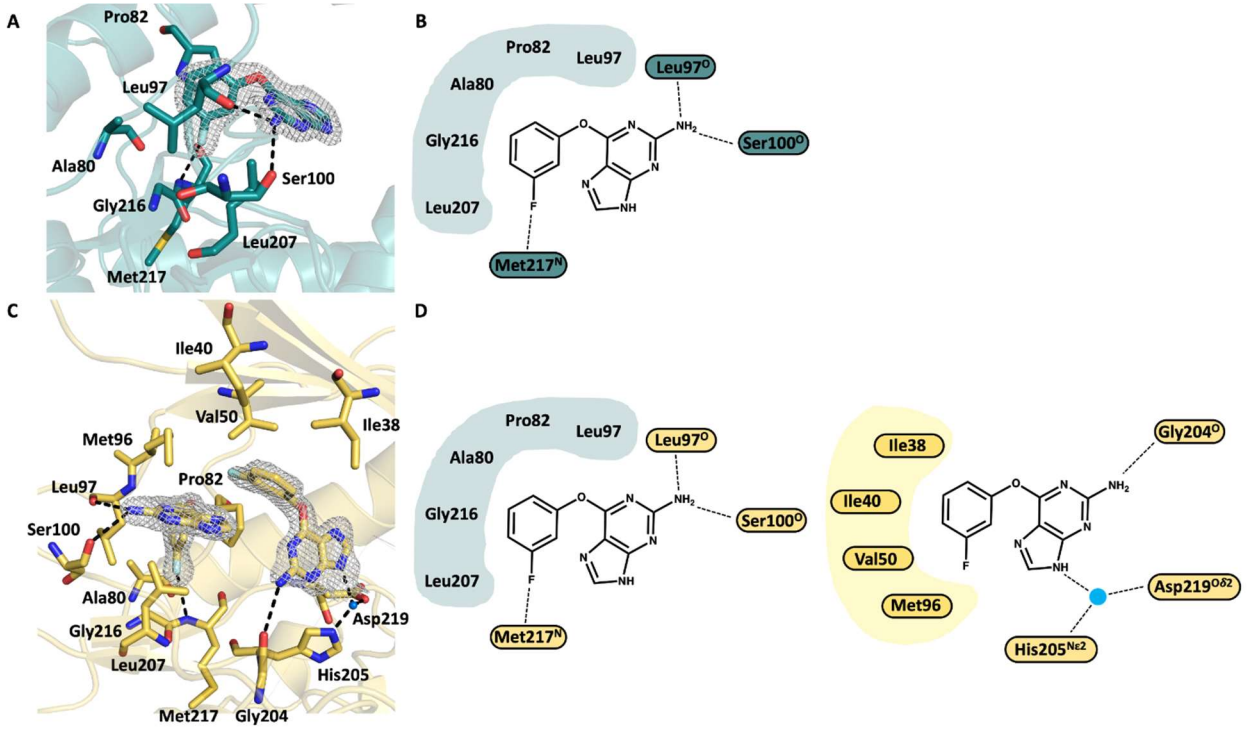

Figure 3-7. MPH(2′)-I hydrogen bond interactions with 6-(3-fluorophenoxy)-7H-purin-2-amine 1 (ABG-1) in *structures one* and *two*. (A) MPH(2′)-I residues involved in hydrogen bond interaction with ABG-1 and formation of hydrophobic pocket in *structure one* depicted as sticks and colored in dark green. ABG-1 is also colored in dark green. Hydrogen bonds are depicted as black dashed lines. The Fo–Fc discovery map is countered to 3σ and colored in gray. **(B)** A 2-dimensional representation of hydrogen bond interactions between ABG-1 and MPH(2′)-I. The side chain of the residues in the green shell contributes to the hydrophobic pocket formation. **(C)** MPH(2′)-I residues involved in hydrogen bond interactions with ABG-1 and formation of hydrophobic pocket in *structure two* depicted as sticks and colored in yellow. ABG-1 is also colored in yellow. Hydrogen bonds are depicted as black dashed lines. The Fo–Fc discovery map is countered to 3σ and colored in gray. The water molecule is depicted as a blue sphere. **(D)** A 2-dimensional representation of hydrogen bond interactions between ABG-1 and MPH(2′)-I. The side chain of the residues in the green and yellow shells contributes to the hydrophobic pocket formation.

Analysis of both structures on the primary binding position of ABG-1 shows that the C2-amine group on the guanine ring forms hydrogen bond interactions with the

backbone's carbonyl oxygen of Leu97 and Ser100 of MPH(2′)-I protein (Figure3-7). These hydrogen bonds improve the affinity of this molecule compared to the original hit fragment (see below).

At the other side of the molecule, the fluorine group on the phenyl ring orients itself pointing downward, contrary to our expectation. In this orientation, the fluorine group can most likely serve as a hydrogen bond acceptor (Auffinger, Hays et al. 2004) from the amino group of Met217 backbone (Figure3-7).

At the secondary binding site (Figure 3-7C, D), the fluoro-phenyl ring aligns parallel to the hydrophobic roof of the nucleotide-binding pocket. This arrangement is assisted by the hydrophobic side chain of Ile38, Ile40, Val50, and Met96. In addition, the guanine ring forms water-mediated hydrogen bonds to Asp219 and His205 through its N9 hydrogen and a hydrogen bond interaction with the backbone carbonyl oxygen of Gly204 through its C2-amino group.

3-3-5 Inhibition studies

Inhibition studies on the hit fragment and ABG-1 indicate that these two molecules act as a competitive inhibitor towards GTP, as expected by previous structural studies. The inhibition studies also display that the first step of elaboration on the hit fragment has significantly increased the affinity of this molecule to MPH(2′)-I (Figure 3-8). At the same time, guanosine shows the highest inhibition constant, which correlates with its higher number of hydrogen bond interactions with MPH(2′)-I compared with two other molecules (Figure 3-5 and Figure 3-7A, B). Preliminary inhibition studies of ABG-1 on MPH(2′)-II also indicated that this molecule is a GTP-competitive inhibitor for this enzyme as well.

The first step in the evolution of the lead inhibitor yielded a molecule with about seven times higher K_i than the hit fragment. Thus, we feel encouraged that we may reach an affinity in the low nanomolar range with additional elaboration steps. The inhibition constant in the nanomolar range is needed to compete with GTP (K_m=47μM), and it is the range seen for ePK inhibitors of kinases with similar K_m values (Knight and Shokat 2005).

Molecules	K_i (μM)	K_m (μM)	K_{cat} (s^{-1})	K_{cat}/K_m (s^{-1} μM^{-1})
MPH(2′)-I				
Hit fragment	(77.1 ± 11.0) x 10	35.5 ± 3.1	1.70 ± (1.79 x 10^{-2})	(4.79 ± 0.47) x 10^{-2}
Guanosine	(1.48 ± 0.27) x 10	28.2 ± 4.9	1.69 ± (3.11 x 10^{-2})	(5.99 ± 1.15) x 10^{-2}
ABG-1	(9.96 ± 1.44) x 10	43.4 ± 3.9	1.25 ± (1.69 x 10^{-2})	(2.88 ± 0.30) x 10^{-2}
MPH(2′)-II				
ABG-1	(6.47 ± 2.16) x 10	77.5 ± 9.8	3.45 ± (7.36 x 10^{-2})	(4.45 ± 0.66) x 10^{-2}

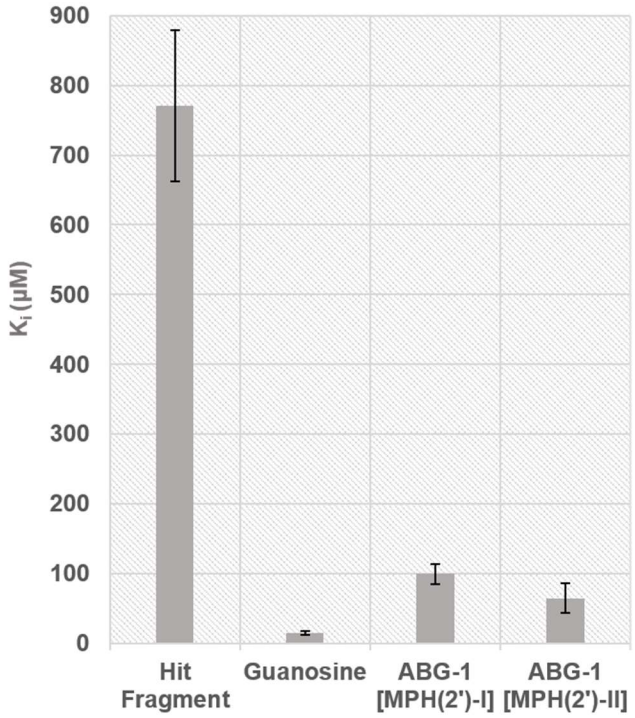

Figure 3-8. Inhibitory constant and kinetic parameters for the hit fragment, guanosine, and ABG-1.

3-3-6 Possibility of cross-reactivity of MPH inhibitors with human GTP-binding proteins

A remaining concern in this effort has been the possibility of cross-reactivity of MPH inhibitors with human protein kinases. However, ABG-1 contains the guanine core of GTP and it has been shown that this core has a different interaction pattern to that observed for adenine core (in ATP) in ePKs. Specifically, the interaction with the carbonyl oxygen of guanine is of particular relevance because it confers binding selectivity toward ATP (Rogne, Rosselin et al. 2018). At the same time, the inability to find leads for MPHs in an array of protein kinase inhibitors suggests that exploiting these libraries for adjuvant development is unlikely to be fruitful (Shakya, Stogios et al. 2011).

On the other hand, many different protein families bind GTP in a human cell, such as the Ras superfamily of GTPases and a diverse subset of other GTP binding proteins. Hence, the probability of the off-target effects for ABG-1 was explored through structural analyses done on the GTP binding pocket of five members of the RAS-superfamily (M-RAS, Rho-E, Rab-1B, ARF, and Ran) and four GTP binding proteins (eEF1A, eIF2, CK2, and G-protein α-subunit of the G_i family of heterotrimeric G-proteins). Following the overlay of these proteins using the GTP's guanine ring, we observed similarities in the architecture of the GTP-binding pocket and the orientation of GTP across the classes of eukaryotic GTP binding proteins. However, ABG-1 modeling in the GTP binding pocket revealed clashes between the fluoro-phenyl ring in ABG-1 to one side of the GTP pocket in these eukaryotic proteins (Figure 3-9). This modeling endeavor has therefore been favorable towards ABG-1, but additional human-cell experiments are needed to verify these results.

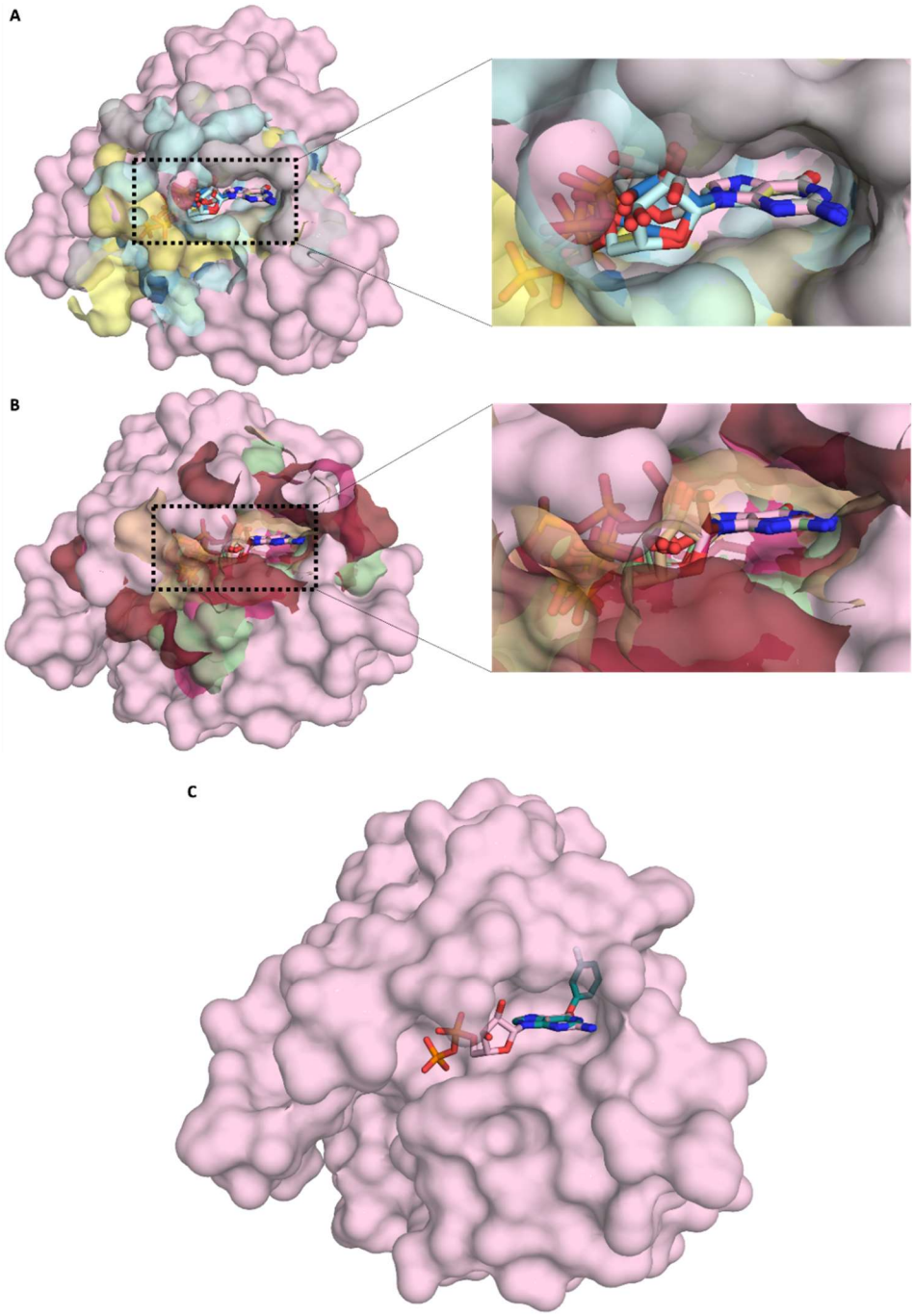

Figure 3-9. Structural modeling of ABG-1 in the GTP pocket of human GTP-binding proteins. (A) Overlay of five proteins in the RAS superfamily using the GTP's guanine ring. M-RAS in light pink (PDB code:1X1R), RAN in light blue (PDB code:1K5G), ARF1 in dark blue (PDB code:1RRF), RhoE in yellow (PDB code:1M7B), and Rab1b in gray (PDB code:4HLQ). **(B)** Overlay of M-RAS and four eukaryotic GTP-binding proteins using the GTP's guanine ring. M-RAS in light pink (PDB:1X1R), EF1A in green (PDB code:1G7C), G-protein α-subunit in light brown (PDB code:1GIT), CK2 in dark brown (PDB code:1LP4), and IF2 in dark pink (PDB code:2QMU). **(C)** 6-(3 -fluorophenoxy)-7H-purin-2-amine (ABG-1) modeling in GTP pocket of M-RAS protein. ABG-1 is depicted in dark green and GTP in light pink. The fluoro-phenyl ring clashes with one side of this pocket.

3-3-7 All-inclusive MPH inhibitor design

At least 15 gene subtypes of MPHs have been reported, which are designated *mph*(A) to (O) (O'Hara, Kanda et al. 1989, Kono, O'Hara et al. 1992, Kim, Baek et al. 1996, Matsuoka, Endou et al. 1998, Roberts, Sutcliffe et al. 1999, Matsuoka, Inoue et al. 2003, Schlüter, Szczepanowski et al. 2007, Pawlowski, Wang et al. 2016, Pawlowski, Stogios et al. 2018). Among these subtypes, MPH(2′)-I and -II, the products of *mph*(A) and *mph*(B) genes respectively, are the main two resistance factors in human pathogens and have been characterized structurally (Fyfe, Grossman et al. 2016, Fong, Burk et al. 2017, Gomes, Ruiz-Roldán et al. 2019). Although we obtained the crystal structure of the ABG-1 with MPH(2′)-I, preliminary inhibition studies of ABG-1 on MPH(2′)-II confirm its ability to inhibit this enzyme.

Furthermore, following structure-based sequence alignment on fourteen MPH subtypes (only a partial sequence is available for the *mph*(D) gene), we performed a conservation prediction analysis on the ten residues surrounding ABG-1 binding pocket. This analysis showed that seven of these residues are more than 60% conserved in all MPHs (Figure 3-10). Thus, the high conservation scores among these residues suggest with high confidence the possibility of using this inhibitor as an all-inclusive MPH inhibitor.

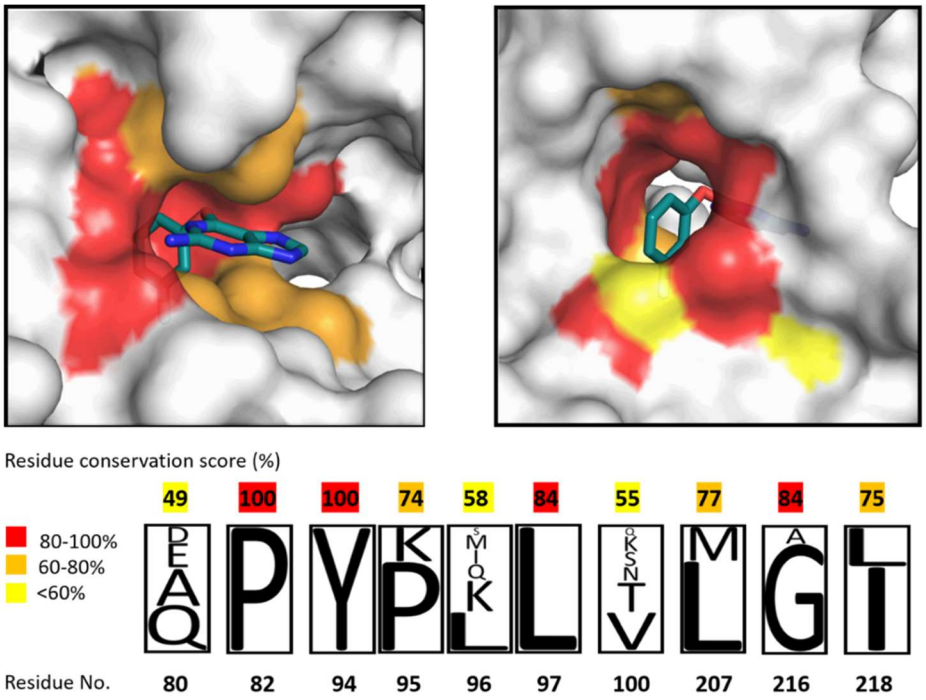

Figure 3-10. Conservation prediction of ten residues surrounding ABG-1 is shown on MPH(2′)-I structure in complex with this molecule. ABG-1 is depicted as dark green.

3-4 Conclusion

In summary, applying fragment-based drug design approaches, we intended to develop a GTP-competitive inhibitor for resistance-conferring macrolide phosphotransferases, MPH(2′)-I and MPH(2′)-II. We present, here, crystal structures of a hit fragment and a lead molecule complexed with MPH(2′)-I. The lead molecule was designed using ‘growing’ and ‘merging’ strategies to enhance the binding affinity of the hit fragment. Comparison of the inhibition constant of the hit fragment and the lead molecule for MPH(2′)-I, and its solved binding position in our structure confirm the success of our strategy. Besides, the preliminary inhibition studies on MPH(2′)-II confirm the inhibitory effects of this lead on this enzyme as well. Furthermore, structural modeling of this lead onto nine selected eukaryotic GTP-binding proteins reduces our concern for

its cross-reactivity to these enzymes. Finally, residue conservation studies of all reported macrolide phosphotransferase at the binding pocket of our suggested lead, validates this inhibitor as a putative all-inclusive MPH inhibitor. We, therefore, propose this lead molecule to be used as a framework inhibitor that can be further elaborated with the outlook of efficacy enhancement and drug delivery.

3-5 Experimental Procedures

3-5-1 MPH(2')-I and MPH(2'')-II Expression, and Purification

One liter of auto-induction medium (Studier 2005) was inoculated with 1 mL of a 5-hour culture of *E. coli* BL21(DE3) carrying the plasmid containing the *mph*(A) or *mph*(B) genes (Fong, Burk et al. 2017). The 1L culture was grown at 37°C with aeration for 3 hours and the temperature was then decreased to 20°C for about 21 hours of expression. Cells were harvested by centrifugation at 6000g for 20 minutes. The cell pellet was resuspended in 50 mL of lysis buffer containing 50 mM Tris pH 7.5, 500 mM NaCl, 10 mM imidazole and then lysed by sonication. The sonicated lysate was then cleared by centrifugation at 20000 X g for 20 minutes and filtered through a 0.45 mm filter. Affinity chromatography on 5-mL Ni-NTA Superflow cartridge (QIAGEN) and thrombin digestion were carried out as previously described (Fong, Burk et al. 2017). MPH(2′)-I and -II fractions were desalted on HiPrep 26/10 Desalting column (Cytiva) equilibrated in 25 mM BIS-TRIS propane pH 7.0. The desalted material was applied on HiLoad 16/10 DEAE® FF column equilibrated in the identical buffer and eluted with 0–1M NaCl gradient over 20 column volumes. Peak fractions were pooled, and buffer exchange was then performed on the same desalting column equilibrated in the final storage buffer consisting of 25 mM Tris, pH 7.5. for MPH(2′)-I and pH 8.0 for MPH(2′)-II.

3-5-2 Fragment-Based Library

An in-house fragment library containing 257 compounds grouped into 34 cocktail stocks in 100% DMSO was used. The stock concentration of each constituent compound

in each cocktail was standardized at 100 mM. This fragment library was adopted from Dr. Wim Hol group (Verlinde, Fan et al. 2009) (see Appendix).

3-5-3 6-(3-fluorophenoxy)-7H-purin-2-amine (ABG-1) Synthesis

Synthesis of 6-(3-fluorophenoxy)-7H-purin-2-amine was performed at CHEMSPACE (NJ, USA).

3-5-4 NMR Studies

STD and WaterLOGSY on cocktails

Saturation transfer difference (STD) (Mayer and Meyer 2001) and Water-Ligand Observed via Gradient SpectroscopY experiments (WaterLOGSY) (Dalvit, Fogliatto et al. 2001) were performed for both MPH(2′)-I and MPH(2′)-II using each cocktail. Cocktails with positive peaks for both proteins were chosen and a separate STD and waterLOGSY experiment was carried out with 500 µM of each compound from the respective cocktail in 600 µl of NMR solution composed of 10 µM enzyme, 100 mM potassium phosphate pH 7.5, 150 mM NaCl, and 10% D2O.

NMR spectra were recorded on a 500 MHz Varian INOVA NMR spectrometer equipped with a triple-resonance HCN probe with Z-axis gradient.

1D proton spectra were recorded using a double-pulsed field gradient stimulated echo (dpfgse_water) sequence with a sweep width of 8000 Hz, 2s acquisition time and 2.5s relaxation delay.

STD spectra were recorded using a double-pulsed field gradient stimulated echo sequence with interleaved acquisition of on and off resonance saturation pulses and

internal subtraction (dpfgse_satxfer). Sweep width was 8000 Hz, with 1s acquisition time, and 1.5s d1, with a total of 1024 scans. On-resonance (0 ppm) and off-resonance (32.3 ppm) saturation pulses of 1 - 1.5s were applied as a train of 50ms gaussian pulses, exciting a range of 100 Hz (Mayer and Meyer 2001).

WaterLOGSY (wlogsy_noe) spectra were recorded with a sweep width of 8000 Hz, 1s acquisition time and 1.2s relaxation delay. A 1.5s mixing time was used, and 512 scans were recorded (Dalvit, Fogliatto et al. 2001).

WaterLOGSY competition assay

WaterLOGSY competition experiments were carried out with 500 µM of each of the 16 candidate binders and 500 µM of guanosine in 600 µl of NMR solution composed of 10 µM enzyme, 100 mM potassium phosphate pH 7.5, 150 mM NaCl, and 10% D2O. The Waterlogsy spectra were recorded for the candidate binder, guanosine, and mixture of the binder and guanosine.

Waterlogsy spectra were recorded on a 600 MHz Bruker Avance III HD NMR spectrometer equipped with a TCI cryoprobe. The ephogsygpno sequence was used to record spectra with a sweep width of 9615 Hz, with 1.7s acquisition time and 2s relaxation delay. Residual protein signal was suppressed with a 15ms CLEANEX spinlock. A 2s mixing time was used, and 256 scans were recorded (Dalvit, Fogliatto et al. 2001).

3-5-5 MPH-I Co-crystallization With 6-phenoxy pyridine 3-amine and 6-(3-fluorophenoxy)-7H-purin-2-amine

Crystals of the MPH(2′)-I and 6-phenoxy pyridine 3-amine complex were grown at 4°C using the sitting-drop vapour diffusion method. Drops contained a 3:1 volume ratio of

10 mg mL^{-1} of MPH(2′)-I in storage buffer supplemented with 1.5 mM 6-phenoxy pyridine 3-amine, 3 mM $MgCl_2$, and reservoir solution. Crystals of the MPH(2′)-I complex grew when the reservoir solution consisted of 0.2 M Ca Acetate, 0.1 M imidazole pH 8.0, and 4% PEG 8K. Crystals were transferred into a cryoprotecting solution consisting of the same reservoir solution supplemented with 25% PEG400 and flash-frozen in liquid nitrogen.

Crystals of the MPH(2′)-I and 6-(3-fluorophenoxy)-7H-purin-2-amine (ABG-1) complex were grown at 4°C using the sitting-drop vapour diffusion method. The crystals presenting one binding site for the compound grew in six crystallization conditions listed here:

1. Drops contained 1:1 volume ratio of 10 mg mL^{-1} of MPH(2′)-I in storage buffer supplemented with 3 mM ABG-1 and 3 mM $MgCl_2$, and reservoir solution, when reservoir solution consisted of 0.08M Na cacodylate pH 6.5, 20% glycerol, 0.16M Ca Acetate, and 14.4% w/v PEG 8K.

2. Drops contained 3:1 volume ratio of 10 mg mL^{-1} of MPH(2′)-I in storage buffer supplemented with 1.5 mM ABG-1 and 3 mM $MgCl_2$, and reservoir solution, when reservoir solution consisted of 0.1M Na cacodylate pH 6.5, 0.2M $MgCl_2$, and 20%PEG 1K.

3. Drops contained 1:1 volume ratio of 10 mg mL^{-1} of MPH(2′)-I in storage buffer supplemented with 3 mM ABG-1 and 3 mM $MgCl_2$, and reservoir solution, when reservoir solution consisted of 0.08M Na cacodylate pH 6.5, 20% glycerol, 0.16M Mg Acetate, and 16% w/v PEG 8K.

4. Drops contained 3:1 volume ratio of 10 mg mL^{-1} of MPH(2′)-I in storage buffer supplemented with 1.5 mM ABG-1 and 3 mM $MgCl_2$, and reservoir solution when reservoir solution consisted of 0.1M TRIS pH 8.5, 0.16M $CaCl_2$, and 16% PEG 4K.

5. Drops contained 3:1 volume ratio of 10 mg mL^{-1} of MPH(2′)-I in storage buffer supplemented with 1.5 mM ABG-1 and 3 mM $MgCl_2$, and reservoir solution, when reservoir solution consisted of 0.1M TRIS pH 8.5, 0.18M $CaCl_2$, and 16% PEG 4K.

6. Drops contained 3:1 volume ratio of 10 mg mL^{-1} of MPH(2′)-I in storage buffer supplemented with 1.5 mM ABG-1 and 3 mM $MgCl_2$, and reservoir solution, when reservoir solution consisted of 0.1M TRIS pH 8.5, 0.2M $CaCl_2$, and 16% PEG 4K.

Drops of the crystals displaying two binding sites for the compound contained a 3:1 volume ratio of 10 mg mL^{-1} of MPH(2′)-I in storage buffer supplemented with 1.5 mM ABG-1 and 3 mM $MgCl_2$, and reservoir solution. These crystals grew when reservoir solution consisted of 0.085 M HEPES pH 7.5, 15% glycerol, 8.5% v/v 2-propanol, and 17% w/v PEG 4K.

3-5-6 Data Collection, Structure Solution, and Refinement

Diffraction data for the optimized crystal of the MPH(2′)-I in complex with 6-phenoxy pyridine 3-amine was collected on a Bruker D8 Venture home source consisting of a METALJET X-ray source (liquid gallium anode) coupled with a PHOTON II CAPD detector. The dataset was integrated, scaled, and reduced in the Bruker PROTEUM3 suite. The structure was solved by molecular replacement (MR) with the previously solved structure of MPH(2′)-I in complex with guanosine and erythromycin (PDB ID: 5IGT)

stripped of all non-protein atoms as the search model using PHASER (McCoy, Grosse-Kunstleve et al. 2007).

Diffraction data for all of the crystals of MPH(2′)-I in complex with ABG-1 were collected at CMCF beamline 08B1-1 at the Canadian Light Source using MxDC (Fodje, Janzen et al. 2012). These datasets were processed using AutoProcess. This CLS in-house software program process the datasets by using xia2 pipeline (Winter 2010) [XDS (Kabsch 2010), POINTLESS (Evans 2006)]. The structures were determined using Fourier synthesis performed by phenix.refine (Adams, Afonine et al. 2010) using our previously solved MPH(2′)-I in complex with 6-phenoxy pyridine 3-amine stripped of all non-protein atoms. The structure solved from the first crystallization condition mentioned above with the highest resolution of diffraction (1.59 Å) was chosen for further refinement cycles. The highest resolution of diffraction for other structures solved from other crystallization conditions were, 2^{nd} condition: 2.11 Å, 3^{rd} condition: 1.70 Å, 4^{th} condition: 2.06 Å, 5^{th} condition: 2.10 Å, and 6^{th} condition: 2.02 Å.

All of the structures were refined by iterative cycles of reciprocal-space refinement with phenix.refine (Adams, Afonine et al. 2010) and real-space refinement and model building in Coot (Emsley, Lohkamp et al. 2010). The ligand restraints for 6-phenoxy pyridine 3-amine and 6-(3-fluorophenoxy)-7H-purin-2-amine were generated using eLBOW (Moriarty, Grosse-Kunstleve et al. 2009).

3-5-7 Inhibition Assay

Inhibitory activity of the hit fragment (6-phenoxy pyridine 3-amine), guanosine and 6-(3-fluorophenoxy)-7H-purin-2-amine were assessed to determine the K_i of these molecules against GTP using Thermo Fisher NanoDrop One^C Spectrometer.

The phosphorylation of oleandomycin was measured in a pyruvate kinase/lactate dehydrogenase coupled assay in which the hydrolysis of GTP is coupled to the oxidation of NADH to NAD+, which can be monitored by a decrease in absorbance at 340nm. This assay was previously used for measuring the enzyme kinetics for both MPH(2′)-I and MPH(2′)-II (Fong, Burk et al. 2017).

The assay was carried out in a 0.8 mL quartz cuvette (pathlength 1 cm), in a buffer containing 50 mM MOPS pH 6.5, 40 mM potassium chloride, 10 mM magnesium chloride, 2.5 mM phosphoenolpyruvate, 3 mM oleandomycin, 0.560 mM β-nicotinamide adenine dinucleotide (reduced), 18-30 U/ml pyruvate kinase, and 28-43 U/ml lactate dehydrogenase and varying concentrations of GTP (0.5625, 1.125, 2.25, 4.5, 9 and 18 mM). The reaction was initiated by the addition of the MPH(2′)-I or MPH(2′)-II enzymes (2 μM, final concentration), where UV absorbance was measured over 5 min at 22 °C. Assays were run in triplicates and the kinetic properties were measured against 6-phenoxy pyridine 3-amine (0, 156.25, 312.5, 625, 1250, 2500 μM), guanosine (0, 25, 50, 100, 200, 400 μM), and 6-(3-fluorophenoxy)-7H-purin-2-amine (0, 12.5, 25, 50, 100, 200, 400 μM) for MPH(2′)-I and against 6-(3-fluorophenoxy)-7H-purin-2-amine (0, 25, 35, 50 μM) for MPH(2′)-II. Data analysis was performed using the GraphPad5 software. Kinetic parameters were obtained by fitting the kinetic data nonlinearly with the Michaelis-Menten equation for competitive inhibition.

Table 3-1 Data collection and refinement statistics of MPH(2′)-I in complex with the hit fragment and ABG-1.

	MPH(2')-I ● 6Phenoxy Pyridine 3-Amine	MPH(2')-I ● ABG-1 (*structure one*)	MPH(2')-I ● ABG-1 ● ABG-1 (*structure two*)
Data collection			
Space group	P 21 21 21	P 21 21 21	P 21 21 21
Cell dimensions			
***a*, *b*, *c* (Å)**	49.56, 64.14, 96.21	50.92, 63.51, 97.35	51.18, 63.44, 97.83
α, β, γ (°)	90, 90, 90	90, 90, 90	90, 90, 90
Resolution (Å)	32.07 - 2.29 (2.372 - 2.29)	39.73 - 1.68 (1.74 - 1.68)	38.74 - 1.7 (1.76 - 1.7)
R_{merge}	0.1288 (0.6226)	0.03584 (0.9383)	0.04649 (0.5427)
I / σ	17.72 (4.20)	37.65 (2.88)	26.47 (3.80)
Completeness (%)	99.64 (96.90)	99.94 (99.89)	98.32 (93.07)
Redundancy	13.0 (8.9)	12.3 (11.4)	10.4 (7.6)
Refinement			
Total no. reflections	185669(12253)	452389 (41417)	364681 (24874)
Unique reflections	14314(1379)	36714 (3621)	35189 (3276)
R_{work} / R_{free}	0.1686/ 0.2331	0.1806/0.2026	0.1838/0.2102
No. atoms	2625	2712	2854
Macromolecules	2382	2411	2506
Ligand/ion	34	32	62
Water	209	269	286
***B*-factors (Å²)**	28.09	43.24	34.43
Macromolecules	27.73	42.85	33.68
Ligand/ion	35.5	48.16	38.91
Water	30.91	46.20	40.07
R.m.s. deviations			
Bond lengths (Å)	0.008	0.010	0.007
Bond angles (°)	1.26	1.16	0.94
Ramachandran favorded (%)	98.00	97.67	97.00
Ramachandran outliners (%)	0.00	0.00	0.00

One crystal used for data collection of each structure. *Values in parentheses are for the highest-resolution shell.

Chapter 4 — Thesis Conclusion

In the preceding chapters, we have undertaken structure-based approaches to advance drug design in the context of antibiotic resistance. We have focused on two available strategies in this avenue; modifying existing antibiotics to overcome resistance factors and designing antibiotic adjuvants to block the activity of resistance-conferring antibiotic modifying enzymes.

Chapter two revolves around plazomicin, the newest semi-synthetic aminoglycoside and the first to be approved by the FDA in nearly 40 years. Pursuing structural studies of the bacterial ribosome bound to plazomicin, we solved the first crystal structure of this drug bound to its target, and we examined the structural basis for plazomicin mechanism of action. In addition, this structure resolved the structural consequences of ribosome methylation and 2′ acetylation of plazomicin, the two clinically recognized resistance mechanisms for this aminoglycoside. Furthermore, we extend our knowledge on plazomicin resistance by structural studies of the only reported modifying enzyme for this drug, acetyltransferase AAC(2′)-Ia. Finally, integrating the structural knowledge on drug-target and drug-resistome provided us with insights for next-generation aminoglycoside design. Our collaborators at Clemson University are pursuing the synthetic pathways to these next-generation drugs guided by our studies.

A somewhat puzzling result presented in chapter two is the structural basis for the resistance-conferring properties of 2′-acetylation. In the chapter, we proposed three structural outcomes for 2′-acetylation of plazomicin by AAC(2′)-Ia; the steric clash/strain, loss of hydrogen bonds, and loss of charge interactions. We noted that individually these

factors seem insufficient to prevent the binding of acetylated plazomicin, and thus we speculate that together, they cause resistance to this aminoglycoside. In order to further probe the basis of AAC(2′) mediated resistance, we are pursuing a collaborative follow-up study using isothermal titration calorimetry (ITC).

Here, we are performing a 2′ acetylation of plazomicin using AAC(2′)-Ia in a biphasic reaction (Figure 4-1). This reaction is adapted from a previous study (Llano-Sotelo, Azucena Jr et al. 2002) and optimized to meet our needs.

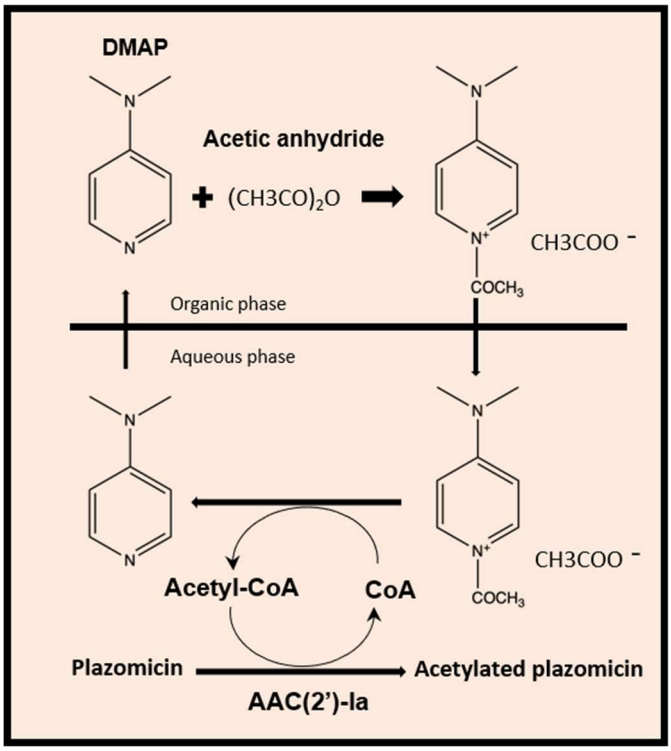

Figure 4-1. Acetylation of plazomicin at 2′ position, using AAC(2′)-Ia in a biphasic reaction. In this reaction, CoA can be recycled to make acetyl-CoA used by the AAC(2′)-Ia enzyme. Acetylated dimethyl aminopyridine (DMAP) is the carrier of the acetyl group to the aqueous phase and converts CoA to acetyl-CoA. DMAP goes back to the organic phase, and the cycle will be repeated.

Following this reaction, the acetylated plazomicin is purified using column chromatography followed by mass spectrometry analysis of aliquots of the eluted molecules (Figure 4-2).

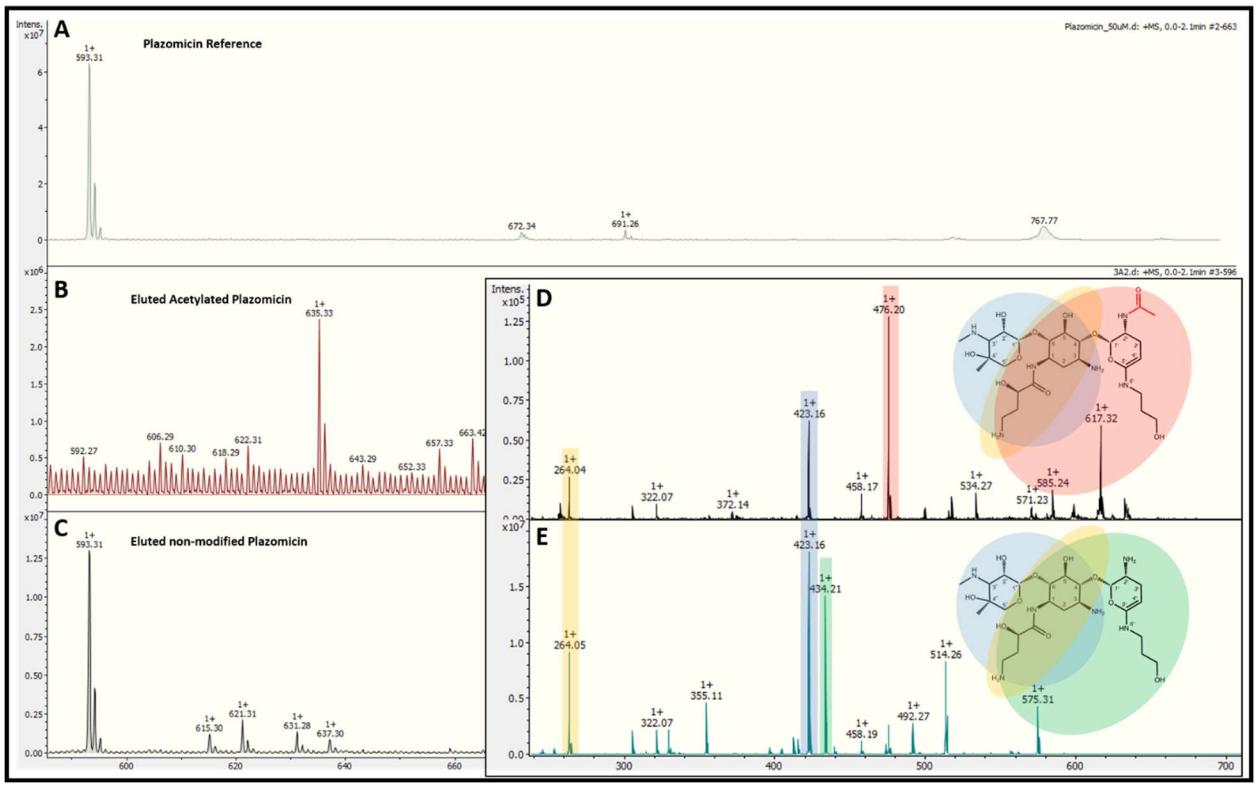

Figure 4-2. Mass spectrometry analysis of eluted samples after column chromatography. This analysis not only differentiates the acetylated plazomicin but also confirms the position of acetylation on this molecule. **(A)** The 'reference' mass peak for plazomicin (593.3 Da). **(B)** The mass peak for eluted acetylated plazomicin (635.3 Da). **(C)** The mass peak for eluted non-modified plazomicin (593.3 Da). **(D)** Signature fragment masses for acetylated plazomicin. The mass for the central ring of plazomicin is highlighted in yellow (264 Da). The mass for the combined central ring and the double-prime ring is highlighted in blue (423.1 Da). The mass for the combined central ring and the prime ring is highlighted in red (476.2). **(E)** Signature fragment masses for non-modified plazomicin. The mass for the central ring and combined central ring and the double-prime ring is as shown in D, but the mass for the combined central ring and the prime ring is highlighted in green (434.2 Da). The difference in the mass of the peak highlighted in green, and the peak highlighted in red is 42 Da. This mass represents the acetyl group added to the 2′ position of this molecule.

In the last step, the ITC experiments will be carried out by our collaborators and the binding affinity of acetylated plazomicin to minimal ribosomal A-site will be compared

to plazomicin. We anticipate that plazomicin binding to the minimal ribosomal A-site would enhance the thermal stability of the A-site with an exothermic enthalpy profile, as suggested by studies on other aminoglycosides (Kaul and Pilch 2002, Dudek, Romanowska et al. 2014). This may not be the case for acetylated plazomicin. In particular, we would expect to see an increase in the dissociation constant for acetylated plazomicin compared to plazomicin, which reflects its lower binding affinity to the A-site.

In chapter three, we pursued fragment-based drug design techniques to develop an inhibitor for resistance-conferring MPH(2′)-I and MPH(2′)-II enzymes to be used as an adjuvant for the macrolide class of antibiotics. We have solved the crystal structure of one of the hit fragments identified as GTP-competitive molecules in the NMR WaterLOGSY competition assays. This hit fragment was elaborated using “growing” and “merging” strategies, and two crystal structures for this elaborated molecule (ABG-1) in complex with MPH(2′)-I were determined. The primary binding site of ABG-1 upheld our evolution strategies for the hit fragment. Furthermore, the inhibition assay showed ABG-1 competitive nature against GTP for MPH(2′)-I and MPH(2′)-II (K_i = 99.6 ± 14.4 μM for MPH(2′)-I and K_i = 64.7 ± 21.6 μM for MPH(2′)-II). In addition, we achieved a significant increase in the inhibition constant for ABG-1 compared to the hit fragment (K_i = 771 ± 110 μM for MPH(2′)-I) after only one step of hit fragment elaboration.

In chapter three, we also predicted the feasibility of using ABG-1 as an all-inclusive MPHs inhibitor with residue conservation studies for the ABG-1 primary binding site. Additionally, structural modeling of ABG-1 in the nucleotide-binding pocket of nine selected eukaryotic GTP-binding proteins reduced our concerns for the off-target effects of this molecule.

In the direction of developing a more potent drug (with the inhibition constant in the nanomolar range), the ABG-1 can be further elaborated. Two paths can be suggested by examining our structures (see Figure 3-7). On the first path, ABG-1 can be further expanded at the side of the fluoro-phenyl ring (Figure 4-3). The determined orientation for the fluorine group in the primary binding site of ABG-1, gives us room for expansion of the molecule on the opposing meta- and ortho-position of this ring. The arrangement of one conserved water molecule that connects the backbone of Pro95 and Asp83 in all of our solved structures inspires us to add a hydroxyl or amino group at the meta-position. Another version can also be suggested with a methyl group at this position, which may flip the orientation of the fluorine group in its bound structure. The opposing ortho position can also be filled by a hydroxyl group, putatively replacing the same conserved water molecule. These four elaborated versions of ABG-1 have been ordered for synthesis, and we are ready to perform inhibition studies on them as soon as they arrive.

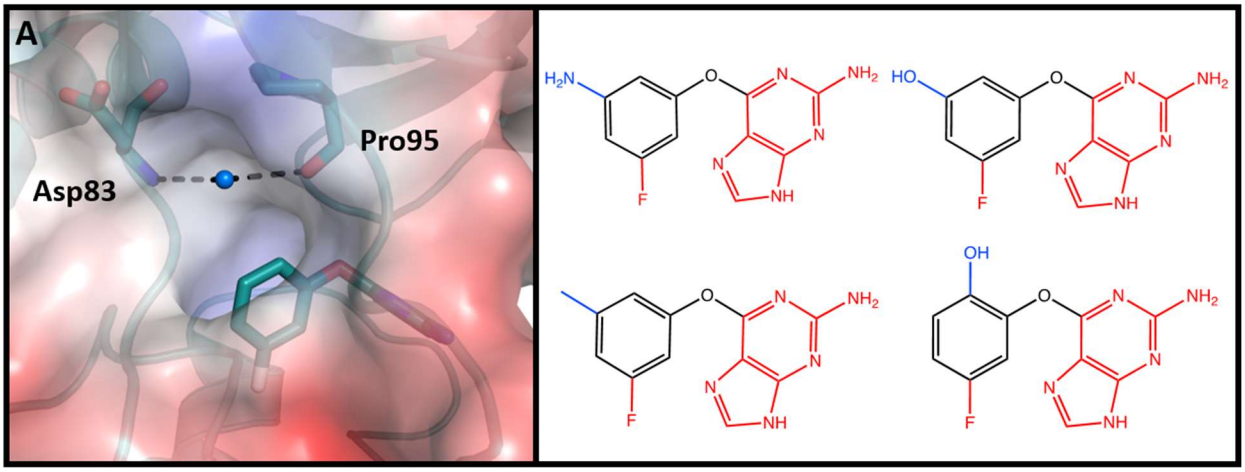

Figure 4-3 Chemical structures of the four elaborated versions of ABG-1. **(A)** Further evolution of ABG-1 is suggested based on the positioning of the fluorine group and the arrangement of one conserved water molecule in all solved structures. The first-step elaborations on the hit fragment are depicted in **red**, and the suggested second-step modifications on ABG-1 are depicted in **blue**.

On the second path, elaborations on the side of the guanine ring can be pursued based on “linking” strategies. Guiding by the structure of MPH(2′)-I complexed with two molecules of ABG-1 in the GTP-binding pocket (see Figure 3-7C, D), two molecules of ABG-1 can be coupled with the addition of a propyl linker. We, therefore, propose two elaborated versions of the previous four compounds (Figure 4-4). The synthesis of any of these molecules should be pursued after selecting the best lead in the previous elaboration step.

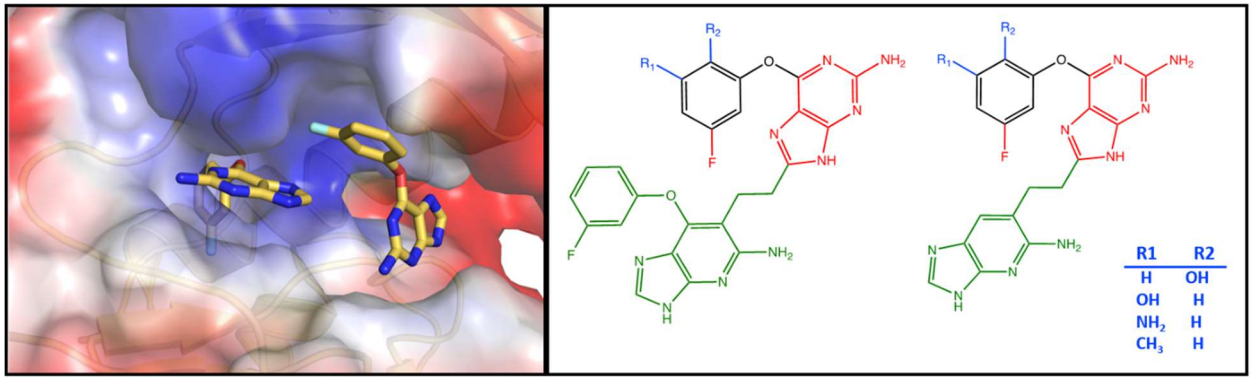

Figure 4-4. Chemical structures of the two proposed inhibitors based on *structure two* for ABG-1. The first-step elaborations on the hit fragment are depicted in **red**, the suggested second-step modifications on ABG-1 are depicted in **blue**, and the third suggested step of expansion is depicted in **green**.

Considerations on drug delivery should also be contemplated while suggesting further elaboration strategies. This inhibitor needs to reach the cytoplasm of bacterial cells to act on macrolide phosphotransferases. This is a rather challenging route as it passes the outer membrane and plasma membrane in the case of Gram-negative, and the peptidoglycan layer and plasma membrane for Gram-positive bacteria. Therefore, it will be necessary to perform preliminary studies on the effects of this inhibitor on the minimal inhibitory concentrations (MIC) of macrolides on macrolide-resistance bacteria, with only the MPH-related mechanism of resistance.

The two chapters of this thesis represent practical examples of pursuing structure-based drug design while tackling antibiotic resistance. Pursuing a two-pronged approach, firstly, we advanced the domain of drug design for the class of aminoglycosides by suggesting modifications on plazomicin molecule. Secondly, we developed a framework molecule that can be used as an adjuvant that can come to the rescue in the context of resistance for the macrolide class of antibiotics.

Finally, we would like to reiterate what we have discussed in the introduction chapter: Tackling antibiotic resistance demands a collaborative and integrative effort of multiple disciplines both on a local and global level. The struggle against antibiotic resistance cannot come to fruition unless we, as teachers, scientists, physicians, farmers, and policymakers in a global community, all contribute to achieve this goal.

References

Abraham, E. P. and E. Chain (1940). "An enzyme from bacteria able to destroy penicillin." Nature **146**(3713): 837-837.

Achaogen (2018). "Drug approval package: ZEMDRI (plazomicin)." U.S. Food and Drug Administration.

Adams, P. D., P. V. Afonine, G. Bunkóczi, V. B. Chen, I. W. Davis, N. Echols, J. J. Headd, L.-W. Hung, G. J. Kapral and R. W. Grosse-Kunstleve (2010). "PHENIX: a comprehensive Python-based system for macromolecular structure solution." Acta Crystallographica Section D: Biological Crystallography **66**(2): 213-221.

Aggen, J. B., E. S. Armstrong, A. A. Goldblum, P. Dozzo, M. S. Linsell, M. J. Gliedt, D. J. Hildebrandt, L. A. Feeney, A. Kubo and R. D. Matias (2010). "Synthesis and spectrum of the neoglycoside ACHN-490." Antimicrobial agents and chemotherapy **54**(11): 4636-4642.

Ahmed, M. O. and K. E. Baptiste (2018). "Vancomycin-resistant enterococci: a review of antimicrobial resistance mechanisms and perspectives of human and animal health." Microbial Drug Resistance **24**(5): 590-606.

Alangaden, G. J., B. N. Kreiswirth, A. Aouad, M. Khetarpal, F. R. Igno, S. L. Moghazeh, E. K. Manavathu and S. A. Lerner (1998). "Mechanism of resistance to amikacin and kanamycin in Mycobacterium tuberculosis." Antimicrobial agents and chemotherapy **42**(5): 1295-1297.

Aminov, R. I. and R. I. Mackie (2007). "Evolution and ecology of antibiotic resistance genes." FEMS microbiology letters **271**(2): 147-161.

Antanasijevic, A., C. Kingsley, A. Basu, T. L. Bowlin, L. Rong and M. Caffrey (2016). "Application of virus-like particles (VLP) to NMR characterization of viral membrane protein interactions." Journal of biomolecular NMR **64**(3): 255-265.

Antanasijevic, A., B. Ramirez and M. Caffrey (2014). "Comparison of the sensitivities of WaterLOGSY and saturation transfer difference NMR experiments." Journal of biomolecular NMR **60**(1): 37-44.

Attwood, M. M., D. Fabbro, A. V. Sokolov, S. Knapp and H. B. Schiöth (2021). "Trends in kinase drug discovery: Targets, indications and inhibitor design." Nature Reviews Drug Discovery: 1-23.

Auffinger, P., F. A. Hays, E. Westhof and P. S. Ho (2004). "Halogen bonds in biological molecules." Proceedings of the National Academy of Sciences **101**(48): 16789-16794.

Bacot-Davis, V. R., A. V. Bassenden and A. M. Berghuis (2016). "Drug-target networks in aminoglycoside resistance: hierarchy of priority in structural drug design." MedChemComm **7**(1): 103-113.

Ban, N., P. Nissen, J. Hansen, P. B. Moore and T. A. Steitz (2000). "The complete atomic structure of the large ribosomal subunit at 2.4 Å resolution." Science **289**(5481): 905-920.

Bassenden, A. V., L. Dumalo, J. Park, J. Blanchet, K. Maiti, D. P. Arya and A. M. Berghuis (2021). "Structural and phylogenetic analyses of resistance to next-generation aminoglycosides conferred by AAC (2′) enzymes." Scientific reports **11**(1): 1-13.

Bassenden, A. V., D. Rodionov, K. Shi and A. M. Berghuis (2016). "Structural analysis of the tobramycin and gentamicin clinical resistome reveals limitations for next-generation aminoglycoside design." ACS chemical biology **11**(5): 1339-1346.

Bassett, E. J., M. S. Keith, G. J. Armelagos, D. L. Martin and A. R. Villanueva (1980). "Tetracycline-labeled human bone from ancient Sudanese Nubia (AD 350)." Science **209**(4464): 1532-1534.

Bernal, P., C. Molina-Santiago, A. Daddaoua and M. A. Llamas (2013). "Antibiotic adjuvants: identification and clinical use." Microbial biotechnology **6**(5): 445-449.

Bolam, D. N., S. Roberts, M. R. Proctor, J. P. Turkenburg, E. J. Dodson, C. Martinez-Fleites, M. Yang, B. G. Davis, G. J. Davies and H. J. Gilbert (2007). "The crystal structure of two macrolide glycosyltransferases provides a blueprint for host cell antibiotic immunity." Proceedings of the National Academy of Sciences **104**(13): 5336-5341.

Boll, M., J. Radziejewska-Lebrecht, C. Warth, D. Krajewska-Pietrasik and H. Mayer (1994). "4-Amino-4-deoxy-L-arabinose in LPS of enterobacterial R-mutants and its possible role for their polymyxin reactivity." FEMS Immunology & Medical Microbiology **8**(4): 329-341.

Borovinskaya, M. A., R. D. Pai, W. Zhang, B. S. Schuwirth, J. M. Holton, G. Hirokawa, H. Kaji, A. Kaji and J. H. D. Cate (2007). "Structural basis for aminoglycoside inhibition of bacterial ribosome recycling." Nature structural & molecular biology **14**(8): 727-732.

Brodersen, D. E., W. M. Clemons Jr, A. P. Carter, R. J. Morgan-Warren, B. T. Wimberly and V. Ramakrishnan (2000). "The structural basis for the action of the antibiotics tetracycline, pactamycin, and hygromycin B on the 30S ribosomal subunit." Cell **103**(7): 1143-1154.

Bryan, L. and S. Kwan (1981). "Mechanisms of aminoglycoside resistance of anaerobic bacteria and facultative bacteria grown anaerobically." Journal of Antimicrobial Chemotherapy **8**(suppl_D): 1-8.

Burk, D. L., N. Ghuman, L. E. Wybenga-Groot and A. M. Berghuis (2003). "X-ray structure of the AAC (6′)-Ii antibiotic resistance enzyme at 1.8 Å resolution; examination of oligomeric arrangements in GNAT superfamily members." Protein science **12**(3): 426-437.

Caldwell, S. J. and A. M. Berghuis (2018). "Plasticity of Aminoglycoside Binding to Antibiotic Kinase APH (2 ″)-Ia." Antimicrobial Agents and Chemotherapy **62**(7).

Carter, A. P., W. M. Clemons, D. E. Brodersen, R. J. Morgan-Warren, B. T. Wimberly and V. Ramakrishnan (2000). "Functional insights from the structure of the 30S ribosomal subunit and its interactions with antibiotics." Nature **407**(6802): 340-348.

Castanheira, M., A. P. Davis, A. W. Serio, K. M. Krause and R. E. Mendes (2019). "In vitro activity of plazomicin against Enterobacteriaceae isolates carrying genes encoding aminoglycoside-modifying enzymes most common in US Census divisions." Diagnostic microbiology and infectious disease **94**(1): 73-77.

Castanheira, M., L. M. Deshpande, L. N. Woosley, A. W. Serio, K. M. Krause and R. K. Flamm (2018). "Activity of plazomicin compared with other aminoglycosides against isolates from European and adjacent countries, including Enterobacteriaceae molecularly characterized for aminoglycoside-modifying enzymes and other resistance mechanisms." Journal of Antimicrobial Chemotherapy **73**(12): 3346-3354.

Cayama, E., A. Yépez, F. Rotondo, E. Bandeira, A. C. Ferreras and F. J. Triana-Alonso (2000). "New chromatographic and biochemical strategies for quick preparative isolation of tRNA." Nucleic acids research **28**(12): e64-e64.

Celma, M., R. Monro and D. Vazquez (1970). "Substrate and antibiotic binding sites at the peptidyl transferase centre of *E. coli* ribosomes." FEBS letters **6**(3): 273-277.

Chahine, E. B., J. A. Dougherty, K.-A. Thornby and E. H. Guirguis (2021). "Antibiotic Approvals in the Last Decade: Are We Keeping Up With Resistance?" Annals of Pharmacotherapy: 10600280211031390.

Chen, L. (2017). "Notes from the field: pan-resistant New Delhi metallo-beta-lactamase-producing Klebsiella pneumoniae—Washoe County, Nevada, 2016." MMWR. Morbidity and mortality weekly report **66**.

Chesneau, O., K. Tsvetkova and P. Courvalin (2007). "Resistance phenotypes conferred by macrolide phosphotransferases." FEMS microbiology letters **269**(2): 317-322.

Chu, S., G. Zhou and M. Gochin (2017). "Evaluation of ligand-based NMR screening methods to characterize small molecule binding to HIV-1 glycoprotein-41." Organic & biomolecular chemistry **15**(24): 5210-5219.

Collaborative, C. P. (1994). "The CCP4 suite: programs for protein crystallography." Acta crystallographica. Section D, Biological crystallography **50**(Pt 5): 760.

Cox, E. C., J. R. White and J. G. Flaks (1964). "Streptomycin action and the ribosome." Proceedings of the National Academy of Sciences of the United States of America **51**(4): 703.

Cox, G., L. Ejim, P. J. Stogios, K. Koteva, E. Bordeleau, E. Evdokimova, A. O. Sieron, A. Savchenko, A. W. Serio and K. M. Krause (2018). "Plazomicin retains antibiotic activity against most aminoglycoside modifying enzymes." ACS infectious diseases **4**(6): 980-987.

Credito, K. L., L. M. Ednie, M. R. Jacobs and P. C. Appelbaum (1999). "Activity of telithromycin (HMR 3647) against anaerobic bacteria compared to those of eight other agents by time-kill methodology." Antimicrobial agents and chemotherapy **43**(8): 2027-2031.

D'Costa, V. M., C. E. King, L. Kalan, M. Morar, W. W. Sung, C. Schwarz, D. Froese, G. Zazula, F. Calmels and R. Debruyne (2011). "Antibiotic resistance is ancient." Nature **477**(7365): 457-461.

Daigle, D. M., G. A. McKay and G. D. Wright (1997). "Inhibition of aminoglycoside antibiotic resistance enzymes by protein kinase inhibitors." Journal of Biological Chemistry **272**(40): 24755-24758.

Dalvit, C., G. Fogliatto, A. Stewart, M. Veronesi and B. Stockman (2001). "WaterLOGSY as a method for primary NMR screening: practical aspects and range of applicability." Journal of biomolecular NMR **21**(4): 349-359.

Davies, J. and B. D. Davis (1968). "Misreading of ribonucleic acid code words induced by aminoglycoside antibiotics: the effect of drug concentration." Journal of Biological Chemistry **243**(12): 3312-3316.

Davies, J., W. Gilbert and L. Gorini (1964). "Streptomycin, suppression, and the code." Proceedings of the National Academy of Sciences of the United States of America **51**(5): 883.

Davies, J. E. (1964). "Studies on the ribosomes of streptomycin-sensitive and resistant strains of Escherichia coli." Proceedings of the National Academy of Sciences of the United States of America **51**(4): 659.

Davis, A. R., D. W. Gohara and M.-N. F. Yap (2014). "Sequence selectivity of macrolide-induced translational attenuation." Proceedings of the National Academy of Sciences **111**(43): 15379-15384.

Davis, B. and N. Anand (1960). "Effect of streptomycin on Escherichia coli." Nature **185**: 22-24.

Delcour, A. H. (2009). "Outer membrane permeability and antibiotic resistance." Biochimica et Biophysica Acta (BBA)-Proteins and Proteomics **1794**(5): 808-816.

Descours, G., C. Ginevra, N. Jacotin, F. Forey, J. Chastang, E. Kay, J. Etienne, G. Lina, P. Doublet and S. Jarraud (2017). "Ribosomal mutations conferring macrolide resistance in Legionella pneumophila." Antimicrobial agents and chemotherapy **61**(3): e02188-02116.

Doi, Y., J.-i. Wachino and Y. Arakawa (2016). "Aminoglycoside resistance: the emergence of acquired 16S ribosomal RNA methyltransferases." Infectious disease clinics of North America **30**(2): 523.

Domagk, G. (1935). "Ein beitrag zur chemotherapie der bakteriellen infektionen." DMW-Deutsche Medizinische Wochenschrift **61**(07): 250-253.

Douafer, H., V. Andrieu, O. Phanstiel IV and J. M. Brunel (2019). "Antibiotic adjuvants: make antibiotics great again!" Journal of medicinal chemistry **62**(19): 8665-8681.

Drawz, S. M., K. M. Papp-Wallace and R. A. Bonomo (2014). "New β-lactamase inhibitors: a therapeutic renaissance in an MDR world." Antimicrobial agents and chemotherapy **58**(4): 1835-1846.

Du, D., X. Wang-Kan, A. Neuberger, H. W. van Veen, K. M. Pos, L. J. Piddock and B. F. Luisi (2018). "Multidrug efflux pumps: structure, function and regulation." Nature Reviews Microbiology **16**(9): 523-539.

Dudek, M., J. Romanowska, T. Wituła and J. Trylska (2014). "Interactions of amikacin with the RNA model of the ribosomal A-site: computational, spectroscopic and calorimetric studies." Biochimie **102**: 188-202.

Ehrlich, P. and S. Halta (1910). Die experimentelle chemotherapie der Spirillosen, Springer.

Eliopoulos, G. M., V. G. Meka and H. S. Gold (2004). "Antimicrobial resistance to linezolid." Clinical Infectious Diseases **39**(7): 1010-1015.

Eljaaly, K., A. Alharbi, S. Alshehri, J. K. Ortwine and J. M. Pogue (2019). "Plazomicin: A Novel Aminoglycoside for the Treatment of Resistant Gram-Negative Bacterial Infections." Drugs **79**(3): 243-269.

Elkins, C. A. and L. B. Mullis (2007). "Substrate competition studies using whole-cell accumulation assays with the major tripartite multidrug efflux pumps of Escherichia coli." Antimicrobial agents and chemotherapy **51**(3): 923-929.

Emsley, P., B. Lohkamp, W. G. Scott and K. Cowtan (2010). "Features and development of Coot." Acta Crystallographica Section D: Biological Crystallography **66**(4): 486-501.

Endres, B. T., E. Bassères, M. J. Alam and K. W. Garey (2017). "Cadazolid for the treatment of Clostridium difficile." Expert opinion on investigational drugs **26**(4): 509-514.

Espejo, R. T. and N. Plaza (2018). "Multiple ribosomal RNA operons in bacteria; their concerted evolution and potential consequences on the rate of evolution of their 16S rRNA." Frontiers in microbiology **9**: 1232.

Ettayebi, M., S. M. Prasad and E. A. Morgan (1985). "Chloramphenicol-erythromycin resistance mutations in a 23S rRNA gene of *Escherichia coli*." Journal of bacteriology **162**(2): 551-557.

Evans, P. (2006). "Scaling and assessment of data quality." Acta Crystallographica Section D: Biological Crystallography **62**(1): 72-82.

Fernandes, P., E. Martens and D. Pereira (2017). "Nature nurtures the design of new semi-synthetic macrolide antibiotics." The Journal of antibiotics **70**(5): 527-533.

Fleming, A. (1929). "On the antibacterial action of cultures of a penicillium, with special reference to their use in the isolation of B. influenzae." British journal of experimental pathology **10**(3): 226.

Fodje, M., K. Janzen, R. Berg, G. Black, S. Labiuk, J. Gorin and P. Grochulski (2012). "MxDC and MxLIVE: software for data acquisition, information management and remote access to macromolecular crystallography beamlines." Journal of synchrotron radiation **19**(2): 274-280.

Fong, D. H. and A. M. Berghuis (2002). "Substrate promiscuity of an aminoglycoside antibiotic resistance enzyme via target mimicry." The EMBO journal **21**(10): 2323-2331.

Fong, D. H., D. L. Burk, J. Blanchet, A. Y. Yan and A. M. Berghuis (2017). "Structural basis for kinase-mediated macrolide antibiotic resistance." Structure **25**(5): 750-761. e755.

Fong, D. H., B. Xiong, J. Hwang and A. M. Berghuis (2011). "Crystal structures of two aminoglycoside kinases bound with a eukaryotic protein kinase inhibitor." PloS one **6**(5): e19589.

François, B., R. J. Russell, J. B. Murray, F. Aboul-ela, B. Masquida, Q. Vicens and E. Westhof (2005). "Crystal structures of complexes between aminoglycosides and decoding A site oligonucleotides: role of the number of rings and positive charges in the specific binding leading to miscoding." Nucleic acids research **33**(17): 5677-5690.

Fraser, I. (1984). "Penicillin: early trials in war casualties." British medical journal (Clinical research ed.) **289**(6460): 1723.

Fyfe, C., T. H. Grossman, K. Kerstein and J. Sutcliffe (2016). "Resistance to Macrolide Antibiotics in Public Health Pathogens." Cold Spring Harbor perspectives in medicine **6**(10): a025395.

Gabashvili, I. S., S. T. Gregory, M. Valle, R. Grassucci, M. Worbs, M. C. Wahl, A. E. Dahlberg and J. Frank (2001). "The polypeptide tunnel system in the ribosome and its gating in erythromycin resistance mutants of L4 and L22." Molecular Cell **8**(1): 181-188.

Galani, I., K. Nafplioti, P. Adamou, I. Karaiskos, H. Giamarellou, M. Souli and S. Collaborators (2019). "Nationwide epidemiology of carbapenem resistant Klebsiella pneumoniae isolates from

Greek hospitals, with regards to plazomicin and aminoglycoside resistance." BMC infectious diseases **19**(1): 167.

Gillis, E. P., K. J. Eastman, M. D. Hill, D. J. Donnelly and N. A. Meanwell (2015). "Applications of fluorine in medicinal chemistry." Journal of medicinal chemistry **58**(21): 8315-8359.

Golkar, T., M. Zieliński and A. M. Berghuis (2018). "Look and outlook on enzyme-mediated macrolide resistance." Frontiers in microbiology **9**: 1942.

Gomes, C., S. Martínez-Puchol, N. Palma, G. Horna, L. Ruiz-Roldán, M. J. Pons and J. Ruiz (2017). "Macrolide resistance mechanisms in Enterobacteriaceae: focus on azithromycin." Critical reviews in microbiology **43**(1): 1-30.

Gomes, C., L. Ruiz-Roldán, J. Mateu, T. J. Ochoa and J. Ruiz (2019). "Azithromycin resistance levels and mechanisms in Escherichia coli." Scientific reports **9**(1): 1-10.

Gordon, N., K. Png and D. Wareham (2010). "Potent synergy and sustained bactericidal activity of a vancomycin-colistin combination versus multidrug-resistant strains of Acinetobacter baumannii." Antimicrobial agents and chemotherapy **54**(12): 5316-5322.

Guillon, J.-M., T. Meinnel, Y. Mechulam, C. Lazennec, S. Blanquet and G. Fayat (1992). "Nucleotides of tRNA governing the specificity of Escherichia coli methionyl-tRNAfMet formyltransferase." Journal of molecular biology **224**(2): 359-367.

Gupta, V. and P. Datta (2019). "Next-generation strategy for treating drug resistant bacteria: Antibiotic hybrids." The Indian journal of medical research **149**(2): 97.

Haas, L. (1999). "Papyrus of Ebers and Smith." Journal of Neurology, Neurosurgery & Psychiatry **67**(5): 578-578.

Hajduk, P. J., J. Dinges, J. M. Schkeryantz, D. Janowick, M. Kaminski, M. Tufano, D. J. Augeri, A. Petros, V. Nienaber and P. Zhong (1999). "Novel inhibitors of Erm methyltransferases from NMR and parallel synthesis." Journal of medicinal chemistry **42**(19): 3852-3859.

Hansen, J. L., J. A. Ippolito, N. Ban, P. Nissen, P. B. Moore and T. A. Steitz (2002). "The structures of four macrolide antibiotics bound to the large ribosomal subunit." Molecular Cell **10**(1): 117-128.

Hernández, A., M. B. Sanchez and J. L. Martínez (2011). "Quinolone resistance: much more than predicted." Frontiers in microbiology **2**: 22.

Hon, W.-C., G. A. McKay, P. R. Thompson, R. M. Sweet, D. S. Yang, G. D. Wright and A. M. Berghuis (1997). "Structure of an enzyme required for aminoglycoside antibiotic resistance reveals homology to eukaryotic protein kinases." Cell **89**(6): 887-895.

Hutchings, M. I., A. W. Truman and B. Wilkinson (2019). "Antibiotics: past, present and future." Current opinion in microbiology **51**: 72-80.

Ingolia, N. T., S. Ghaemmaghami, J. R. Newman and J. S. Weissman (2009). "Genome-wide analysis in vivo of translation with nucleotide resolution using ribosome profiling." science **324**(5924): 218-223.

Jelić, D. and R. Antolović (2016). "From erythromycin to azithromycin and new potential ribosome-binding antimicrobials." Antibiotics **5**(3): 29.

Juhas, M., E. Widlake, J. Teo, D. L. Huseby, J. M. Tyrrell, Y. S. Polikanov, O. Ercan, A. Petersson, S. Cao and A. F. Aboklaish (2019). "In vitro activity of apramycin against multidrug-, carbapenem-and aminoglycoside-resistant Enterobacteriaceae and Acinetobacter baumannii." Journal of Antimicrobial Chemotherapy **74**(4): 944-952.

Jünemann, R., J. Wadzack, F. J. Triana-Alonso, J.-U. Bittner, J. Caillet, T. Meinnel, K. Vanatalu and K. H. Nierhaus (1996). "In vivo deuteration of transfer RNAs: overexpression and large-scale purification of deuterated specific tRNAs." Nucleic acids research **24**(5): 907-913.

Kabsch, W. (2010). "XDS." Acta Crystallogr. D **66**: 125-132.

Kaul, M. and D. S. Pilch (2002). "Thermodynamics of aminoglycoside− rRNA recognition: the binding of neomycin-class aminoglycosides to the A site of 16S rRNA." Biochemistry **41**(24): 7695-7706.

Kehrenberg, C., S. Schwarz, L. Jacobsen, L. H. Hansen and B. Vester (2005). "A new mechanism for chloramphenicol, florfenicol and clindamycin resistance: methylation of 23S ribosomal RNA at A2503." Molecular microbiology **57**(4): 1064-1073.

Kim, C., D. Hesek, J. Zajíček, S. B. Vakulenko and S. Mobashery (2006). "Characterization of the bifunctional aminoglycoside-modifying enzyme ANT (3 ‘’)-Ii/AAC (6 ‘)-IId from Serratia marcescens." Biochemistry **45**(27): 8368-8377.

Kim, C., A. Villegas-Estrada, D. Hesek and S. Mobashery (2007). "Mechanistic Characterization of the Bifunctional Aminoglycoside-Modifying Enzyme AAC (3)-Ib/AAC (6 ‘)-Ib ‘from Pseudomonas aeruginosa." Biochemistry **46**(17): 5270-5282.

Kim, S.-Y., D. H. Kim, S. M. Moon, J. Y. Song, H. J. Huh, N. Y. Lee, S. J. Shin, W.-J. Koh and B. W. Jhun (2021). "Association between 16S rRNA gene mutations and susceptibility to amikacin in Mycobacterium avium Complex and Mycobacterium abscessus clinical isolates." Scientific reports **11**(1): 1-8.

Kim, S., M. Baek, S. Choi, B. Kim and E. Choi (1996). "Nucleotide sequence, expression and transcriptional analysis of the *Escherichia coli* mphK gene encoding macrolide-phosphotransferase K." Molecules and Cells (Korea Republic).

Knight, Z. A. and K. M. Shokat (2005). "Features of selective kinase inhibitors." Chemistry & biology **12**(6): 621-637.

Kondo, S. and K. Hotta (1999). "Semisynthetic aminoglycoside antibiotics: development and enzymatic modifications." Journal of Infection and Chemotherapy **5**(1): 1-9.

Kono, M., K. O'Hara and T. Ebisu (1992). "Purification and characterization of macrolide 2′-phosphotransferase type II from a strain of *Escherichia coli* highly resistant to macrolide antibiotics." FEMS microbiology letters **97**(1-2): 89-94.

Krause, K. M., A. W. Serio, T. R. Kane and L. E. Connolly (2016). "Aminoglycosides: an overview." Cold Spring Harbor perspectives in medicine **6**(6): a027029.

Lescoute, A. and E. Westhof (2006). "The A-minor motifs in the decoding recognition process." Biochimie **88**(8): 993-999.

Lesher, G. Y., E. J. Froelich, M. D. Gruett, J. H. Bailey and R. P. Brundage (1962). "1, 8-Naphthyridine derivatives. A new class of chemotherapeutic agents." Journal of Medicinal Chemistry **5**(5): 1063-1065.

Li, Q. (2020). "Application of fragment-based drug discovery to versatile targets." Frontiers in Molecular Biosciences **7**: 180.

Li, X.-Z., P. Plésiat and H. Nikaido (2015). "The challenge of efflux-mediated antibiotic resistance in Gram-negative bacteria." Clinical microbiology reviews **28**(2): 337-418.

Lim, C. L. L., A. Q. Chua, J. Q. M. Teo, Y. Cai, W. Lee and A. L.-H. Kwa (2018). "Importance of control groups when delineating antibiotic use as a risk factor for carbapenem resistance, extreme-drug resistance, and pan-drug resistance in Acinetobacter baumannii and Pseudomonas aeruginosa: A systematic review and meta-analysis." International Journal of Infectious Diseases **76**: 48-57.

Livermore, D., S. Mushtaq, M. Warner, J.-C. Zhang, S. Maharjan, M. Doumith and N. Woodford (2011). "Activity of aminoglycosides, including ACHN-490, against carbapenem-resistant Enterobacteriaceae isolates." Journal of Antimicrobial Chemotherapy **66**(1): 48-53.

Llano-Sotelo, B., E. F. Azucena Jr, L. P. Kotra, S. Mobashery and C. S. Chow (2002). "Aminoglycosides modified by resistance enzymes display diminished binding to the bacterial ribosomal aminoacyl-tRNA site." Chemistry & biology **9**(4): 455-463.

Long, K. S. and B. Vester (2012). "Resistance to linezolid caused by modifications at its binding site on the ribosome." Antimicrobial agents and chemotherapy **56**(2): 603-612.

Lovmar, M., K. Nilsson, E. Lukk, V. Vimberg, T. Tenson and M. Ehrenberg (2009). "Erythromycin resistance by L4/L22 mutations and resistance masking by drug efflux pump deficiency." The EMBO journal **28**(6): 736-744.

Lowy, F. D. (2003). "Antimicrobial resistance: the example of Staphylococcus aureus." The Journal of clinical investigation **111**(9): 1265-1273.

Magnet, S. and J. S. Blanchard (2005). "Molecular insights into aminoglycoside action and resistance." Chemical reviews **105**(2): 477-498.

Martin, P., E. Jullien and P. Courvalin (1988). "Nucleotide sequence of Acinetobacter baumannii aphA-6 gene: evolutionary and functional implications of sequence homologies with nucleotide-binding proteins, kinases and other aminoglycoside-modifying enzymes." Molecular microbiology **2**(5): 615-625.

Matsuoka, M., K. Endou, H. Kobayashi, M. Inoue and Y. Nakajima (1998). "A plasmid that encodes three genes for resistance to macrolide antibiotics in *Staphylococcus aureus*." FEMS Microbiology Letters **167**(2): 221-227.

Matsuoka, M., M. Inoue, Y. Endo and Y. Nakajima (2003). "Characteristic expression of three genes, msr (A), mph (C) and erm (Y), that confer resistance to macrolide antibiotics on *Staphylococcus aureus*." FEMS Microbiology Letters **220**(2): 287-293.

Mayer, M. and B. Meyer (2001). "Group epitope mapping by saturation transfer difference NMR to identify segments of a ligand in direct contact with a protein receptor." Journal of the American Chemical Society **123**(25): 6108-6117.

McCoy, A. J., R. W. Grosse-Kunstleve, P. D. Adams, M. D. Winn, L. C. Storoni and R. J. Read (2007). "Phaser crystallographic software." Journal of applied crystallography **40**(4): 658-674.

Melander, R. J. and C. Melander (2017). "The challenge of overcoming antibiotic resistance: an adjuvant approach?" ACS infectious diseases **3**(8): 559-563.

Melnikova, I. and J. Golden (2004). "Targeting protein kinases." Nat Rev Drug Discov **3**(12): 993-994.

Mendelson, M. and M. P. Matsoso (2015). "The World Health Organization global action plan for antimicrobial resistance." SAMJ: South African Medical Journal **105**(5): 325-325.

Mitcheltree, M. J., A. Pisipati, E. A. Syroegin, K. J. Silvestre, D. Klepacki, J. D. Mason, D. W. Terwilliger, G. Testolin, A. R. Pote and K. J. Wu (2021). "A synthetic antibiotic class overcoming bacterial multidrug resistance." Nature: 1-6.

Moazed, D. and H. F. Noller (1987). "Chloramphenicol, erythromycin, carbomycin and vernamycin B protect overlapping sites in the peptidyl transferase region of 23S ribosomal RNA." Biochimie **69**(8): 879-884.

Moore, S. D. and R. T. Sauer (2008). "Revisiting the mechanism of macrolide-antibiotic resistance mediated by ribosomal protein L22." Proceedings of the National Academy of Sciences **105**(47): 18261-18266.

Morar, M., K. Bhullar, D. W. Hughes, M. Junop and G. D. Wright (2009). "Structure and mechanism of the lincosamide antibiotic adenylyltransferase LinB." Structure **17**(12): 1649-1659.

Moriarty, N. W., R. W. Grosse-Kunstleve and P. D. Adams (2009). "electronic Ligand Builder and Optimization Workbench (eLBOW): a tool for ligand coordinate and restraint generation." Acta Crystallographica Section D: Biological Crystallography **65**(10): 1074-1080.

Muir, M. E., D. R. Hanwell and B. J. Wallace (1981). "Characterization of a respiratory mutant of Escherichia coli with reduced uptake of aminoglycoside antibiotics." Biochimica et Biophysica Acta (BBA)-Bioenergetics **638**(2): 234-241.

Murray, C. W. and D. C. Rees (2009). "The rise of fragment-based drug discovery." Nature chemistry **1**(3): 187-192.

Nguyen, F., A. L. Starosta, S. Arenz, D. Sohmen, A. Dönhöfer and D. N. Wilson (2014). "Tetracycline antibiotics and resistance mechanisms." Biological chemistry **395**(5): 559-575.

Nichols, L. (2019). "Death from pan-resistant superbug." Autopsy & case reports **9**(3).

Nikaido, H. (1994). "Prevention of drug access to bacterial targets: permeability barriers and active efflux." Science **264**(5157): 382-388.

O'Hara, K., T. Kanda and M. Kono (1988). "Structure of a phosphorylated derivative of oleandomycin, obtained by reaction of oleandomycin with an extract of an erythromycin-resistant strain of *Escherichia coli*." The Journal of antibiotics **41**(6): 823-827.

O'Hara, K., T. Kanda, K. Ohmiya, T. Ebisu and M. Kono (1989). "Purification and characterization of macrolide 2'-phosphotransferase from a strain of *Escherichia coli* that is highly resistant to erythromycin." Antimicrobial agents and chemotherapy **33**(8): 1354-1357.

O'Neill, J. (2014). Antimicrobial Resistance: Tackling a Crisis for the Health and Wealth of Nations: December 2014, Review on antimicrobial resistance.

Oefner, C., A. d'Arcy, J. Daly, K. Gubernator, R. Charnas, I. Heinze, C. Hubschwerlen and F. Winkler (1990). "Refined crystal structure of β-lactamase from Citrobacter freundii indicates a mechanism for β-lactam hydrolysis." Nature **343**(6255): 284-288.

Oleinick, N. L. and J. W. Corcoran (1969). "Two types of binding of erythromycin to ribosomes from antibiotic-sensitive and-resistant Bacillus subtilis 168." Journal of Biological Chemistry **244**(3): 727-735.

Ouyang, Y., J. Li, Y. Peng, Z. Huang, Q. Ren and J. Lu (2020). "The role and mechanism of thiol-dependent antioxidant system in bacterial drug susceptibility and resistance." Current medicinal chemistry **27**(12): 1940-1954.

Pawlowski, A. C., P. J. Stogios, K. Koteva, T. Skarina, E. Evdokimova, A. Savchenko and G. D. Wright (2018). "The evolution of substrate discrimination in macrolide antibiotic resistance enzymes." Nature communications **9**(1): 112.

Pawlowski, A. C., W. Wang, K. Koteva, H. A. Barton, A. G. McArthur and G. D. Wright (2016). "A diverse intrinsic antibiotic resistome from a cave bacterium." Nature communications **7**: 13803.

Pawlowski, A. C., E. L. Westman, K. Koteva, N. Waglechner and G. D. Wright (2018). "The complex resistomes of Paenibacillaceae reflect diverse antibiotic chemical ecologies." The ISME Journal **12**(3): 885.

Pfister, P., S. Jenni, J. Poehlsgaard, A. Thomas, S. Douthwaite, N. Ban and E. C. Böttger (2004). "The structural basis of macrolide–ribosome binding assessed using mutagenesis of 23 S rRNA positions 2058 and 2059." Journal of molecular biology **342**(5): 1569-1581.

Polikanov, Y. S., I. A. Osterman, T. Szal, V. N. Tashlitsky, M. V. Serebryakova, P. Kusochek, D. Bulkley, I. A. Malanicheva, T. A. Efimenko and O. V. Efremenkova (2014). "Amicoumacin A inhibits translation by stabilizing mRNA interaction with the ribosome." Molecular cell **56**(4): 531-540.

Polikanov, Y. S., T. Szal, F. Jiang, P. Gupta, R. Matsuda, M. Shiozuka, T. A. Steitz, N. Vázquez-Laslop and A. S. Mankin (2014). "Negamycin interferes with decoding and translocation by simultaneous interaction with rRNA and tRNA." Molecular cell **56**(4): 541-550.

Poole, K. (2005). "Aminoglycoside resistance in Pseudomonas aeruginosa." Antimicrobial agents and Chemotherapy **49**(2): 479-487.

Priebe, G. P. and J. B. Goldberg (2014). "Vaccines for Pseudomonas aeruginosa: a long and winding road." Expert review of vaccines **13**(4): 507-519.

Ramirez, M. S. and M. E. Tolmasky (2010). "Aminoglycoside modifying enzymes." Drug resistance updates **13**(6): 151-171.

Ramirez, M. S. and M. E. Tolmasky (2017). "Amikacin: uses, resistance, and prospects for inhibition." Molecules **22**(12): 2267.

Rammelkamp, C. H. and T. Maxon (1942). "Resistance of Staphylococcus aureus to the Action of Penicillin." Proceedings of the Society for Experimental Biology and Medicine **51**(3): 386-389.

Rasko, D. A. and V. Sperandio (2010). "Anti-virulence strategies to combat bacteria-mediated disease." Nature reviews Drug discovery **9**(2): 117-128.

Recht, M. I., S. Douthwaite and J. D. Puglisi (1999). "Basis for prokaryotic specificity of action of aminoglycoside antibiotics." The EMBO journal **18**(11): 3133-3138.

Redi, D., C. S. Raffaelli, B. Rossetti, A. De Luca and F. Montagnani (2018). "Staphylococcus aureus vaccine preclinical and clinical development: current state of the art." New Microbiol **41**(3): 208-213.

Roberts, M. C. (2008). "Update on macrolide–lincosamide–streptogramin, ketolide, and oxazolidinone resistance genes." FEMS microbiology letters **282**(2): 147-159.

Roberts, M. C., J. Sutcliffe, P. Courvalin, L. B. Jensen, J. Rood and H. Seppala (1999). "Nomenclature for macrolide and macrolide-lincosamide-streptogramin B resistance determinants." Antimicrobial Agents and Chemotherapy **43**(12): 2823-2830.

Roca, I., M. Akova, F. Baquero, J. Carlet, M. Cavaleri, S. Coenen, J. Cohen, D. Findlay, I. Gyssens and O. Heure (2015). "The global threat of antimicrobial resistance: science for intervention." New microbes and new infections **6**: 22-29.

Rogne, P., M. Rosselin, C. Grundström, C. Hedberg, U. H. Sauer and M. Wolf-Watz (2018). "Molecular mechanism of ATP versus GTP selectivity of adenylate kinase." Proceedings of the National Academy of Sciences **115**(12): 3012-3017.

Rohde, C., J. Wittmann and E. Kutter (2018). "Bacteriophages: A therapy concept against multi-drug–resistant bacteria." Surgical infections **19**(8): 737-744.

Santajit, S. and N. Indrawattana (2016). "Mechanisms of antimicrobial resistance in ESKAPE pathogens." BioMed research international **2016**.

Sati, G. C., V. A. Sarpe, T. Furukawa, S. Mondal, M. Mantovani, S. N. Hobbie, A. Vasella, E. C. Böttger and D. Crich (2019). "Modification at the 2′-Position of the 4, 5-Series of 2-Deoxystreptamine Aminoglycoside Antibiotics To Resist Aminoglycoside Modifying Enzymes and Increase Ribosomal Target Selectivity." ACS infectious diseases **5**(10): 1718-1730.

Schatz, A., E. Bugle and S. A. Waksman (1944). "Streptomycin, a Substance Exhibiting Antibiotic Activity Against Gram-Positive and Gram-Negative Bacteria.∗." Proceedings of the Society for Experimental Biology and Medicine **55**(1): 66-69.

Schluenzen, F., A. Tocilj, R. Zarivach, J. Harms, M. Gluehmann, D. Janell, A. Bashan, H. Bartels, I. Agmon and F. Franceschi (2000). "Structure of functionally activated small ribosomal subunit at 3.3 Å resolution." cell **102**(5): 615-623.

Schlünzen, F., J. M. Harms, F. Franceschi, H. A. Hansen, H. Bartels, R. Zarivach and A. Yonath (2003). "Structural basis for the antibiotic activity of ketolides and azalides." Structure **11**(3): 329-338.

Schlünzen, F., R. Zarivach, J. Harms, A. Bashan, A. Tocilj, R. Albrecht, A. Yonath and F. Franceschi (2001). "Structural basis for the interaction of antibiotics with the peptidyl transferase centre in eubacteria." Nature **413**(6858): 814.

Schlüter, A., R. Szczepanowski, N. Kurz, S. Schneiker, I. Krahn and A. Pühler (2007). "Erythromycin resistance-conferring plasmid pRSB105, isolated from a sewage treatment plant, harbors a new macrolide resistance determinant, an integron-containing Tn402-like element, and a large region of unknown function." Applied and environmental microbiology **73**(6): 1952-1960.

Selmer, M., C. M. Dunham, F. V. Murphy, A. Weixlbaumer, S. Petry, A. C. Kelley, J. R. Weir and V. Ramakrishnan (2006). "Structure of the 70S ribosome complexed with mRNA and tRNA." Science **313**(5795): 1935-1942.

Serpersu, E. H., C. Özen and E. Wright (2008). Studies of enzymes that cause resistance to aminoglycosides antibiotics. New Antibiotic Targets, Springer**:** 261-271.

Shaeer, K. M., M. T. Zmarlicka, E. B. Chahine, N. Piccicacco and J. C. Cho (2019). "Plazomicin: A Next-Generation Aminoglycoside." Pharmacotherapy: The Journal of Human Pharmacology and Drug Therapy **39**(1): 77-93.

Shakya, T., P. J. Stogios, N. Waglechner, E. Evdokimova, L. Ejim, J. E. Blanchard, A. G. McArthur, A. Savchenko and G. D. Wright (2011). "A small molecule discrimination map of the antibiotic resistance kinome." Chemistry & biology **18**(12): 1591-1601.

Shaw, K., P. Rather, R. Hare and G. Miller (1993). "Molecular genetics of aminoglycoside resistance genes and familial relationships of the aminoglycoside-modifying enzymes." Microbiological reviews **57**(1): 138-163.

Shi, K. and A. M. Berghuis (2012). "Structural basis for dual nucleotide selectivity of aminoglycoside 2 ″-phosphotransferase IVa provides insight on determinants of nucleotide specificity of aminoglycoside kinases." Journal of Biological Chemistry **287**(16): 13094-13102.

Shi, K., S. J. Caldwell, D. H. Fong and A. M. Berghuis (2013). "Prospects for circumventing aminoglycoside kinase mediated antibiotic resistance." Frontiers in cellular and infection microbiology **3**: 22.

Shrivastava, S. R., P. S. Shrivastava and J. Ramasamy (2018). "World health organization releases global priority list of antibiotic-resistant bacteria to guide research, discovery, and development of new antibiotics." Journal of Medical Society **32**(1): 76.

Slee, A., M. Wuonola, R. McRipley, I. Zajac, M. Zawada, P. Bartholomew, W. Gregory and M. Forbes (1987). "Oxazolidinones, a new class of synthetic antibacterial agents: in vitro and in vivo activities of DuP 105 and DuP 721." Antimicrobial agents and chemotherapy **31**(11): 1791-1797.

Sobhanifar, S., L. J. Worrall, D. T. King, G. A. Wasney, L. Baumann, R. T. Gale, M. Nosella, E. D. Brown, S. G. Withers and N. C. Strynadka (2016). "Structure and mechanism of Staphylococcus aureus TarS, the wall teichoic acid β-glycosyltransferase involved in methicillin resistance." PLoS pathogens **12**(12): e1006067.

Sommer, M. O., C. Munck, R. V. Toft-Kehler and D. I. Andersson (2017). "Prediction of antibiotic resistance: time for a new preclinical paradigm?" Nature Reviews Microbiology **15**(11): 689-696.

Sonousi, A., V. A. Sarpe, M. Brilkova, J. Schacht, A. Vasella, E. C. Böttger and D. Crich (2018). "Effects of the 1-N-(4-amino-2 S-hydroxybutyryl) and 6′-N-(2-hydroxyethyl) substituents on ribosomal selectivity, cochleotoxicity, and antibacterial activity in the sisomicin class of aminoglycoside antibiotics." ACS infectious diseases **4**(7): 1114-1120.

Spotts, C. R. and R. Stanier (1961). "Mechanism of streptomycin action on bacteria: a unitary hypothesis." Nature **192**: 633-637.

Springer, B., Y. G. Kidan, T. Prammananan, K. Ellrott, E. C. Böttger and P. Sander (2001). "Mechanisms of streptomycin resistance: selection of mutations in the 16S rRNA gene conferring resistance." Antimicrobial agents and chemotherapy **45**(10): 2877-2884.

Steitz, T. A. (2008). "A structural understanding of the dynamic ribosome machine." Nature reviews Molecular cell biology **9**(3): 242-253.

Stogios, P. J., G. Cox, P. Spanogiannopoulos, M. C. Pillon, N. Waglechner, T. Skarina, K. Koteva, A. Guarné, A. Savchenko and G. D. Wright (2016). "Rifampin phosphotransferase is an unusual antibiotic resistance kinase." Nature communications **7**(1): 1-12.

Studier, F. W. (2005). "Protein production by auto-induction in high-density shaking cultures." Protein expression and purification **41**(1): 207-234.

Su, W., V. Kumar, Y. Ding, R. Ero, A. Serra, B. S. T. Lee, A. S. W. Wong, J. Shi, S. K. Sze and L. Yang (2018). "Ribosome protection by antibiotic resistance ATP-binding cassette protein." Proceedings of the National Academy of Sciences **115**(20): 5157-5162.

Sugantino, M. and S. L. Roderick (2002). "Crystal structure of Vat (D): an acetyltransferase that inactivates streptogramin group A antibiotics." Biochemistry **41**(7): 2209-2216.

Svetlov, M. S., E. Plessa, C.-W. Chen, A. Bougas, M. G. Krokidis, G. P. Dinos and Y. S. Polikanov (2019). "High-resolution crystal structures of ribosome-bound chloramphenicol and erythromycin provide the ultimate basis for their competition." RNA **25**(5): 600-606.

Svetlov, M. S., E. A. Syroegin, E. V. Aleksandrova, G. C. Atkinson, S. T. Gregory, A. S. Mankin and Y. S. Polikanov (2021). "Structure of Erm-modified 70S ribosome reveals the mechanism of macrolide resistance." Nature Chemical Biology **17**(4): 412-420.

Svetlov, M. S., N. Vázquez-Laslop and A. S. Mankin (2017). "Kinetics of drug–ribosome interactions defines the cidality of macrolide antibiotics." Proceedings of the National Academy of Sciences **114**(52): 13673-13678.

Tacconelli, E., E. Carrara, A. Savoldi, S. Harbarth, M. Mendelson, D. L. Monnet, C. Pulcini, G. Kahlmeter, J. Kluytmans and Y. Carmeli (2018). "Discovery, research, and development of new

antibiotics: the WHO priority list of antibiotic-resistant bacteria and tuberculosis." The Lancet Infectious Diseases **18**(3): 318-327.

Taubman, S., A. So, F. Young, E. Davie and J. Corcoran (1963). "Effect of erythromycin on protein biosynthesis in *Bacillus subtilis* " Antimicrobial agents and chemotherapy **161**: 395-401.

Taubman, S. B., N. R. Jones, F. E. Young and J. W. Corcoran (1966). "Sensitivity and resistance to erythromycin in *Bacillus subtilis* 168: the ribosomal binding of erythromycin and chloramphenicol." Biochimica et Biophysica Acta (BBA)-Nucleic Acids and Protein Synthesis **123**(2): 438-440.

Tenorio, C., M. Zarazaga, C. Martinez and C. Torres (2001). "Bifunctional enzyme 6′-N-aminoglycoside acetyltransferase-2"-O-aminoglycoside phosphotransferase in Lactobacillus and Pediococcus isolates of animal origin." Journal of Clinical Microbiology **39**(2): 824-825.

Theuretzbacher, U. and L. J. Piddock (2019). "Non-traditional antibacterial therapeutic options and challenges." Cell host & microbe **26**(1): 61-72.

Tomlinson, J. H., G. S. Thompson, A. P. Kalverda, A. Zhuravleva and A. J. O'Neill (2016). "A target-protection mechanism of antibiotic resistance at atomic resolution: insights into FusB-type fusidic acid resistance." Scientific reports **6**(1): 1-12.

Traxler, M. F. and R. Kolter (2015). "Natural products in soil microbe interactions and evolution." Natural product reports **32**(7): 956-970.

Tu, D., G. Blaha, P. B. Moore and T. A. Steitz (2005). "Structures of MLSBK antibiotics bound to mutated large ribosomal subunits provide a structural explanation for resistance." Cell **121**(2): 257-270.

Unemo, M., D. Golparian, V. Skogen, A. O. Olsen, H. Moi, G. Syversen and S. O. Hjelmevoll (2013). "Neisseria gonorrhoeae strain with high-level resistance to spectinomycin due to a novel resistance mechanism (mutated ribosomal protein S5) verified in Norway." Antimicrobial agents and chemotherapy **57**(2): 1057-1061.

Van Bambeke, F. and V. J. Lee (2006). "Inhibitors of bacterial efflux pumps as adjuvants in antibiotic treatments and diagnostic tools for detection of resistance by efflux." Recent patents on anti-infective drug discovery **1**(2): 157-175.

Vazquez, D. (1966). "Binding of chloramphenicol to ribosomes the effect of a number of antibiotics." Biochimica et Biophysica Acta (BBA)-Nucleic Acids and Protein Synthesis **114**(2): 277-288.

Verlinde, C. L., E. Fan, S. Shibata, Z. Zhang, Z. Sun, W. Deng, J. Ross, J. Kim, L. Xiao, T. L. Arakaki, J. Bosch, J. M. Caruthers, E. T. Larson, I. Letrong, A. Napuli, A. Kelly, N. Mueller, F. Zucker, W. C. V. Voorhis, F. S. Buckner, E. A. Merritt and W. G. J. Hol (2009). "Fragment-based

cocktail crystallography by the medical structural genomics of pathogenic protozoa consortium." Current topics in medicinal chemistry **9**(18): 1678-1687.

Wachino, J.-i. and Y. Arakawa (2012). "Exogenously acquired 16S rRNA methyltransferases found in aminoglycoside-resistant pathogenic Gram-negative bacteria: an update." Drug Resistance Updates **15**(3): 133-148.

Waksman, S. A. (1947). "What is an antibiotic or an antibiotic substance?" Mycologia **39**(5): 565-569.

Waksman, S. A., A. Schatz and D. M. Reynolds (2010). "Production of antibiotic substances by actinomycetes." Annals of the New York Academy of Sciences **1213**(1): 112-124.

Walkty, A., J. A. Karlowsky, M. R. Baxter, H. J. Adam and G. G. Zhanel (2019). "In vitro activity of plazomicin against gram-negative and gram-positive bacterial pathogens isolated from patients in Canadian hospitals from 2013 to 2017 as part of the CANWARD surveillance study." Antimicrobial Agents and Chemotherapy **63**(1).

Wang, C., Z. Sui, S. O. Leclercq, G. Zhang, M. Zhao, W. Chen and J. Feng (2015). "Functional characterization and phylogenetic analysis of acquired and intrinsic macrolide phosphotransferases in the *Bacillus cereus* group." Environmental microbiology **17**(5): 1560-1573.

Wekselman, I., E. Zimmerman, C. Davidovich, M. Belousoff, D. Matzov, M. Krupkin, H. Rozenberg, A. Bashan, G. Friedlander and J. Kjeldgaard (2017). "The Ribosomal Protein uL22 Modulates the Shape of the Protein Exit Tunnel." Structure **25**(8): 1233-1241. e1233.

WHO, W. H. O. (2021). "Global antimicrobial resistance and use surveillance system (GLASS) report: 2021."

Wimberly, B. T., D. E. Brodersen, W. M. Clemons Jr, R. J. Morgan-Warren, A. P. Carter, C. Vonrhein, T. Hartsch and V. Ramakrishnan (2000). "Structure of the 30S ribosomal subunit." Nature **407**(6802): 327.

Wimberly, B. T., D. E. Brodersen, W. M. Clemons, R. J. Morgan-Warren, A. P. Carter, C. Vonrhein, T. Hartsch and V. Ramakrishnan (2000). "Structure of the 30S ribosomal subunit." Nature **407**(6802): 327-339.

Winter, G. (2010). "xia2: an expert system for macromolecular crystallography data reduction." Journal of applied crystallography **43**(1): 186-190.

Winter, G., D. G. Waterman, J. M. Parkhurst, A. S. Brewster, R. J. Gildea, M. Gerstel, L. Fuentes-Montero, M. Vollmar, T. Michels-Clark and I. D. Young (2018). "DIALS: implementation and evaluation of a new integration package." Acta Crystallographica Section D **74**(2): 85-97.

Yahav, D., C. G. Giske, A. Grāmatniece, H. Abodakpi, V. H. Tam and L. Leibovici (2020). "New β-lactam–β-lactamase inhibitor combinations." Clinical Microbiology Reviews **34**(1): e00115-00120.

Zhanel, G. G., M. Dueck, D. J. Hoban, L. M. Vercaigne, J. M. Embil, A. S. Gin and J. A. Karlowsky (2001). "Review of macrolides and ketolides." Drugs **61**(4): 443-498.

Zieliński, M., J. Park, B. Sleno and A. M. Berghuis (2021). "Structural and functional insights into esterase-mediated macrolide resistance." Nature communications **12**(1): 1-9.

Zubay, G. (1962). "The isolation and fractionation of soluble ribonucleic acid." Journal of Molecular Biology **4**(5): 347-356.

Zuckerman, J. M., F. Qamar and B. R. Bono (2011). "Review of macrolides (azithromycin, clarithromycin), ketolids (telithromycin) and glycylcyclines (tigecycline)." Medical Clinics **95**(4): 761-791.

Appendix

Fragment library cocktail numbers and compound names. This fragment library was adopted from Dr. Wim Hol group (Verlinde, Fan et al. 2009). Thus, the original cocktail number is written when necessary. This library contains 257 compounds grouped into 34 cocktail stocks in 100% DMSO. The stock concentration of each constituent compound in each cocktail was standardized at 100 mM.

Cocktail 1

Fragment Name	CAS
❖ 2-CHLOROQUINOXALINE 98%	1448-87-9
❖ 3-CYCLOPROPYL-1-METHYL-1H-PYRAZOL-5-AMINE	118430-74-3
❖ KYNURENIC ACID	492-27-3
❖ 6-METHOXYQUINALDINE	1078-28-0
❖ (R)-(+)-Alpha-(1-NAPHTHYL)ETHYLAMINE	3886-70-2
❖ 1,8-NAPHTHALIMIDE	81-83-4

Cocktail 2

Fragment Name	CAS
❖ 4-AMINOQUINALDINE	6628-04-2
❖ BENZO[C]CINNOLINE	230-17-1
❖ 2,3-DIHYDRO-1,4-BENZODIOXINE-6-CARBOXYLIC ACID	4442-54-0
❖ 1-(4-METHOXYPHENYL)-1-CYCLOPROPANECARBOXYLIC ACID	16728-01-1
❖ 5,5-PENTAMETHYLENEHYDANTOIN	702-62-5
❖ QUINOLINE-8-CARBOXYLIC ACID	86-59-9
❖ DECAHYDRO-2-NAPHTHOL	825-51-4

Cocktail 3

Fragment Name	CAS
❖ 9-AMINOACRIDINE HCL SALT	90-45-9
❖ 1,4-BENZODIOXAN-6-AMINE	22013-33-8
❖ 6-CHLOROTHIOCHROMAN-4-ONE 98%	37674-72-9
❖ CYCLOPROPYL 2-THIENYL KETONE	6193-47-1
❖ 6-HYDROXY-1-NAPHTHOIC ACID	2437-17-4
❖ 4,7-PHENANTHROLINE	230-07-9
❖ 9H-PYRIDO[3,4-B]INDOLE	244-63-3
❖ 6-QUINOXALINECARBOXYLIC ACID	6925-00-4

Cocktail 4

Fragment Name	CAS
❖ 3-AMINOQUINOLINE	580-17-6
❖ 1,2,3,4-TETRAHYDRO-3-ISOQUINOLINECARBOXYLIC ACID HYDROCHLORIDE	74163-81-8
❖ 6-METHOXY-1,2,3,4-TETRAHYDROQUINOLINE	120-15-0
❖ 2-NAPHTHOL	135-19-3
❖ S-TRIAZOLO(4,3-A)QUINOLINE	235-06-3
❖ Benz[cd]indo-2(1H)-one	130-00-7
❖ 6-AMINO-1,2,3,4-TETRAHYDRONAPHTHALEN-1-ONE	3470-53-9
❖ 1-AZAXANTHONE	6537-46-8
❖ 6-HYDROXY-2-NAPHTHOIC ACID	16712-64-4

Cocktail 5

Fragment Name	CAS
❖ 6-AMINO-1-NAPHTHOL	23894-12-4
❖ 6-METHOXY-1-TETRALONE	1078-19-9
❖ 5-AMINOQUINOLINE	611-34-7
❖ 5-AMINO-2-NAPHTHOL	86-97-5
❖ 8-HYDROXYQUINOLINE-2-CARBOXYLIC ACID	1571-30-8
❖ 6-HYDROXY-1-TETRALONE	3470-50-6
❖ 2-NAPHTHYLAMINE	91-59-8
❖ QUINALDIC ACID	93-10-7

Cocktail 6

Fragment Name	CAS
❖ CYCLOPENTYLAMINE	1003-03-8
❖ 2-AMINO-4,5-DIMETHOXYBENZOIC ACID	5653-40-7
❖ AMINODIPHENYLMETHANE	91-00-9
❖ URIC ACID	69-93-2
❖ 2-PROPIONYLTHIAZOLE	43039-98-1
❖ (2-METHYL-5-PHENYL-3-FURYL)METHANOL	111787-91-8
❖ 3-ACETYL-2,4-DIMETHYLPYRROLE	2386-25-6

Cocktail 7

Fragment Name	CAS
❖ 2-AMINO-5-PHENYL-[1,3,4]-THIADIAZOLE	2002-03-1, 312619-47-9
❖ N,N'-DIACETYLGLYCINE ANHYDRIDE	21827-92-9, 3027-05-2
❖ 3-METHYLPHENETHYLAMINE	5470-40-6
❖ 3,5-DIAMINOBENZOIC ACID	535-87-5
❖ 3,3,5-TRIMETHYLCYCLOHEXANOL	116-02-9
❖ 2-AMINO-1-METHYL-2-IMIDAZOLIN-4-ONE HEMISULFATE SALT	31377-28-3, 60-27-5
❖ PSEUDOTHIOHYDANTOIN	556-90-1
❖ 5-(2-FURYL)CYCLOHEXANE-1,3-DIONE	1774-11-4
❖ 3-ETHYNYLPYRIDINE	2510-23-8

Cocktail 8

Fragment Name	CAS
❖ D-GLUCURONAMIDE	3789-97-7
❖ N-(2-CARBOXYPHENYL)GLYCINE	612-42-0
❖ 1-((PYRROLIDINE-1-CARBONYL)METHYL)PIPERAZINE	39890-45-4
❖ 2-ETHYL-4-METHYLIMIDAZOLE	931-36-2
❖ 2-ETHOXY-4-METHYLPHENOL	2563-07-7
❖ 1-AMINOMETHYL-1-CYCLOHEXANOL HYDROCHLORIDE	19968-85-5

Cocktail 9

Fragment Name	CAS
❖ BROMOBENZENE	108-86-1
❖ 5-(HYDROXYMETHYL)URACIL	4433-40-3
❖ 2-PYRROLIDONE-5-CARBOXYLIC ACID	149-87-1
❖ 4-PHENYLIMIDAZOLE	670-95-1
❖ 2-(1,3-DIOXOLAN-2-YL)ETHANAMINE	5754-35-8
❖ 1,2-DIACETYLBENZENE	704-00-7
❖ SODIUM SACCHARIN	128-44-9
❖ BENZOGUANAMINE	91-76-9
❖ 4-METHYLPYRIDAZINE	1120-88-3
❖ 1-AMINOINDAN	34698-41-4

Cocktail 10 (Originally cocktail 11)

Fragment Name	CAS
❖ 4-CHLOROPHTHALIC ACID MONOSODIUM SALT	56047-23-5
❖ 3,6-BIS(HYDROXYMETHYL)DURENE	7522-62-5
❖ 3-TERT-BUTYL-1-METHYL-2-PYRAZOLIN-5-ONE	87031-30-9
❖ N-PHENYLBENZAMIDINE	1527-91-9
❖ 3-AMINO-5-METHYLTHIO-1H-1,2,4-TRIAZOLE	45534-08-5
❖ 1-METHYL-2(1H)-QUINOLINONE	606-43-9

Cocktail 11 (Originally cocktail 12)

Fragment Name	CAS
❖ (5-FLUORO-2-METHYLPHENYL)ACETIC ACID	261951-75-1
❖ P-AZIDOACETOPHENONE	20062-24-2
❖ (2,2-DIMETHYL-2,3-DIHYDRO-1-BENZOFURAN-7-YL)METHANOL	38002-89-0
❖ 4-CHLORO-2-(METHYLTHIO)PYRIMIDINE	49844-90-8
❖ CAFFEINE	58-08-2
❖ 2-AMINOIMIDAZOLE SULFATE	1450-93-7
❖ 3-(2-THENOYL)-PROPIONIC ACID	4653-08-1
❖ 1,4-BIS(1-METHYL-1-HYDROXYETHYL)BENZENE	2948-46-1

Cocktail 12 (Originally cocktail 14)

Fragment Name	CAS
❖ (4R,5S)-(-)-1,5-DIMETHYL-4-PHENYL-2-IMIDAZOLIDINONE	92841-65-1
❖ (+/-)-3,4,8,8A-TETRAHYDRO-8A-METHYL-1,6(2H,7H)-NAPHTHALENEDIONE	20007-72-1
❖ 3-HYDROXY-1,2-DIMETHYL-4(1H)-PYRIDONE	30652-11-0
❖ 2-CHLORO-6-FLUOROPHENETHYLAMINE	149488-93-7
❖ XANTHOPTERIN MONOHYDRATE	5979-01-1

Cocktail 13 (Originally cocktail 15)

Fragment Name	CAS
❖ 6,7-DIMETHOXY-3,4-DIHYDROISOQUINOLINE HYDROCHLORIDE	20232-39-7
❖ PYRIDINE-2-THIOAMIDE	5346-38-3
❖ PHENYLMALONIC ACID	2855-13-2
❖ ISOPHORONEDIAMINE	2568-34-5
❖ (BENZOYL-METHYL-AMINO)-ACETIC ACID	621-04-5
❖ 1-ETHYL-3-PHENYLUREA	77-04-3
❖ PYRITHYLDIONE	16867-03-1
❖ 2-AMINO-3-HYDROXYPYRIDINE	2855-13-2

Cocktail 14 (Originally cocktail 21)

Fragment Name	CAS
❖ 9-METHYL-3,4-DIHYDRO-2H-PYRIDO[1,2-A]PYRIMIDIN-2-ONE	61751-44-8
❖ 2,3-DIMETHYLCYCLOHEXANAMINE	42195-92-6
❖ 3,5-PYRIDINEDICARBOXYLIC ACID	499-81-0
❖ 2-(METHYLTHIO)CYCLOHEXANONE	52190-35-9
❖ 3-BROMOTHIOPHENE	872-31-1
❖ 2-METHYLPHENYLACETONE	51052-00-7

Cocktail 15 (Originally cocktail 22)

Fragment Name	CAS
❖ 5-CHLORO-2,3-DIHYDROXYPYRIDINE	53233-89-9
❖ 4-PHENYLPYRIMIDINE	3438-48-0
❖ 3-BENZYLIDENE-2,4-PENTANEDIONE	4335-90-4
❖ SHIKIMIC ACID	138-59-0
❖ 2-ETHYLTHIOPHENE	872-55-9
❖ 1-ACETYL-4-METHYL-2,5-DIHYDRO-1H-PYRROL-2-ONE	34581-92-5
❖ ARECAIDINE HYDROCHLORIDE	6018-28-6

Cocktail 16 (Originally cocktail 23)

Fragment Name	CAS
❖ (PHENYLSULPHONYL)ACETAMIDE	35008-50-5
❖ N,N-DIETHYLNICOTINAMIDE	59-26-7
❖ 2-BROMOANISOLE	578-57-4
❖ DL-PANTOLACTONE	79-50-5
❖ 2,4-THIAZOLIDINEDIONE	2295-31-0
❖ 2-AMINO-4-PHENYLPHENOL	1134-36-7
❖ 2-METHOXYNICOTINIC ACID	16498-81-0
❖ 1-TETRAHYDRO-FURFURYLPIPERAZINE	82500-35-4

Cocktail 17 (Originally cocktail 25)

Fragment Name	CAS
❖ 1-PIPERIDINECARBOTHIOAMIDE	14294-09-8
❖ TETRAHYDRO-3-FUROIC ACID	89364-31-8
❖ 3-(DIMETHYLAMINO)-5,5-DIMETHYL-2-CYCLOHEXEN-1-ONE	31039-88-0
❖ ETHYL 3,4-DIAMINOBENZOATE	37466-90-3
❖ 4-(HYDROXYMETHYL)IMIDAZOLE HYDROCHLORIDE	32673-41-9, 822-55-9
❖ 4-AMINOPHTHALIMIDE	3676-85-5
❖ 2-ETHYLBENZYL ALCOHOL	767-90-8
❖ 4(3H)-PYRIMIDINONE	4562-27-0
❖ 3-BENZOYLPYRIDINE	5424-19-1

Cocktail 18 (Originally cocktail 27)

Fragment Name	CAS
❖ 1-METHYL-3-INDOLEACETIC ACID	1912-48-7
❖ 1-METHYLIMIDAZOLE-2-CARBOXYLIC ACID, LITHIUM SALT	20485-43-2
❖ TRIGONELLINE HYDROCHLORIDE	6138-41-6
❖ 4-AMINO-3-BROMOPYRIDINE	13534-98-0
❖ HYDROXYECTOINE	165542-15-4

Cocktail 19 (Originally cocktail 28)

Fragment Name	CAS
❖ 4-FLUOROVERATROLE	398-62-9
❖ 5-PHENYLCYCLOHEXANE-1,3-DIONE	493-72-1, 35376-44-4
❖ 4-AMINOBENZYL ALCOHOL	623-04-1
❖ 3-HYDROXYDIPHENYLAMINE	101-18-8
❖ (S)-(+)-2-(METHOXYMETHYL)PYRROLIDINE	63126-47-6

Cocktail 20 (Originally cocktail 29)

Fragment Name	CAS
❖ 1-(4-METHYLPHENYL)-1-PROPANOL	25574-04-3
❖ 5-OXO-2,3-DIHYDRO-5H-PYRIMIDO[2,1-B][1,3]THIAZOLE-6-CARBOXYLIC ACID	32084-55-2
❖ 3-ETHOXYANILINE	621-33-0
❖ 4-METHYL-3,4-DIHYDRO-2H-1,4-BENZOXAZINE-7-CARBOXYLIC ACID	90563-93-2
❖ N-(HYDROXYMETHYL)BENZAMIDE	6282-02-6

Cocktail 21 (Originally cocktail 34)

Fragment Name	CAS
❖ 4-FLUOROANILINE	371-40-4
❖ 4-PIPERIDINOPIPERIDINE	4897-50-1
❖ 3-METHYL-2(5H)-FURANONE	22122-36-7
❖ 4-PROPYLPYRIDINE	1122-81-2
❖ 5-(2-FURYL)-2,4-DIHYDRO-[1,2,4]-TRIAZOLE-3-THIONE	35771-65-4
❖ 3-METHYLPYRAZOLE-1-CARBOXAMIDE	873-50-7
❖ METHYL 5-AMINO-2-FUROATE	22600-30-2

Cocktail 22 (Originally cocktail 35)

Fragment Name	CAS
❖ 3-ETHYL-4-METHYL-3-PYRROLIN-2-ONE	766-36-9
❖ 4-TERT-BUTYLPYRIDINE	3978-81-2
❖ 4-(HYDROXYMETHYL) PHENYLACETIC ACID	73401-74-8
❖ 2-(2-THIENYL)PYRIDINE	3319-99-1
❖ (2H)1,4-BENZOTHIAZIN-3(4H)-ONE	5325-20-2

Cocktail 23 (Originally cocktail 36)

Fragment Name	CAS
❖ 6-PHENOXY-3-PYRIDINAMINE	25194-67-6
❖ 2-(DIMETHYLAMINOMETHYL)-3-HYDROXYPYRIDINE	2168-13-0
❖ CIS-1,2-CYCLOPENTANEDIOL	5057-98-7
❖ 1-METHYL-1H-IMIDAZOLE-4-SULFONAMIDE	111124-90-4
❖ 4-PHENYLPIPERIDINE	771-99-3
❖ 3-(3,4-DIHYDROXYPHENYL) PROPIONIC ACID	1078-61-1
❖ BUTYROPHENONE	495-40-9
❖ METHYL 4(AMINOMETHYL) BENZOATE HYDROCHLORIDE	6232-11-7

Cocktail 24 (Originally cocktail 39)

Fragment Name	CAS
❖ 4'-METHOXYACETOPHENONE	100-06-1
❖ 4-METHYL-1,3-OXAZOL-2-AMINE	35629-70-0
❖ 1,3-BENZENEDIMETHANOL	626-18-6
❖ 1-FURFURYLPYRROLE	1438-94-4
❖ 3-BROMOIMIDAZO[1,2-A]PYRIDINE	4926-47-0
❖ N,N-DIMETHYLBENZOTRIAZOLEMETHANAMINE	57684-30-7
❖ PHTHALAN	496-14-0
❖ 1-(HYDROXYMETHYL)-2-PYRROLIDINONE	15438-71-8
❖ 2-METHYL-1-PHENYL-2-PROPEN-1-OL	4383-08-8

Cocktail 25 (Originally cocktail 41)

Fragment Name	CAS
❖ PROPYLENE CARBONATE	108-32-7
❖ 5-(METHYLTHIO)THIOPHENE-2-CARBOXYLIC ACID	20873-58-9
❖ N-ETHYLANILINE	103-69-5
❖ 4'-CHLOROPROPIOPHENONE	6285-05-8
❖ 3,5-DIISOPROPYLPYRAZOLE	17536-00-4
❖ 2-AMINO-3-BROMO-6-METHYLPYRIDINE	126325-46-0

Cocktail 26 (Originally cocktail 44)

Fragment Name	CAS
❖ 2,3-DIMETHYLFURAN	14920-89-9
❖ 2-(1-CYCLOHEXENYL) ETHYLAMINE	3399-73-3
❖ 1-BENZYLIMIDAZOLE	4238-71-5
❖ 1-BENZYL-3-PYRROLIDINONE	775-16-6
❖ PYRIDOXINE	65-23-6
❖ ETHYL 4-HYDROXYBENZIMIDATE HYDROCHLORIDE	54998-28-6
❖ CYCLOHEXANECARBOXAMIDE	1122-56-1
❖ 2-(CARBOXYMETHYLTHIO) PYRIMIDINE	88768-45-0
❖ 2-(4-CHLOROPHENYL)-2-METHYLPROPIONIC ACID	6258-30-6
❖ 2'-BROMOACETOPHENONE	2142-69-0

Cocktail 27 (Originally cocktail 48)

Fragment Name	CAS
❖ 6-METHYL-3(2H)-PYRIDAZINONE	13327-27-0
❖ 5-METHOXY-2-BENZIMIDAZOLINONE	2080-75-3
❖ 3-BENZYL-1,3-OXAZOLIDINE	13657-16-4
❖ 2,2'-BIPYRIMIDINE	34671-83-5
❖ 3-BROMOPHENOL	591-20-8
❖ 2-(PHENYLSULFONYL)ETHANOL	20611-21-6
❖ 4-FLUOROPHENYLUREA	659-30-3
❖ METHYL 4-OXO-3-PIPERIDINECARBOXYLATE HYDROCHLORIDE	71486-53-8
❖ 3-(2-HYDROXYPROPYL)-5-METHYL-2-OXAZOLIDINONE	3375-84-6
❖ 3-BROMOBENZYLAMINE	10269-01-9

Cocktail 28 (Originally cocktail 49)

Fragment Name	CAS
❖ 4-FLUOROPHENOL	371-41-5
❖ 2-MERCAPTOPURINE	28128-19-0
❖ 4-(AMINOMETHYL)PIPERIDINE	7144-05-0
❖ 4-BROMO-3-METHYLPYRAZOLE	13808-64-5
❖ 2-METHYL-3-PHENYL-2-PROPEN-1-OL	1504-55-8
❖ (S)-(+)-5-(HYDROXYMETHYL)-2-PYRROLIDINONE	17342-08-4
❖ 4,5,6,7-TETRAHYDROINDAZOLE	2305-79-5

Cocktail 29 (Originally cocktail 53)

Fragment Name	CAS
❖ 3-CHLORO-2,5-DIMETHYLPYRAZINE	95-89-6
❖ 2-(METHYLAMINO)BENZAMIDE	7505-81-9
❖ 2-DIMETHYLAMINOPYRIDINE	5683-33-0
❖ 4-CHLOROBENZENE-1-CARBOXIMIDAMIDE HYDROCHLORIDE	115297-57-9
❖ 5-METHOXYRESORCINOL	2174-64-3
❖ 2-BROMOPYRIMIDINE	4595-60-2
❖ D-CYCLOSERINE	68-41-7
❖ 4-BROMOPYRAZOLE	2075-45-8

Cocktail 30 (Originally cocktail 59)

Fragment Name	CAS
❖ BENZOFURAZAN-5-CARBOXYLIC ACID	19155-88-5
❖ N-(3-PYRROLIDINYL)ACETAMIDE	79286-74-1
❖ (1,5-DIMETHYL-1H-PYRAZOL-3-YL)METHANOL	153912-60-8
❖ 1-ISOPROPYL-PIPERAZINE	4318-42-7
❖ (5-METHYL-2-FURYL)METHANOL	3857-25-8
❖ 4-(2-HYDROXYETHYL)-3-METHYL-2-PYRAZOLIN-5-ONE	7721-54-2
❖ 1-BENZYL-4-PIPERIDONE	3612-20-2
❖ 4-(1H-PYRAZOL-1-YL)ANILINE	17635-45-9
❖ 1-BENZOTHIOPHENE-3-CARBOXIMIDAMIDINE HYDROCHLORIDE HYDRATE	465515-36-0

Cocktail 31 (Originally cocktail 60)

Fragment Name	CAS
❖ (S)-(-)-1-PHENYLPROPYLAMINE	2941-20-0
❖ 4'-AMINOACETOPHENONE	99-92-3
❖ 2-ACETYL-1-ETHYLPYRROLE	39741-41-8
❖ 3-PIPERIDINEMETHANOL	4606-65-9
❖ HOMOSULFAMINE HYDROCHLORIDE	138-37-4
❖ N-(2-FLUOROPHENYL) METHANESULFONAMIDE	98611-90-6
❖ QUINOLINE-3-CARBOXYLIC ACID	6480-68-8
❖ 4-(METHYLTHIO) BENZYL ALCOHOL	3446-90-0
❖ METHYL 2-CYCLOPENTANONE CARBOXYLATE	10472-24-9

Cocktail 32 (Originally cocktail 61)

Fragment Name	CAS
❖ 1-BENZYL-3-PYRROLIDINOL	775-15-5, 10472-24-9
❖ 6-AMINO-M-CRESOL	2835-98-5
❖ 3-CYCLOHEXENE-1-CARBOXYLIC ACID METHYL ESTER	6493-77-2
❖ 4-METHOXYTHIOBENZAMIDE	2362-64-3
❖ CYCLOPENTYLACETIC ACID	1123-00-8
❖ 3-METHYLCYCLOHEXANOL	591-23-1
❖ 2-(1-PIPERAZINYL)PYRIMIDINE	20980-22-7

Cocktail 33 (Originally cocktail 63)

Fragment Name	CAS
❖ 2-(4-CHLOROPHENYL)ETHANETHIOAMIDE	17518-48-8
❖ 1,3-DIMETHYL-3,4,5,6-TETRAHYDRO-2(1H)-PYRIMIDINONE	7226-23-5
❖ 3-HYDROXYPHENETHYL ALCOHOL	13398-94-2
❖ 1,1-DIMETHYL-4-PHENYLPIPERAZINIUM IODIDE	54-77-3
❖ (4-CHLOROPHENYL)METHANOL	873-76-7
❖ 2-CYCLOHEXYLETHANOL	4442-79-9
❖ 3-BROMO-N-METHYLANILINE	66584-32-5
❖ N-METHYL-N-PHENYLTHIOUREA	4104-75-0
❖ (1S,2S)-2-METHOXYCYCLOHEXANOL	2979-24-0, 134108-92-2
❖ METHYL 3-AMINOTHIOPHENE-4-CARBOXYLATE HYDROCHLORIDE	39978-14-8

Cocktail 34 (Originally cocktail 68)

Fragment Name	CAS
❖ 2-AMINO-6-BROMOPYRIDINE	19798-81-3
❖ 5-FLUOROINDOLE-2-CARBOXYLIC ACID	399-76-8
❖ 3-AMINOPYRROLIDINE	116183-82-5
❖ 5-AMINO-2-BROMOPYRIDINE	13534-97-9
❖ 2-(2,5-DIMETHYL-1,3-THIAZOL-4-YL)ACETIC ACID	306937-38-2
❖ 5-PHENYL-2-FUROIC ACID	52938-97-3
❖ 3-BROMOPYRIDINE	626-55-1
❖ 5-BROMOPYRIMIDINE	4595-59-9
❖ 3-AMINO-2-BROMOPYRIDINE	39856-58-1